European School of Molecular Medicine

Sede di Napoli

EUROPEAN SCHOOL OF MOLECULAR MEDICINE

SEDE DI NAPOLI

UNIVERSITA' DEGLI STUDI DI NAPOLI "FEDERICO II"

Ph.D. in Molecular Medicine – Ciclo VI/XXIV

Curricula Human Genetics

Study of the functional role of microRNAs in the regulatory networks underlying vertebrate eye development

Tutor:
Prof. Sandro Banfi

Ph.D. student:
Dr. Sabrina Carrella

Internal Supervisor:
Prof. Antonio Simeone

External Supervisor:
Prof. Paola Bovolenta

Coordinator:
Prof. Francesco Salvatore

Academic Year: 2011-2012

TABLE OF CONTENTS

ABSTRACT

MicroRNAs (miRNAs) are small non-coding RNAs that negatively regulate gene expression at the post-transcriptional level. They exert diverse functions in controlling normal tissue and organ development and physiology. Many miRNAs show spatially and temporally restricted expression patterns during vertebrate eye development but the roles of individual miRNAs in controlling this process remain however, largely unknown. The aim of my thesis was to shed further light on the role of specific miRNAs in regulating basic processes of ocular development mainly by exploiting the medakafish (*Oryzias latipes*) model system. In particular, I focused my attention on the miRNA subfamily constituted by miR-181a and miR-181b, which are expressed in the Inner Nuclear Layer (INL) and Ganglion Cell Layer (GCL) of the vertebrate retina. Morpholino-mediated combined knockdown of miR-181a/b function in medakafish results in a specific retinal phenotype characterized by the reduction of Inner Plexiform Layer (IPL) thickness, without any apparent reduction in the number of retinal cells. To dissect this phenotype further, I studied the consequences of miR-181a/b ablation in two medakafish transgenic lines, namely GFP-Six3.2 and GFP-Ath5, in which GFP expression can be specifically visualized in amacrine and retinal ganglion cells (RGCs), respectively. This analysis revealed that miR-181a/b exert a role in the specification and growth of amacrine and RGC axons. The above alterations translate into an impairment of retinal circuits assembly and to visual function defects, as assessed by the evaluation of the Optokinetic Response (OKR) behavioral test. Using a combination of bioinformatic, as well as on *in vitro* and *in vivo* experimental approaches, I identified *ERK2,* a kinase member of the MAPK signaling cascade, as one of

the direct targets of these two microRNAs. I demonstrated that the function of miR-181a/b in growth cone cytoskeleton remodeling during retinal development are largely mediated by *ERK2* targeting and by the modulation of its downstream signaling cascade. Moreover I provide, for the first time, *in vivo* evidence of an antagonism between the TGF-β pathway and the ERK2 cascade in the regulation of retinal axon specification and growth, which is exerted via TGF-β regulation of miR-181a/b levels. These data expand our knowledge on the role of miRNAs in eye patterning in vertebrates, and demonstrate that miR-181a/b-targeting of ERK2 and the consequent modulation of the MAPK cascade, in concert with TGF-β-action, play important roles in the signaling network that define the correct wiring and assembly of functional retina neural circuits.

1.INTRODUCTION

1.1 The vertebrate eye development

The eye is a bilateral organ, part of the central nervous system, deputed to the visual perception of the surroundings. The complexity of this organ is reached through a series of inductive and morphogenetic events, coordinated by specific genetic programs, which are conserved among different vertebrate species (Fig. 1 A-C).

The eye originates at late gastrula stages with the specification of retinal precursors cells within the eye field in the anterior neural plate. During neurulation, eye progenitor cells converge medially and are surrounded rostrally and laterally by telencephalic precursors and caudally and medially by cells that will form the diencephalon. The first morphological sign of eye development in vertebrates is the bilateral evagination of anterior diencephalon in the early neurula (Fig. 1 A, D, D'). Continued evagination of the optic primordial leads to the formation of the optic vesicles connected to the diencephalon by a small canal, the optic stalk. The optic vescicle extend towards the overlying, non-neural surface ectoderm that will ultimately give rise to the lens and cornea. At this stage, the presumptive lens also shows the first morphological signs of development. This is characterized by formation of the lens placode, a thickening of the surface ectoderm that comes into contact with the optic vesicle (Chow and Lang, 2001) (Fig. 1 E'). Coordinated invagination of the lens placode and the optic vesicle results in the formation of the lens vesicle and a double-layered optic cup and provides the first indication of the final shape of the eye (Fig. 1 C, F, F') . The inner layer of the optic cup (facing the lens) forms the

neural retina (NR), while the outer layer of the optic cup gives rise to the retinal pigment epithelium (RPE) which will be formed of a single layer of cells containing melanin. The proximal ventral region will instead originate the optic fissure, from which the optic nerve derives. This structure provides a channel for blood vessels within the eye and it allows the egression of retinal axons from the eye cup. The transition zone between the future retina and the RPE forms the Ciliary Margin (CM), or periphery of the retina (Fig. 1 F'). The Ciliary Margin differentiates into non neural structures: the proximal part into the ciliary epithelium while the distal part becomes the iris (Beebe, 1986).

In vertebrates, the morphogenetic movements and the tissue interaction are orchestrated by specific genetic programs regulated by the interplay between a reduced number of signaling pathways and transcription factors. Information, in the form of signaling molecules derived also from the surrounding tissues, modulate and restrict the expression of different transcription factors driving the differentiation towards a specific cell type.

In the optic cup formation, extracellular signals, derived from the surface ectoderm in contact with the prospective NR or from the periocular mesenchyme surrounding the presumptive RPE, pattern the distal optic vesicle. The surface ectoderm secretes high levels of two members of Fibroblast Growth Factor (FGF) signaling molecules family, FGF1 and FGF2, (Nguyen and Arnheiter, 2000) while members of the Transforming Growth Factor-β (TGF-β) signaling molecules superfamily, such as activins or the related Bone Morphogenetic Proteins (Bmp) - Bmp4 and Bmp7 - are expressed in the surrounding mesenchyme and/or the presumptive RPE itself (Fuhrmann et al., 2000) (Fig. 1A). FGF and TGF-β/BMP signaling act antagonistically on the specification of RPE and NR precursors. The first activates NR specification but

inhibits RPE formation by activation of the mitogen-activated protein kinase (MAPK) cascade which, in turn, promote the expression of Ceh10 homeodomain-contain homolog (*Chx10*), that impose a NR character to the native optic vesicle cells, and reduce the expression of Orthodenticle homeobox 2 (*Otx2*) and Microphtalmia transcriptor-associated factor (*MITF*), transcription factors crucial for the RPE identity. In contrast the induction of TGF-β/BMP signaling by extraocular mesenchyme is essential for turning on the expression of RPE molecular markers such as *MITF*, and has an inhibitory effect on the expression of *Chx10*. Besides those mentioned above, a number of additional transcription factors are also specifically expressed in the presumptive neural retina and RPE. Currently, it is not clear how many of them are really needed to impose tissue specificity.

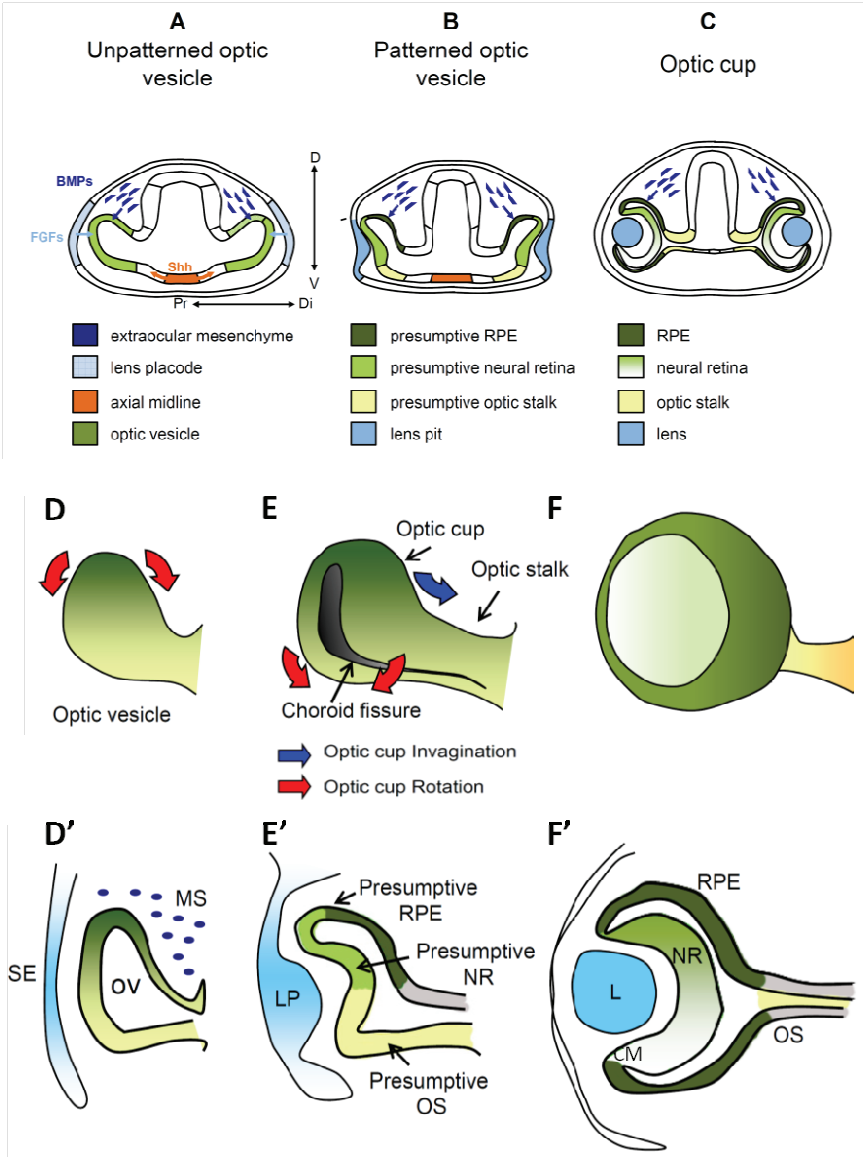

Figure 1. Schematic overview of vertebrate eye development.
(A, B, C) Distribution of inductive signals and transcription factors involved in early patterning of the eye. Progressive tissue specification during the transition from unpatterned (A) to patterned optic vesicle (B) and optic cup (C) where the different colors represent the distinct territories. TGFβ-like signals from the extraocular mesenchyme promote RPE character (dark green in B), whereas FGF signals from the lens placode repress RPE and activate neural retina identity (light green in B). During optic cup formation the graded distribution of BMP4 dorsally and Shh, in the ventral side establish the dorso-ventral polarity of the neural retina (shaded green in C). Shh: Sonic hedgehog; FGFs: Fibroblast grow factors; BMPs: bone morphogenetic proteins.
(D, E, F) Schematic representation of initial eye morphogenesis. D) The optic vesicle appears as a protrusion of the anterior neural tube. E) Folding of the distal and ventral neuroepithelium generates the optic cup and the optic fissure. F) The optic fissure seals and a spherical eye cup forms. D'). The optic vesicle neuroepithelium is composed of the cells that are morphologically and molecularly indistinguishable. E') As the vesicle folds, the dorsal neuroepithelium specifies as presumptive RPE (dark green), the distal region on presumptive neural retina (light green), while the ventral portion in optic stalk (light yellow). The surface ectoderm thickens forming the lens placode (blue). F') Complete folding of the vesicle results in an optic cup, where the RPE completely surround the neural retina. Abbreviations: L: lens; LV: lens vesicle; MS: mesenchyme; NR: neural retina; OS: optic stalk; OV: optic vesicle; RPE: retinal pigment epithelium; SE: surface ectoderm. (Adapted from Bovolenta, Marco-Ferreres and Conte, 2010).

Once established the RPE and NR identities, the retina differentiation process will give rise to an adult mature retina deputed to the transduction of visual stimuli to higher brain centers. The retina comprises seven major classes of cells, six of which are neurons (Wassle, 2004) whose cell bodies and connections are arranged in layers (Fig. 2 A). This laminar organization is stereotypic across species. The connections are restricted to two laminae: the outer plexiform layer (OPL) and the inner plexiform layer (IPL). Rod and cone photoreceptors in the outer nuclear layer (ONL) convert the light information into chemical and electrical signals that are relayed to interneurons. Bipolar interneurons in the inner nuclear layer (INL) are contacted by photoreceptors, in the OPL, and convey signals from the outer retina to the inner retina. The INL also comprises horizontal cells, which modulate the electric signal transmission, and Muller glial cells, which provide important structural and functional support in the maturation of retinal neurons and their connectivity. The bipolar cells form chemical synapses in the IPL with their targets, namely retinal ganglion cells (RGCs) and amacrine interneurons. Amacrine cells modulate the visual signals by regulating the release of neurotransmitters from the bipolar cells and providing inhibition directly onto ganglion cells. Light information leaves the retina via axons of the retinal ganglion cells that collectively form the optic nerve.

Generation of the appropriate cell types, their numbers and distribution derive from cell-intrinsic (genetic) and extrinsic (environmental) signals that act in concert to specify cell fate. Decisions to become one or another type of retinal cell appear to depend on many factors, including the time of cell genesis.

The seven types of cells differentiate from common progenitors in a temporal order widely conserved during evolution from fish to mammals: ganglion cells

first, followed by horizontal cells, cones and amacrine cells, rods and bipolar cells and Müller glial cells last (Fig. 2 B) (Belecky-Adams et al., 1996; Carter-Dawson and LaVail, 1979; Cepko et al., 1996; Hu and Easter, 1999; La Vail et al., 1991; Stiemke and Hollyfield, 1995; Young, 1985).

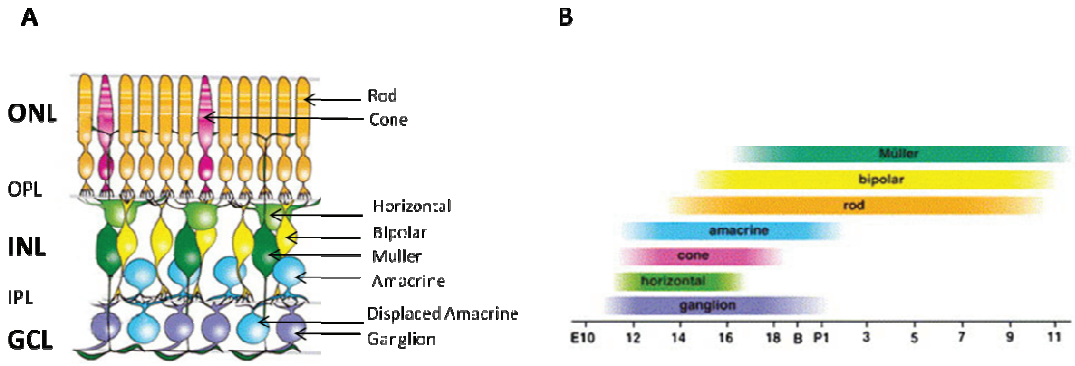

Figure 2. Schematic structure of the neural retina and its differentiation.
A) Vertebrate neural retina composed of seven types of retinal cells which constitute three cellular layers. GCL, ganglion cell layer; INL, inner nuclear layer; ONL, outer nuclear layer. Rod and cone photoreceptors in the outer nuclear layer (ONL) convert the light information into chemical and electrical signals that are relayed to interneurons. Bipolar interneurons in the inner nuclear layer (INL) are contacted by photoreceptors, in the Outer Plexiform Layer (OPL), and convey signals from the outer retina to the inner retina. The INL also comprises horizontal cells, which modulate the electric signal transmission, and Muller glial cells, which provide important structural and functional support. The bipolar cell target amacrine interneurons, that modulate the visual signals, and retinal ganglion cells (RGCs) in the Inner Plexiform Layer (IPL). Light information leaves the retina via axons of the retinal ganglion cells that collectively form the optic nerve. **B)** Retinal cells are differentiated in an order conserved among many species: ganglion cells first and Müller glial cells last. (Adapted from Hatakeyama and Kageyama, 2004).

According to the model of "competence", the different retinal cell types derive from a single common progenitor which change competency over time under the control of extrinsic (such as neurotrophic factors) and intrinsic regulators (such as transcription factors) (Austin et al., 1995; Belliveau and Cepko, 1999; Belliveau et al., 2000; Harris, 1997; Holt et al., 1988; Livesey and Cepko, 2001; Marquardt and Gruss, 2002; Turner and Cepko, 1987; Turner et al., 1990). In this model, progenitors pass through intrinsically determined competence states, during which they are capable of giving rise to a limited subset of cell types under the influence of extrinsic signals (Altshuler et al., 1993; Ezzeddine

et al., 1997; Furukawa et al., 2000; Guillemot and Cepko, 1992; Kelley et al., 1994; Zhang and Yang, 2001).

TGF, EGF (epidermal growth factor) and ILF (leukemia inhibitor factor) are just some examples of extrinsic factors that can stimulate the production of specific retinal cells types, while leading to suppression of other (Lillien and Wancio, 1998). Indeed genes coding for transcription factors of the family b-helix-loop-helix, such as *Ath5*, *mash1*, *NeuroD*, or homeobox genes such as *Otx2*, *Chx10*, *Pax6*, *Six3* and *Crx* act as intrinsic regulators (Bramblett et al., 2004; Brown et al., 2001; Burmeister et al., 1996; Dyer et al., 2003; Inoue et al., 2002; Li et al., 2004; Marquardt et al., 2001; Mathers et al., 1997; Morrow et al., 1999; Satow et al., 2001; Tomita et al., 2000). These genes are important both for differentiation and maintenance of retinal cell types; in fact many of them are expressed at high levels in specific cellular regions also when the retina is completely differentiated. Overall, the development of the eye is a highly complex process, and the sequential and coordinated expression of numerous genes encoding for transcription factors, cofactors, signal transduction molecules, membrane receptors and others, more or less well characterized, play a key role in different stages of eye development and may be responsible, when mutated, for different eye malformations.

1.2 The wiring in the retina

Vision, of course, relies on the proper development of the retina. Following the generation of each cell type, the major developmental events in the retina regard the formation and maintenance of connections between its cellular components and between the retina and its brain targets.

Organization of the retina network occurs progressively and with precision. Accurate processing of visual information requires that the axons and dendrites target their synaptic partners, and that they form the appropriate balance of excitatory and inhibitory connections. For this reason, the various cell types need to express, for intercellular communication, their appropriate neurotransmitters, which together with neurotrophic molecules play essential roles in the establishment of proper retina neural circuits.

The structural development of retinal neuron arbors starts establishing cellular polarity and compartmentalization of neurites into the axons and dendrites. After becoming specified neurons, the cells begin to elaborate neurites. Usually during the polarization process, neurons typically estabilish a single process as axon and the remainder, or the subsequent, processes become dendrites (Horton and Ehlers, 2003). Since the initial event in establishing a polarized neuron is the determination of a single axon, the process was termed “axon specification” (Fukata et al., 2002). During axon specification, one of several seemingly identical nascent neurites undergoes drastic changes in its cytoskeletal and membrane composition, resulting in a neuritic process morphologically and functionally distinct from those that grow and develop into dendrites (Dotti and Banker, 1987; Goslin and Banker, 1989).

Although molecular pathways that regulate neuronal polarity in other neural system have been already defined (Wozard 2002, Shi 2004, Jiang 2005, Yoshimura 2005), our knowledge of the factors that specifically stimulate axonal or dendritic outgrowth in retinal neurons is only just beginning to deepen. Morphological analyses revealed that retinal ganglion cells (RGCs) extend a single axonal process prior to elaborating dendrites (Hinds and Hinds, 1974; Maslim et al, 1986). In 2002, Goldberg et colleagues, demonstrated that purified

rat RGCs display an age-related bias in the rate of growth of axonal versus dendritic processes. Their data suggest the presence of an extrinsic contact-mediated signal responsible for shifting ganglion cell outgrowth from an axon to a dendritic mode. This signal does not come from the axonal target zone but instead from direct contact with amacrine cells within the retina. Other works demonstrated that the development of RGC dendrites is not only regulated by intraretinal signaling but also by neuronal interaction in the brain (Lom and Cohen-Cory, 1999; Lom et al 2002). The Brain-Derived Neurotrophic Factor (BDNF) is endogenously released in the retina as well as in the tectum where RGC axons make synapses. Increasing BDNF levels in the tectum result in more complex RGC dendritic and axonal arborizations, whereas increasing retinal BDNF has opposite effects on dendrites and no effects on axonal complexity, revealing that the effect of individual molecules is dependent also on the site of action.

The RGC arborize in a laminar fashion in the inner plexiform layer (IPL), sometimes occupying single strata within a multilayered array of concentric circuits. In most species, five prominent sublaminae are identifiable in the IPL, termed S1 to S5 (Cajal, 1972). This sublaminae can be divided in the so called ON-region (S3 to S5) and OFF- region (S1 and S2) (Fig. 3). The ON (increments in light intensity) and OFF (decrements in light intensity) stimuli are processed in two vertical pathways and together provide contrast information that are elaborated by specialized circuits in the IPL, and then transmitted through the RGCs to the brain. Initially, it was considered that the ON-pathway cells restrict their arbors to the inner portion of the IPL (the ON region S3-S5), and the OFF-pathway cells occupy the outer region (the OFF region S1,S2) (Famiglietti and Kolb, 1976; Famiglietti et al 1977; Stell et al, 1977; Nelson et al

1978). Later, it was demonstrated that ON- and OFF- responding cells ramify in both regions (Ammermuller and Kolb, 1995).

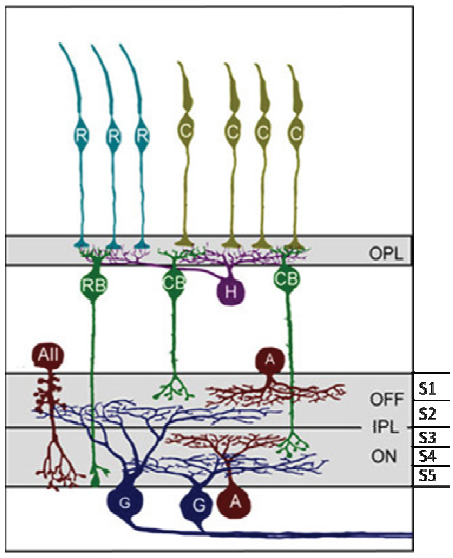

Figure 3. Schematic representation of the Plexiform Layer structures.
Neuronal arbors stratify within the Inner Plexiform Layer (IPL) occupying discrete laminar position. On a gross level, the IPL is split in the OFF- responding circuitry and ON- responding circuitry. Beyond this, the IPL can be divided into finer sublaminea, typically five, S1-S5. Individual retinal circuits are constituted of connection between specific subtypes of bipolar, amacrine and ganglion cells, whose arbors co-stratify within a particular lamina or sublaminae. A: Amacrine cells; RB: Rod-Bipolar cells; CB: Cone-Bipolar cells, G: Retinal Ganglion cells; H: Horizontal cells; R: Rod; C: Cone; OPL: Outer Plexiform Layer; IPL: Inner Plexiform Layer. (Adapted from Morgan and Wong 2005).

Laminated circuits could arise via several non-exclusive strategies (Fig. 4A):

a) Sequential layering: successive strata stacking to either side of preceding networks
b) Remodeling: sublamination being the result of eliminating neurites from inappropriate regions
c) Targeting: neurons extending laterally stratified processes after encountering localized molecular guidance signal
d) Contact-dependent guidance signal
e) Hierarchical: laminar organization following refinement of afferent inputs or efferent target fileds.

The current hypothesis is that the majority of mammalian RGCs progress from an early non-stratified stage - characterised by ON-OFF responses and ramification throughout the depth of the IPL - to a mature stratified stage whereupon they respond as strictly ON or OFF cells and dendritic arbors are restricted to corresponding regions of IPL (Bodnarenko et al, 1995, 1999; Lohmann and Wong 2001; Stacy and Wong 2003). Extensive reorganization, including the retraction of inappropriately placed dendrites, is suggested to lead to their mature stratification pattern (Chalupa and Gunhan, 2004; Maslim and Stone, 1988) (Fig. 4 B).

Cellular ablation studies have provided insights into the understanding of what cellular interrelationships are required to form stratified arborization in the IPL. In a Zebrafish mutant, in which RGCs never develop (lakritz), the bistratification pattern of a transgenically defined amacrine cell subpopulation was found to be nearly normal at maturity, showing only circumscribed areas of disruption (Kay et al 2004).

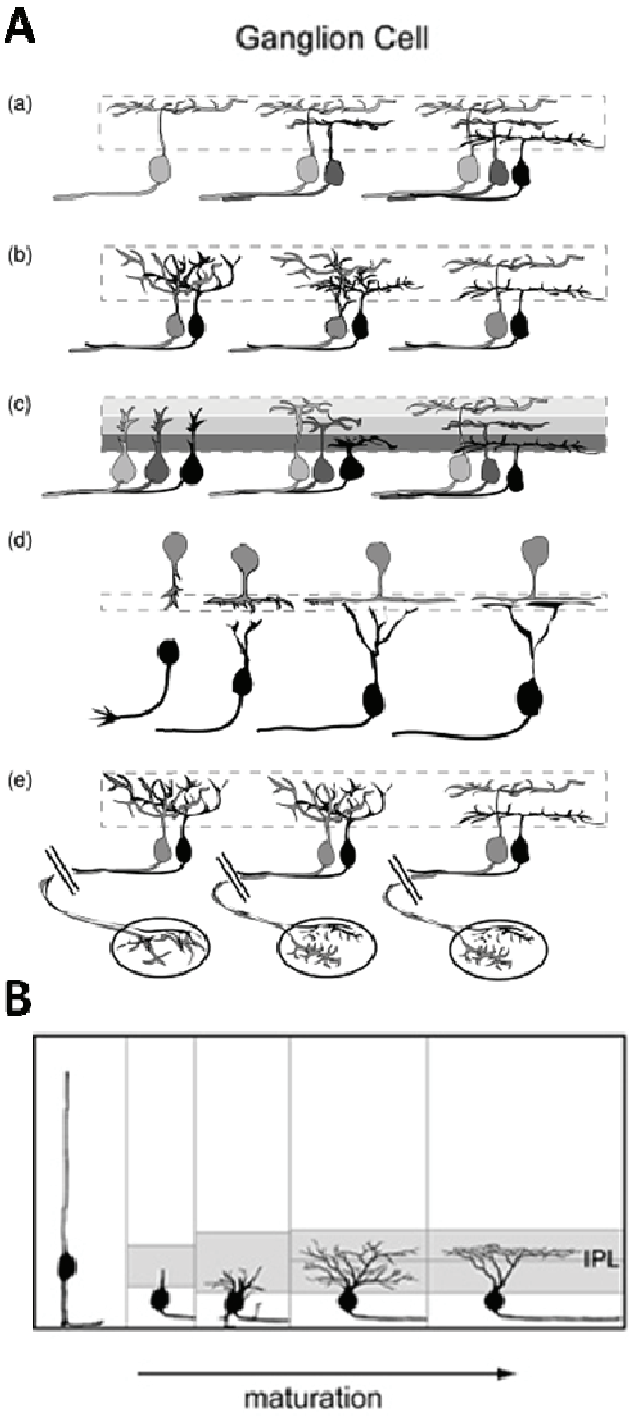

Figure 4. A) Non-exclusive strategies for the formation of laminar circuits.(a) Sequential layering; initial neurons elaborate stratified arbors within the neuropil, subsequent neurons establish strata above or below pre-existing layers. (b) Remodelling; neuritic arbors branch throughout the neuropil initially, subsequent elimination, or selective stabilization, of branches results in stratified patterns at maturity. (c) Targeted (molecular); neurons respond to molecular guidance cues arranged in laminar fashion such that they elaborate leateral processes only in specific sublaminae. (d) Targeted (cellular); neurons respond to contact-dependent cues presented by guidepost cells and/or synaptic partners such that laminar outgrowth is restricted to specific sublaminae. (e) Hierachical; neurons organize axonal and dendritic arbors in a serial fashion such that resolving the axonal target field area precedes dendritic rearrangements or vice versa. (a-e) Dashed box indicates the inner plexiform layer, all panels proceed left to right from immature to mature states. **B)** Proposed sequence of dendritic development of retinal ganglion cells (RGCs). (Adapted from Mumm and Lohmann, 2006; Morgan and Wong 2005).

Despite the detailed studies on the development of RGC morphology, comparatively little is known about factors that shape the arborization of retinal interneurons, amacrine and bipolar cells. However, these data demonstrate that the development of stratified arbor morphologies of bipolar and amacrine cells does not appear to depend on the presence of RGC dendrites. In addition, it has been shown that cholinergic amacrine cells stratify prior to most RGCs and bipolar cells, supporting the idea that some amacrine cells subtype may be positioned upstream, in a hierarchical sense, providing lamination cues for bipolar and RGC subtypes that then ramify in the sublaminae that they establish (Reese at al. 2001).

However, very little information is still available about the molecular signals that regulate amacrine axon specification and stratification patterns. Evidence for general repulsive and/or attractive cues is lacking. The current model proposes that the distance between retinal synaptic partners is small enough that contact may result from polarized outgrowth alone without the need for positional gradients.

To gain insight into the developmental rules that govern amacrine cell stratification and monitor how amacrine neurites contribute to the formation of the IPL, Godinho and colleagues followed individual cells from the time their neurites first elaborate until they stratify (Godinho et al. 2005). Capturing the behavior of amacrine cells prior to their arrival at the interface with the nascent IPL, they showed that during migration, amacrine cell processes did not appear to be polarized towards their eventual target, the IPL. Instead, they had multiple processes emerging from their cell body that were highly dynamic. Even when amacrine cells were detected near the border of the IPL and the forming INL, they continued to elaborate processes that appeared to sample the environment

(Fig. 5 A). Once the processes of amacrine cells reach the forming IPL, amacrine cells project their neurites exclusively towards the GCL, and enter into another phase of dynamic remodeling, resulting in an arbor that demarcates the cell's lateral territory within the forming IPL (Fig. 5 B). Moreover, their arbors lateralize preferentially within the appropriate sublamina, indicating that the amacrine cells directly recognize sublamina-specific cues in the forming IPL (Fig. 5 B). These findings demonstrate that the targeting of amacrine cell neurites is highly directed and does not involve extensive laminar remodeling (Fig. 5 C). The selective elaboration of amacrine neurites within appropriate ON or OFF sublaminae in the IPL suggests the presence of sublamina-specific cues (Godinho et al. 2005).

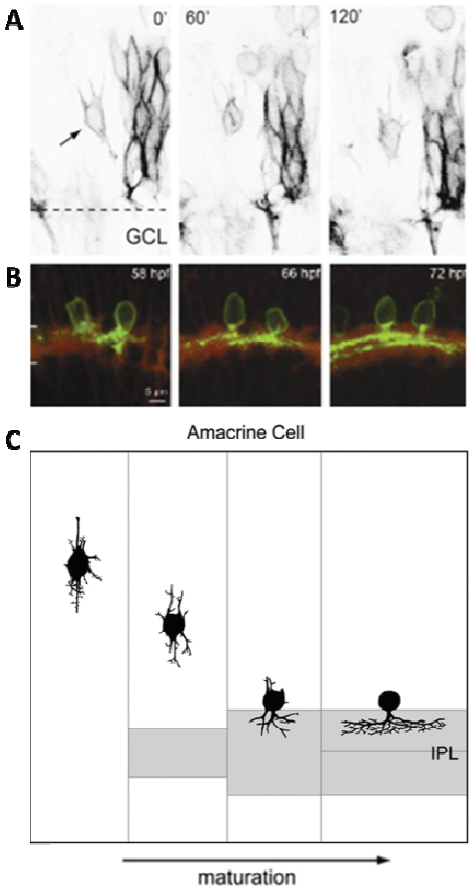

Figure 5. (A-B) *In vivo* analysis of individual amacrine cells from the time their neurites first elaborate until they stratify. During migration, prior to their arrival at the interface with the nascent IPL the amacrine cell processes had multiple processes emerging from their cell body that were highly dynamic. The amacrine cells near the border of the forming IPL continued to

elaborate processes that appeared to sample the environment. At this point amacrine cells project their neurites exclusively towards the GCL, and enter into another phase of dynamic remodeling, resulting in an arbor that demarcates the cell's lateral territory within the forming IPL. The amacrine arbors lateralize preferentially within the appropriate sublamina, indicating that the amacrine cells directly recognize sublamina-specific cues in the forming IPL (Adapted from Godinho et al. 2005). **C)** Proposed sequence of amacrine cell neurite development from serial EM studies (Adapted from Morgan and Wong 2005; Hinds and Hinds, 1978).

As already mentioned, direct cell-cell interactions, rather than molecular gradients, are the more likely candidates for such cues. This is because, compared with other CNS regions in which molecular gradients set up specific axonal arborization patterns (e.g. the tectum or superior colliculus), the IPL is relatively thin and compact. In the IPL, such molecular gradients would need to be very steep to set up not only the ON and OFF sublaminae, but also the multiple strata that lie within each sublamina, as they are only micrometers apart (Wassle and Boycott, 1991; Werblin et al., 2001). One of the most attractive model addresses a key role of adhesion molecules. A large number of cell-cell adhesion molecules are expressed in stratified patterns in the IPL (Wohrn et al.1998; Honjo et al 2000; Drenhaus et al 2003, 2004). In support of this model, disruption of Plexin function, a cell surface co-receptor that mediates the repulsive effects of Semaphorins, results in a failure of IPL formation in the chick retina (Ohta et al, 1992). Another adhesion molecule, N-cadherin, may function specifically to promote proper targeting and lamination of retinal neurons (Masai et al 2004). Recent evidence implicates two members of the immunoglobin supefamily of adhesion molecules, Sidekicks1 and 2, as direct sublamination guidance cues in the chick retina. Sidekick1 and 2 (Sdk1 and 2), have been shown to be differentially expressed in the ON and OFF sublaminae of the chick IPL: Sdk1, expressed in the ON sublamina, has been implicated in establishing connections between ganglion, amacrine and bipolar cells that co-

stratify in this sublamina, whereas Sdk2 has been implicated in establishing connectivity in the OFF sublamina (Yamagata et al. 2002).

Despite the numerous advances in understanding how retinal neurons develop and the relationship between form and function in the retina, there are still many outstanding issues. Finding direct stratification regulators is not an easy challenge since the factors implicated in this complex process usually perform multiple developmental function, moreover the circuit formation may rely on integration of multiple redundant mechanism that simply render it unsusceptible to the loss of individual molecules.

1.3 From the Retina to the Brain

The correct assembly of the wiring in the retina is needed to modulate the visual stimuli, which are then transmitted to the visual processing centers in the brain. This important role is accomplished by the RGCs whose axons, forming the optic nerve, wire the eye to the brain. As for the other retinal neurons, the establishment of functional neural circuits includes three-sequential events: a) the polarized outgrowth of axons and dendrites; b) the axon pathfinding, which, in this case, occurs over long trajectories; and c) the recognition of the appropriate synaptic partner (Fig. 6).

The growth of retinal ganglion cell (RGC) axons to their tectal targets is perhaps one of the best understood cases of axon navigation over an entire pathway. Axon navigation relies on the competence of growth cone to sense and interpret attractive and repulsive cues present along their trajectory, since the earliest phases of the process.

The polarized outgrowth of axons and dendrites:

Axonogenesis is first evident as a polarized thickening of the plasma membrane close to or at the vitreal surface of RGCs (Holt, 1989) (Fig. 6 A). Once axons reach the vitreal surface, they immediately orient and extend along the ganglion cell fiber layer toward a circular region in the centre of the retina, the optic disc, and bundle together to form the optic nerves (Fig. 6 B-D).

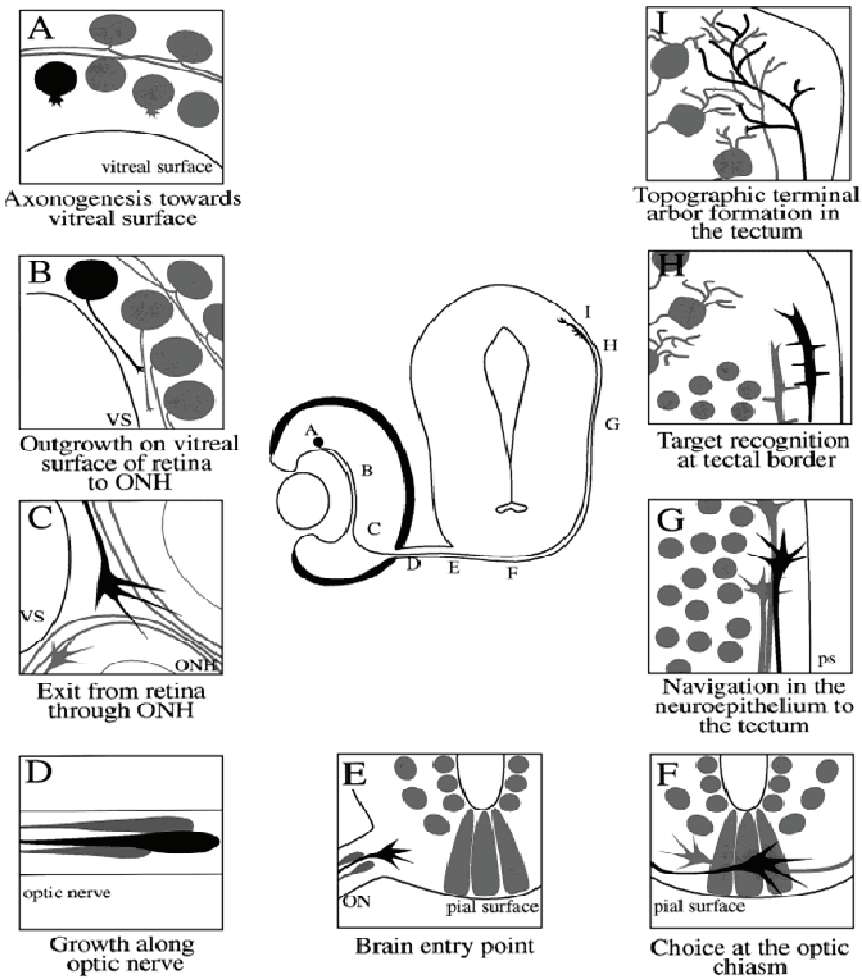

Figure 6. Development of the vertebrate visual system. A) Growth cone dynamics of pioneering axons from the right eye. RGCs from the dorsocentral retina are the first to extend axons. B) These pioneering axons grow ventrally close to the vitreal surface of the eye toward the optic nerve head (ONH). C) At the ONH, growth cones become highly complex as they dive down into the ON. D) Growth cones appear torpedo shaped as they grow along the ON. E) Growth cones then adopt a complex morphology when they reach the ventral diencephalon, at the brain entry point. F) Growth cones cross over to the contralateral side of the brain at the optic chiasm. G) Axons reach the mid–optic tract. H) Growth cones reach the anterior tectum and undergo dramatic morphological changes.I) Within the tectum, terminal arbors develop that form a topographical map. ONH, optic nerve head; ON, optic nerve; vs, vitreal surface; ps, pial surface (Dingwell, Holt and Harris, 2000).

Components of the extracellular matrix (e.g., laminin, fibronectin) and a variety of cell adhesion molecules (CAMs: IgG superfamily, cadherin families) and substrate adhesion molecules (SAMs, integrins) have been shown to promote neurite initiation (Hynes and Lander, 1992). The integrin complex is a structural component of focal adhesions and acts as a link between the plasma membrane and the extracellular matrix (ECM) (Fig. 7A). Substrate-adhesion is essential for generating the forces required for axon outgrowth, but may not be sufficient for promoting axonogenesis. Focal adhesions are not only sites that couple the plasma membrane with the cytoskeleton, but are also macromolecular signaling complexes (Giancotti and Ruoslahti, 1999). Composed of both structural (e.g., cytoskeleton-binding) and signaling proteins, focal adhesions play important roles in axon outgrowth signaling mechanism in addition to cell adhesion. In fact, in addition to CAMs and ECM, axon initiation and outgrowth in the visual system depends on growth factor receptors, such as the fibroblast growth factor receptor (FGFR), expressed in RGC growth cones (Fig.7B).

The axon pathfinding:

The RGCs growth cone is responsible to sense and interpret attractive and repulsive cues, and the dynamics of growth cone morphology varies in a position-specific manner during the development of the visual projection: at different points along the optic pathway, it tends to be more complex at points where important pathway decisions or choice points are made (Harris et al., 1987; Holt, 1989). Growth cones tend to be simple during outgrowth and then acquire a more complex morphology as they reach and turn at key decision points, supporting the idea that these changes reflect responses to cues within

their microenvironment. One of the most dramatic changes in the morphology of RGC growth cones occurs when axons leave the ganglion cell fiber layer and enter the optic nerve head (Fig. 6 E). In this region the growth cone meets an important signaling cue, Netrin-1 (Fig. 7 B, C).

Netrin-1 is a laminin-related secreted protein, produced by glial cells at the optic disk and optic nerve head that appears to act at a short-range to attract RGC growth cones into the optic nerve head. This effect is mediated by signaling involving the netrin-1 receptor, Deleted in Colorectal Cancer (DCC) expressed on RGC axons (de la Torre et al., 1997). Restricted co-expression of laminin-1 and netrin-1 at the entrance to the optic nerve head results in a repulsive signal that serves to 'push' the growth cone away from the retinal surface and grow deep into the attractive netrin-1-rich/laminin-1-poor optic nerve head. Netrin-1 is expressed in the optic disk/nerve head but also further along the optic tract (Fig. 6 G) where it governs RGC axon guidance with a repulsive action. Intrinsic changes in RGC growth cones and extrinsic factors present in the optic tract might modulate the progressive maturational change that occurs in RGC growth cones in response to netrin-1. Netrin-1 functions as a repellent in the distal part of the visual pathway and helps to constrain the growth of RGC axons into the appropriate trajectory. In the tract between the optic nerve head and the optic chiasm the RGC axons are insensitive to Netrin-1. In that point the RGCs growth cones show the second dramatic change in their complexity (Fig. 6 F).

The optic chiasm is an important choice point along the visual pathway where RGC axons have to decide whether or not to cross the ventral midline of the brain. The degree of decussation of RGC axons at the optic chiasm varies according to the species. Fish and birds have no binocular vision and only

crossed projections. In most mammals, all RGCs located in the temporal retina send axons ipsilaterally, whereas in species with less binocular vision uncrossed projections arise from a subpopulation of RGCs in the ventrotemporal (VT) region of the retina. The Eph (**e**rythropoietin-**p**roducing human **h**epatocellular) family of tyrosine kinases receptors is the largest known subfamily of receptor. For Eph receptor activation is required the direct binding with their corresponding ephrin ligands. Because Eph receptors are expressed at high levels in the ventrotemporal retina (Cheng et al., 1995; Drescher et al., 1995), the stage-dependent Eph– ephrin interactions at the chiasm could account for the ipsilateral projection. Ephrin-B ligand forms a repulsive 'barrier' at the chiasm that repels the subpopulation of EphB expressing fibers into the ipsilateral tract. Only this restricted RGC subpopulation in mouse VT retina express a different receptor EphB1 (Williams et al. 2003), responsible for Eph-ephrin interaction needed for ipsilateral projections.

Then the orderly advance of RGC growth cones, is achieved by an integrated response of the growth cone to a variety of environmental cues acting either from a distance through diffusion gradients or by local short range effects that include cell–cell interactions (Tessier-Lavigne and Goodman, 1996). Netrin and Eph/ephrin molecules belong to the growing list of guidance molecules that have been shown to contribute to the accurate development of visual projections. Although they play diverse roles, they share the ability to exert bi-functional activity on growing RGC axons, they are reused along the visual pathway and their role is conserved among vertebrate species.

The recognition of the appropriate synaptic partner:

Once they reach the border of their target, the optic tectum (or superior colliculus in mammals), growth cones undergo a rapid and remarkable change in behavior (Fig. 6 H, J). Their growth rate decreases significantly and they lose their characteristic morphology, becoming highly complex and elongated with lamellipodia and filopodia extending in all directions (Fig. 7 D, E). These changes could be due to a switch in the extracellular environment to one that does not favor axon growth. Molecules that are highly expressed along the optic tract, drop off significantly within the anterior tectum.

One simple model to explain these observations is that during target recognition, growth cones sense a change in FGFR signaling (FGF2 levels), likely from high to low, which then triggers their morphological and behavioral changes. The final result is growth cones switch from active growth to arborization.

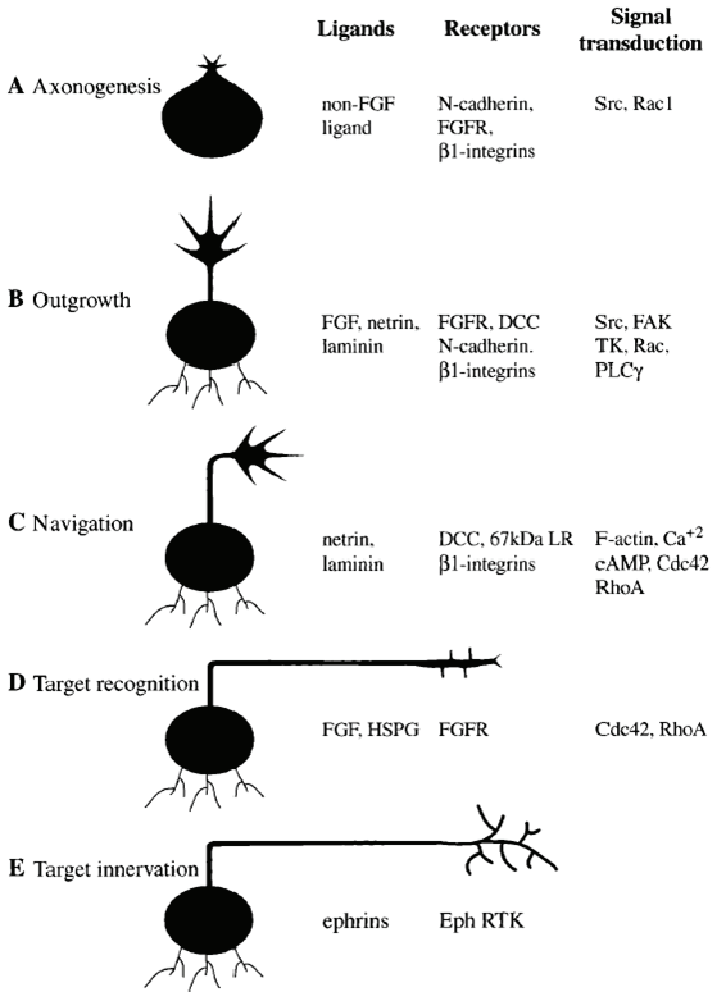

Figure 7. Some of the molecules that regulate RGC growth cones dynamics during the development of the vertebrate visual system. A) Axongenesis occurs at the vitreal surface of RGCs. B) Outgrowth of axons is then stimulated by a variety of molecules within the retina and optic tract. C) Along the visual pathway, growth cones make specific navigational choices leading to a change in their direction of growth. D) Once growth cones have reached their target, they undergo a series of dynamic morphological changes including the loss of the primary growth cone, and the development of branches along the axon shaft. E) Within the target, terminal arbor formation begins in which appropriate topographical choices are made. (Dingwell, Holt and Harris, 2000).

The axons innervate the brain according to specific topographic criteria: axons from the anterior retina project to the posterior tectum, posterior retina axons to the anterior tectum, dorsal retina axons to the ventral tectum, and ventral retina axons to the dorsal tectum. It is now thought that the tyrosine kinases Eph receptor and their ligands, the ephrins, expressed in gradients within the retina

and tectum, respectively, are partially responsible for appropriate topographical mapping (Cheng et al., 1995; Drescher et al., 1995).

1.4 Morphogen guidance cues activate internal signaling cascade at growth cone

Axon navigation depends on the competence of growth cones to sense and interpret guidance cues, along their trajectory. Recently it was demonstrated that the axon guidance process regulation does not relies only on a restricted number of conserved family of ligand-receptor signaling systems (e.g. Netrin/DCC, Ephrin/EPH, Slit/Robo, Semaphorin/Plexin), but some neurons respond also to other secreted signaling molecules, best known for their roles as morphogens in early embryo development, belong to the Sonic hedgehog (SHH), Wingless (WNT) and Transforming Growth Factor/Bone Morphogenetic Protein (TGF-β /BMP) signaling pathways (see for review Bovolenta, 2005; Sanchez-Camacho and Bovolenta, 2009).

Morphogens are secreted proteins produced by a restricted group of cells that, emanating away from their sources, induce distinct cellular responses in a concentration-dependent manner. Binding to specific receptors, morphogens activate particular intracellular cascades that influence cell behavior in a vast number of processes. Recent evidence show that they are not only involved in the early phases of embryo development, but are also reused as axon guidance cues at later developmental stages (Bovolenta, 2005).

Among morphogens, members of the TGF-β /BMP families have been implicated in neuronal polarization (Yi et al. 2010), axon and dendrite development (Kerrison et al.2005; Hocking at al.2007) and axonal pathfinding (Augsburger et al. 1999; Butler and Dodd, 2003), processes that require rapid

and local changes in cytoskeletal organization and plasma membrane components. In fact, as already mentioned, growing axons respond to gradients of chemo-attractant or chemo-repulsive cues translating the external differences into an intracellular signal that could activate different cascades for the different morphogens. In many cases, these intracellular signaling cascades result in the transcriptional activation of nuclear gene targets. However, in the case of axon guidance the participation of nuclear gene transcription may appear a slow and uneconomic way to control local growth cone movement. In fact, the growth cone advance, pause or transformation seem to largely rely on fast and local changes in cell adhesion and cytoskeletal organization mostly due to activation of local protein synthesis and degradation within the growth cone, events that may allow compartmentalized modifications and thus steering.

It was demonstrated that the TGF-β /BMP morphogens mediate axon guidance using a transcription-independent pathway. BMP receptor dimerization in growth cones activates an alternative and completely transcription-independent cascade that culminates in local cytoskeleton regulation. This alternative pathway involves the activation of LIM Kinases (LIMK1 and 2), which in turn phosphorilate and inactivate an Actin Depolimerization Factor (ADF/Cofilin), permitting axon polymerization to occur. Interestingly, prolonged exposure to BMP ligands changes the response from an attraction to a repulsion. This change involved the activation of Slingshot (SSH), a phosphatase known to counteract the effect of LIMK1 on ADF/Cofilin, leading to its activation that results in repulsion (Wen et al. 2007) (Fig. 8).

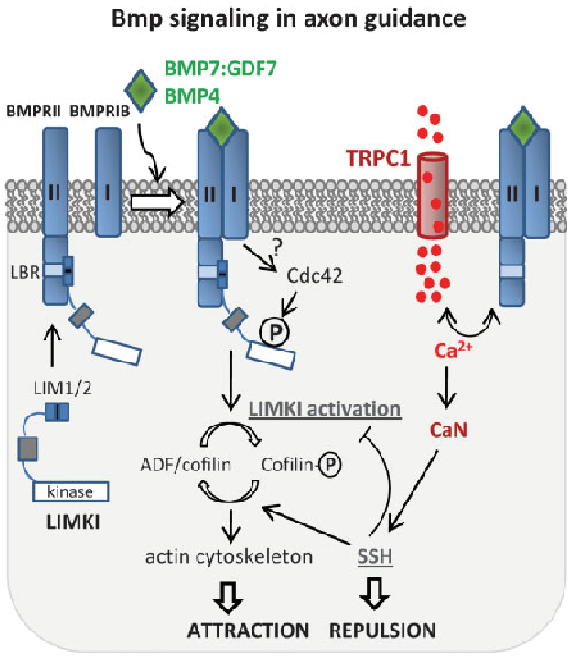

Figure 8. Schematic diagram of the Bmp signalling induced positive and negative responses in growth cones. Positive signal involves interaction of the BMPRII with the LIM1/2 domain of LIM kinase 1 (LIMK1) and inhibits its activity. Ligand binding to the receptor relieves this inhibitory interaction and activates Rho GTPase, Cdc42 and LIMK1. Repulsive response to BMP involves the interaction of TRPC1 with BMPRII, and calcium signalling through calcineurin (CaN) phosphatase for SSH activation. Both pathways converge in the regulation of ADF/cofilin: LIMK1 regulates actin cytoskeleton through phophorylation and inactivation of ADF/cofilin, whereas SSH activates ADF/cofilin by dephosphorylation. (Adapted from Sanchez-Camacho and Bovolenta, 2009)

In 2008 and in 2010, two different studies (Ng J. 2008; Yi J.J. et al 2010) reported other cases of transcriptional-independent signaling, demonstrating that TGF-β signaling specifies axons through distinct Smad-independent mechanism. Yi and colleagues (Yi J.J. et al 2010) demonstrated that the TGF-β-dependent axon specification in brain, is mediated by site-specific phosphorylation of Par6, that recruits the ubiquitin ligase Smurf1, which in turn promotes the proteasomal degradation of RhoA, a GTPase protein (Ozdamar et al. 2005). Axonogenesis in the visual system is particularly sensitive to the unregulated activity of the Rho GTPases. The Rho-dependent control of the actin cytoskeleton has been well characterized in fibroblasts and is now being investigated in neurons (Luo et al. 1997). Activation of myosin-II by Rho-

dependent kinases leads to actinomyosin contraction and growth cone retraction (Burridge and Chrzanowska-Wodnicka, 1996). In the model (Fig. 9) described by Yi and colleagues, the local levels of RhoA can be modified at the site of TGF-β signaling to alter the dynamic actin of axonal growth cones, a well-documented hallmark of axon specification that may account for their rapid outgrowth (Bradke and Dotti, 1999).

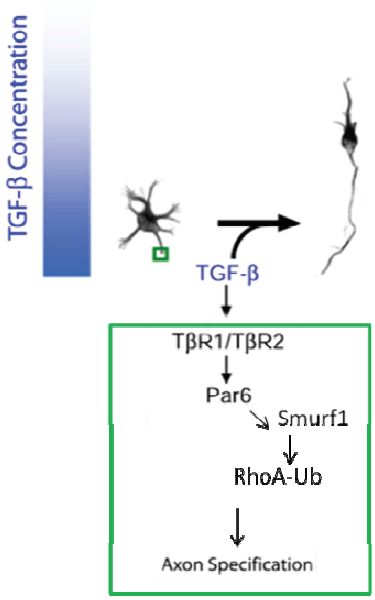

Figure 9. A model for TGF-b-dependent axon specification in developing neocortex. The TGF-β-dependent axon specification in brain, is mediated by site-specific phosphorylation of Par6, that recruits the ubiquitin ligase Smurf1, which in turn promotes the proteasomal degradation of RhoA, a GTPase protein. The local levels of RhoA can be modified at the site of TGF-β signaling to alter the dynamic actin of axonal growth cones, that may account for their rapid outgrowth. (Adapted from Yi et al. 2010).

Using this example, it is possible to hypothesize that cytoskeletal organization could derive not only from biochemical regulation of protein activation/inactivation, but also from activation of local protein synthesis and degradation within the growth cone. Several aspects of growth cone navigation, including the mechanisms by which external signals are transduced within the growth cone, might be regulated by rapid and local changes in protein levels. In Xenopus retinal axons, netrin-1-induced growth cone turning can be blocked

with specific translation inhibitors and proteasomal inhibitors (Campbell and Holt, 2001). EphB-induced collapse, however, does not depend on protein synthesis, but can be blocked with inhibitors of the proteasomal pathway which also inhibit EphB internalization into retinal growth cones (Mann et al. 2003).

The identification of messenger RNAs (mRNAs) present in the axons and growth cone allowed to understand the nature of the proteins involved in mediating growth cone steering.

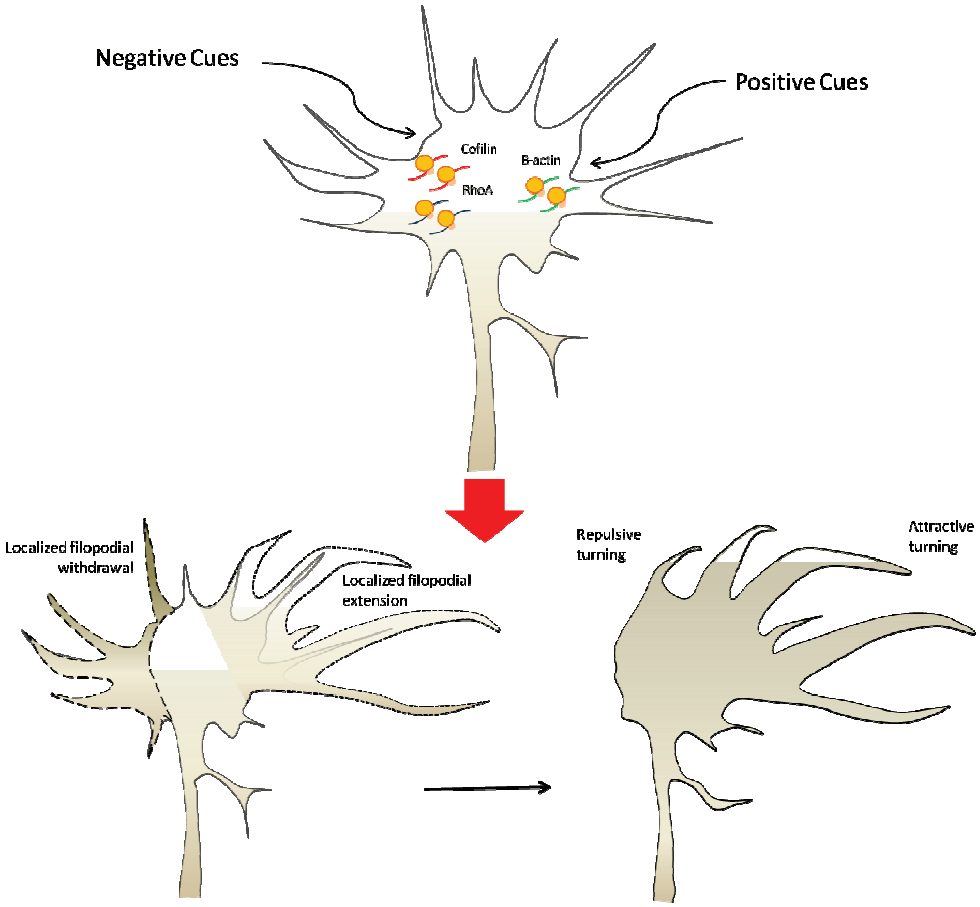

Figure 10. Growth cone turning regulated by differential mRNA translation. Gradients of protein synthesis-inducing guidance cues commonly activate translational activity on the side of the growth cone nearest to the gradient. However, the specific mRNA translated in response to the cue differs depending on whether it is an attractive or repulsive cue and determines the direction of growth cone turning. Stimulation by attractive cues leads to asymmetric synthesis of β-actin on the side near to the source of the gradient. Spatially restricted synthesis of β-actin may lead to actin polymerization, cytoskeletal assembly and attractive turning of the growth cone. By contrast, repulsive cues activate the axonal translation of the actin-depolymerizing proteins RhoA and cofilin when uniformly applied in cell culture. A proposed model is shown, in which localized cytoskeletal disassembly may result in repulsive turning through polarized filopodial collapse.

Cues induce rapid translation of cytoskeletal proteins or regulator based on whether they are attractive or repulsive: proteins induced by attractive cues build up the cytoskeleton, whereas proteins induced by repulsive cues break it down. Attractive cues such as Netrin-1 and BDNF induce b-Actin synthesis, in particular this occurs asymmetrically in response to a gradient of netrin-1 or BDNF (Yao et al, 2006). On the other hand, repulsive cues such as Slit2b and Sema3A induce local synthesis of actin depolymerising molecules such as Cofilin and RhoA (Fig. 10).

Accumulating evidence shows that local protein synthesis (PS) activation in axons and growth cones is also achieved by activation of translation initation factors via mitogen-activated protein kinase (MAPK) and mammalian target of rapamycin (mTOR) which activates translational initiation by phosphorylating its two major substrates 4E-BP1 and S6K (Campbell and Holt, 2001, 2003). Eukaryotic initiation factor 4E (eIF-4E) binds the 5' cap of mRNAs and is the rate-limiting factor for cap-dependent translation. Hypophosphorylated eIF-4Ebinding protein (eIF-4EBP) sequesters eIF-4E, preventing the recruitment of the rest of the translation initiation complex, while phosphorylation of eIF-4EBP releases eIF-4E, thus activating translation (Gebauer and Hentze, 2004). The axon guidance cues induce phosphorylation of eIF-4EBP via MAPK and mTOR pathway and activate eIF-4E by direct phosphorylation via MAPK and Mnk-1 (Campbell and Holt, 2003; Piper et al, 2006). The activation of MAPK pathway is also responsible for mTOR regulation. In fact mTOR activity is positively regulated by a GTP-bound form of RHEB GTPase, which is inactivated by its GTPase-activating proteins TSC1 and TSC2 . Since TSC1 and TSC2 are negatively regulated by AKT and ERK1/2, the guidance cue cascade activate

mTOR pathway also through the mitogen-activated protein kinase (MAPK)–TSC2–RHEB–mTOR pathway by activating MAPK ERK1/2 (Fig.11).

This raises the interesting possibility that cues-induced translational activity in growth cones could be regulated through spatial and temporal integration of diverse receptor-mediated signalling cascades converging on the activation of cap-dependent mRNA translation mediated by the mTOR pathway (see Lin and Holt 2007; Lin and Holt 2008; Jung et al. 2011;Jung et al. 2012, for review).

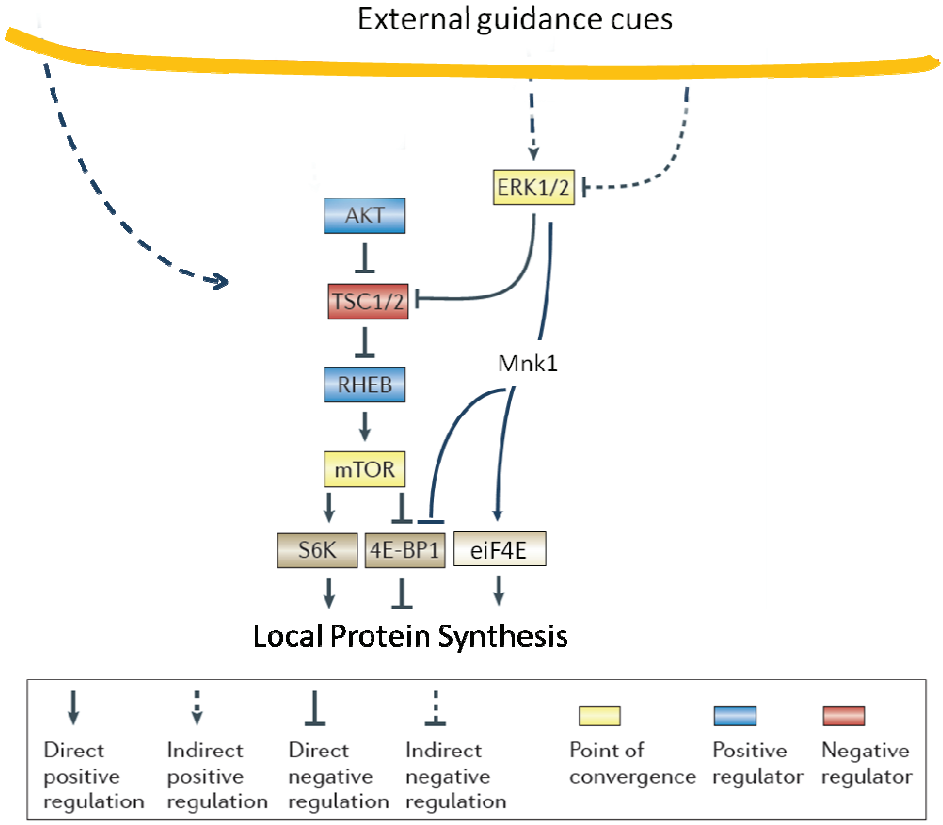

Figure 11. Regulation of global translational activity through MAPK signaling and mTOR pathway. Local protein synthesis (PS) activation in axons and growth cones is achieved by activation of translation initation factors via mitogen-activated protein kinase (MAPK) and mammalian target of rapamycin (mTOR), which regulates cap-dependent mRNA translation by phosphorylating its two major targets: eukaryotic translation initiation factor 4E (eIF4E)-binding protein 1 (4E-BP1) and ribosomal protein S6 kinase (S6K). Eukaryotic initiation factor 4E (eIF-4E) binds the 5' cap of mRNAs and is the rate-limiting factor for cap-dependent translation. Phosphorylation of eIF-4EBP releases eIF-4E, thus activating translation. The axon guidance cues induce phosphorylation of eIF-4EBP via MAPK and mTOR pathway and activate eIF-4E by direct phosphorylation via MAPK and Mnk-1. The activation of MAPK pathway is also responsible for mTOR activity increase through the inhibition of the mTOR negative regulators tuberous sclerosis protein 1 (TSC1) and TSC2. Some cues can inhibit protein synthesis by inhibiting ERK1/2 leading to TSC1/2 activation and mTOR inhibition. Spatiotemporal summation of cue-induced signals converging on mTOR might lead to asymmetric translational activity (Adapted from Jung et al. 2012).

1.5 MicroRNAs

MicroRNAs (miRNAs) are short non-coding RNAs that are viewed as fundamental regulators of cell function (Bartel, 2009;Carthew et al. 2009). MiRNAs are approximately 20–25 nucleotides (nt) long and are generated from double stranded RNA precursors. First discovered in *C. elegans*, (Lee at al. 1993; Wightman et al 1991, 1993), miRNAs are present in both plants and animals and constitute an essential component of gene regulation (Lee at al. 2001; Lau et al.2001; Lagos-Quintana et al.2001; Pasquinelli et al.2000). As summarized in figure 12, miRNAs are transcribed in the nucleus, either independently or as part of introns of protein coding genes (Newman et al 2010; Siomi et al 2010). Genes of functionally related miRNAs are often clustered on the same chromosome, and expressed as a single primary transcript (pri-miRNA). These transcript are generated mainly by RNA polymerase II (Lee et al. 2008). Similar to other Pol II transcripts, pri-miRNAs possess a 5' cap and a 3' poly-A-tail (Cai et al. 2004). Within the primary transcripts, miRNAs form stem-loop structures, which contain the mature miRNA as part of an imperfectly paired double stranded stem connected by a short terminal loop. In the canonical miRNA biogenesis pathway, these structures are recognised by the microprocessor complex, a multiprotein complex with two core components, Drosha and *Di George Syndrome critical region gene 8* (DGCR8). The double-stranded RNA binding protein DGCR8 binds to the base of the stem loop structure and thereby guides the positioning of the RNase III enzyme Drosha, which constitutes the catalytic center of the complex (Han et al.2006). Drosha cleaves the double-stranded stem about 11 bases from the base and generates a two nucleotide (nt) overhang at the 3' end (Gregory et al 2004, Han et al.

2006). This cleavage reaction liberates a hairpin-shaped RNA molecule of 70–100 bases called miRNA precursor or pre-miRNA.

The pre-miRNAs are specifically recognised by the nuclear export receptor Exportin 5 and exported in a Ran-GTP dependent manner (Lund et al. 2004; Yi et al. 2003; Bohnsack et al. 2004). In the cytosol, the pre-miRNA is further processed by the RNase III enzyme Dicer (Grishok et al. 2001). This enzyme binds the 3' overhang of the pre-miRNA with its PAZ domain and thereby positions the substrate correctly for the cleavage by the two catalytic domains 22 bases upstream within the double stranded stem (Macrae et al. 2006; Zhang et al. 2004). The result of Dicer cleavage is a double stranded RNA of 22 bases in length. One of the strands (the mature miRNA) strand interacts with a member of the Ago protein family to form a miRNA-induced silencing complex (miRISC), whereas the other strand (the star (*)-strand) is degraded or also loaded in another miRISC. In mammals, the strand selection and RISC assembly is accomplished by a complex that contains Dicer, Ago and the double stranded RNA binding protein TRBP (Chendrimada et al. 2005; Haase et al. 2005; Gregory et al.2005). Statistical analyses have discovered that generally the strand with the less stable base pairing at the 5' end is chosen as guide strand (Khvorova et al. 2003; Schwarz et al. 2003). Core components of the miRISC include proteins of the argonaute (AGO) family that directly bind the miRNA and GW182 family proteins which mediate translational repression and mRNA decay. The miRNA guides the complex to partially complementary target mRNAs. Most of the target sites are located within the 3' untranslated region (UTR) of mRNAs. However, functional miRNA binding sites in the 5' UTR as well as in the open reading frame have also been reported (Orom et al. 2008; Tay et al. 2008). Nucleotides 2–8 of the miRNA are particularly important for

pairing with the target mRNA. This sequence motif is referred to as the miRNA seed sequence (Bartel, 2009). Depending on the recognition site, binding of miRISC to the cognate target can have different outcomes (Pillai et al. 2007). In the majority of cases the binding is partially complementary to the target sites and leads to repression of translation or degradation of the target transcript (see for a review Krol et al. 2010a). This degradation process involves the recruitment of deadenylase complexes such as the CCR4-NOT complex to the mRNA to remove or shorten the poly(A) tail. Poly(A) tail shortening induces the removal of the 5' cap of the mRNA, a process referred to as de-capping. Uncapped mRNAs are rapidly removed from the cell by 5' to 3' exoribonucleases such as Xrn1 (Huntzinger et al. 2011).

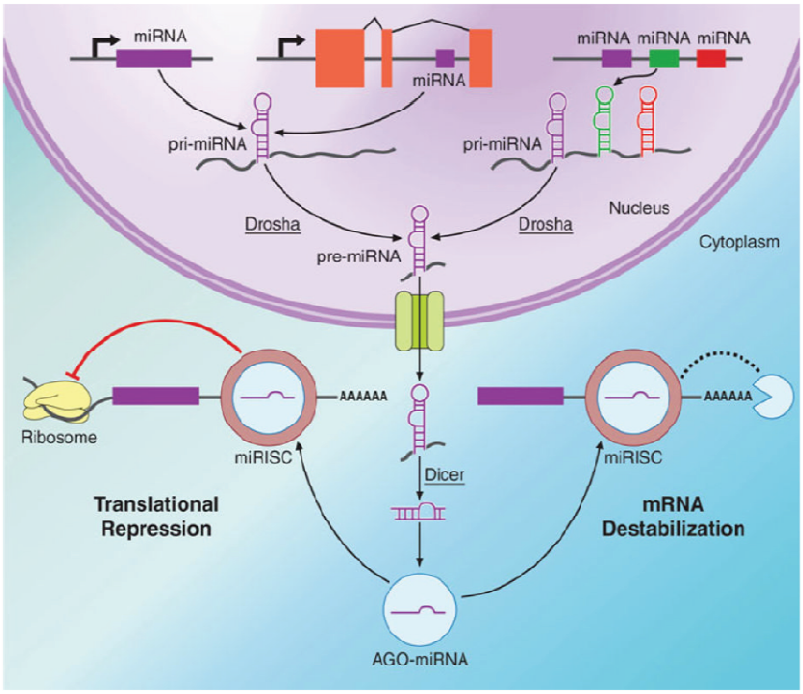

Figure 12. miRNA biogenesis and mechanism of action. miRNAs are transcribed in the nucleus, either independently or as introns of protein coding genes, by RNA Polymerase II. miRNA primary transcripts (pri-miRNAs) fold into hairpin structures, which are recognized by the nuclear microprocessor complex and cleaved by the RNAse III-type enzyme Drosha, generating ~70 nt precursor miRNAs (pre-miRNAs). PremiRNAs are exported to the cytoplasm by exportin-5 and further processed into ~22 nt double-stranded RNAs. One strand is selected and bound by AGO family proteins, then assembled into the RISC, a large ribonucleoprotein effector complex. Imperfect base pairing between the miRNA and target mRNAs recruits the miRISC to target transcripts where it represses their expression either by repressing translation, or enhancing the mRNA decay (Sundermeier and Palczewski 2012)

miRNA-guided regulation of gene expression has been implicated in every cellular pathway. Each cell type expresses a specific subset of miRNAs to ensure that cell type-specific mRNA profiles are established and maintained. For example, expression of a neuron-specific miRNA in non-neuronal cells results in shifting the global gene expression program towards transcript profiles typically found in neurons (Lim et al.2005). miRNAs may be acting in both neuronal remodeling and maintenance of neuronal connections and their roles may be due to the spatial temporal specificity of their expression. Among the multiple classes of sequence-specific RNA regulatory mechanism that contribute in the control of maturation and plasticity in neurons, the role of microRNAs in shaping the neuronal landscape has only begun to be explored.

The knowledge about individual miRNA functions was initially obtained by studying miRNA expression profiles in the nervous system (Wienholds et al. 2005). Experiments using both loss and gain of function have been very informative in the role that miRNAs play at the level of individual neurons and neuronal cell biology, giving us information about the importance of their spatial and temporal control (e.g. Giraldez et al., 2005; Leaman et al., 2005; Krutzfeldt et al., 2005; Lanford et al., 2010). The possible contribution of miRNAs to neuron plasticity can be schematically summarized dividing them into two major category, as depicted in Fig. 13.

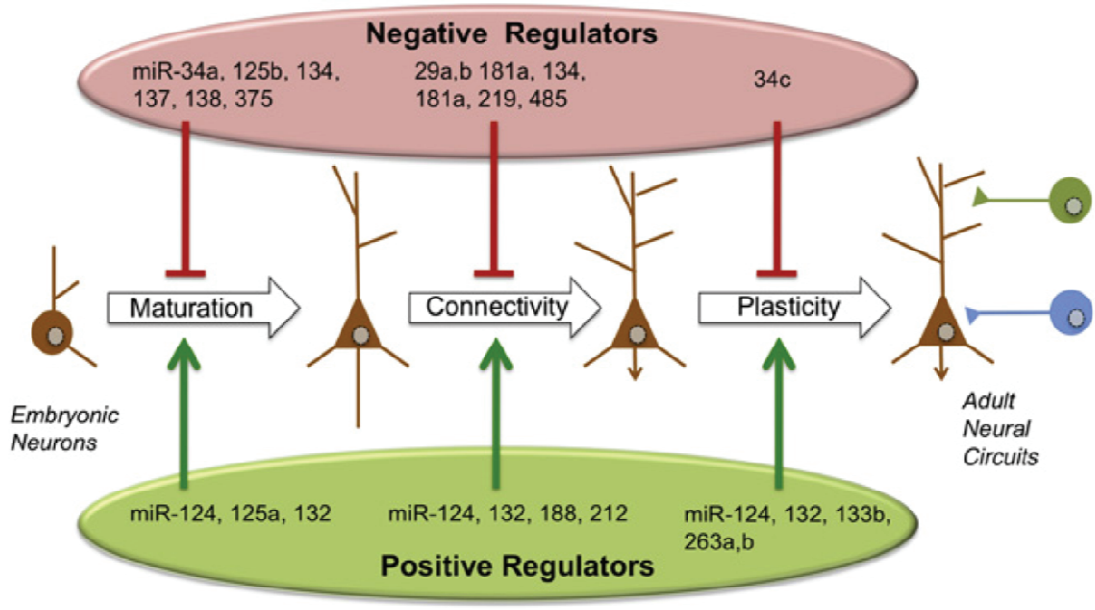

Figure 13. miRNA Involved in Various Aspects of Synaptic Development and Function. Late stages of neuronal differentiation from process formation, axon and dendrite extension, to the developmental and continued plasticity required to form higher-order circuits. Several miRNA have been shown to regulate these steps of neuronal and circuit formation or function as either negative regulators , higher part of the panel, or positive regulators, bottom part of the panel (McNeill and Van Vactor, 2012).

miRNAs can act as both negative and positive regulators of neurite growth depending on their levels and balance, for this reason they are considered as fine-tuners of neurite effector gene networks for the regulation of plasticity.

miRNAs that act as negative regulator of dendritic spine development and synaptic connection:

The miR-138, highly enriched in the brain dendrites, targets *APT1* (*acyl protein thioesterase 1*), negatively regulating the size of dendritic spines in rat hippocampal neurons (Siegel et al., 2009). miR-34a negatively regulates both dendritic outgrowth and synaptic function, possibly via targeting the synaptic components synaptotagmin-1 and syntaxin-1 (Agostini et al., 2011a, 2011b) and miR-375 antagonizes BDNF to inhibit dendritic growth (Abdelmohsen et al., 2010).

Some miRNAs play different roles at different developmental stages. For example, the brain-enriched miR-137 has an early role in neural differentiation targeting *CDK6* (Silber et al., 2008). However, it also controls later processes of neuronal plasticity, as it was found to play a key role in adult neurogenesis (Szulwach et al., 2010), neuronal maturation (Smrt et al., 2010) and dendritic spine growth in which it elicits changes in synapse morphogenesis largely through regulation of the ubiquitin ligase Mind Bomb-1 (Smrt et al., 2010). Also neurotransmitter pathways were examined such as dopamine signaling, which was shown to increase the expression of miR-181a in primary neurons. Overexpression and knockdown of miR-181a in primary neurons demonstrated that miR-181a is a negative posttranscriptional regulator of GluA2 surface expression, spine formation, and mEPSC frequency in hippocampal neuron cultures, establishing a key role for miR-181 in response to neurotransmitters at the synapse (Saba et al., 2012).

miR-134 was identified in hippocampal neurons as a dendritically localized miRNA, and it functions to negatively regulate the size of dendritic spines through the inhibition of LimK1, one of the regulator of actin dynamics already mentioned in the previous chapters. This negative regulation was demonstrated in hippocampal neurons in vitro (Schratt et al., 2006) and in Xenopus spinal neurons in vivo (Han et al. 2011).

miRNAs that act as positive regulator of dendritic spine development and synaptic connection:

Even if the cases of miRNAs with negative impact on synapse regulation are the majority of the reported cases in literature, there are also reported cases of miRNAs that act as positive regulator of dendritic spine development and synaptic connection, such as miR-124, miR-125, miR-132, miR-188, miR-212

and miR-263 (Rajasethupathy et al. 2009; Edbauer et al., 2010; Muddashetty et al., 2011; Magill et al. 20120; Lee et al. 2012; Im et al. 2010; Hollander et al. 2010; Yang et al. 2008). Among them, an example of positive regulation of dendritic spine development is observed in the case of miR-125b, whose overexpression results in longer, thinner processes of hippocampal neurons. Fragile X mental retardation protein (FMRP) knockdown is shown to ameliorate the effect of overexpressed miR-125b on spine morphology. It has been proposed that miR-125b negatively regulates its target NR2A, along with FMRP and AGO1 (Edbauer et al., 2010). Recently, a mechanism was proposed whereby FMRP phosphorylation provides a reversible switch in which AGO2 and miR-125 form an inhibitory complex on PSD-95 mRNA, thus turning off mGluR signaling. However, dephosphorylation of FMRP and subsequent release of Ago2 activates mGluR signaling (Muddashetty et al., 2011). This switching mechanism could provide the means for temporal and spatial control of translation.

These and other observations imply that there are multiple layers of complexity in the regulatory logic of miRNAs in dendritic morphogenesis (see for a review McNeill and Van Vactor, 2012).

Signaling pathways are highly interconnected, and the flow of information they carry is controlled by many feedback loops. This renders their functionality more similar to a network rather than to a linear cascade. In these networks, miRNAs are crucial elements of regulative loops. The miRNAs can act as signaling amplifiers: regulating inhibitors of a signaling cascade they impact on signal strength or duration, or empowering cell responsiveness to otherwise sub-threshold stimuli. A miRNA could simultaneously target distinct branches of a signaling cascade/network, or could impart specificity to the signaling flow by

channelling it towards specific branches. Different miRNAs, such as miR-126, miR-21 and miR-26a, are reported to target both positive or negative regulators of the two pleiotropic pathways RAS-RAF-MAPK and PI3K-AKT cascade (Fish et al. 2008; Kuhnert et al. 2008; Meng et al. 2007; Thum et al. 2008; Huse et al. 2009). The involvement of miRNAs in feed-forward and feed-back motifs makes them important elements in the understanding of signaling pathways properties in the coordination of tissue induction, growth and morphogenesis (see for review Inui, Martello and Piccolo 2010; Inui, Montagner and Piccolo 2012).

Another issue that increases the complexity of this crosstalk between growth factor signaling and miRNAs, is the identification of an emerging group of proteins that can modulate pri-miRNA processing by the microprocessor complex in response to diverse stimuli. For example, activation of Smad proteins by stimulation of cells with bone morphogenic protein (BMP) or tumour growth factor β (TGF-β) can stimulate the maturation of specific miRNAs. This activity is Co-Smad4-independent and leads to increased recruitment of the pri-miRNAs to the microprocessor complex, enabling a more efficient cleavage by Drosha (Davis et al. 2008) (Fig.14).

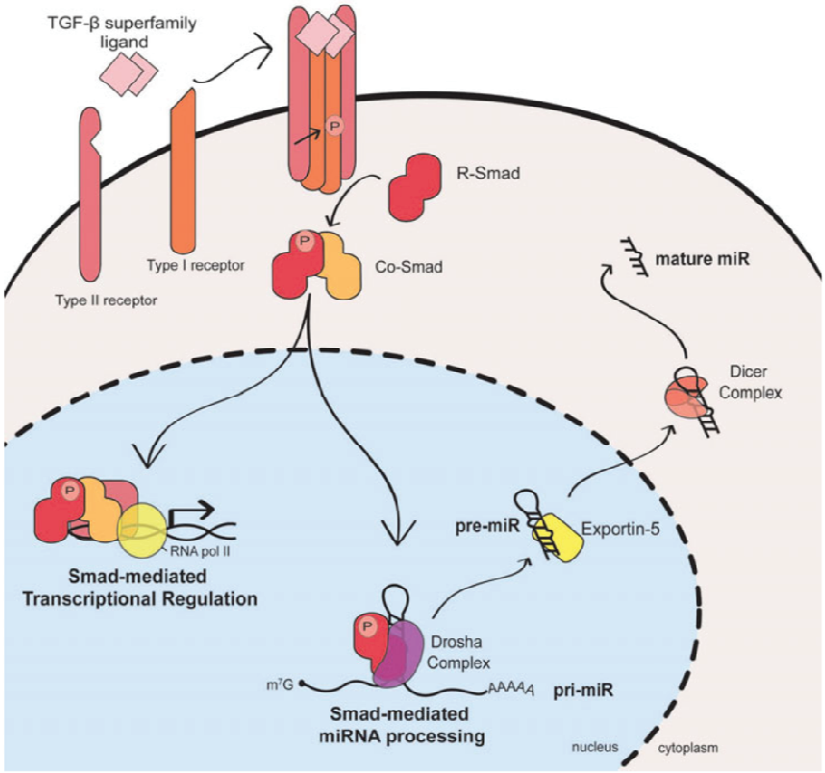

Figure 14. Regulation of miRNA maturation by TGF-β superfamily signaling. TGF-β and BMP signaling stimulates the production of pre-miRNAs by promoting the Drosha-mediated processing by controlling nuclear localization of R-Smad proteins. Thus, Smads regulate gene expression in two distinct manners; a) transcriptional regulation by DNA binding, and b) regulation of miRNA maturation by associating with the Drosha/DGCR8 complex. (Hata and Davis, 2010).

Both negative and positive regulation of synaptic development and remodeling by miRNAs highlight the recurring topic of miRNA dysregulation in neuronal disease. miRNAs are very applicable and exciting tools to better understand neurological diseases and their treatment (Ceman and Saugstad, 2011; Bian and Sun, 2011). Given their importance in neuropathology, several strategies to manipulate miRNA activity and expression are being pursued as therapeutic models.

1.6 MicroRNAs in the eye

Congruent with the complexity of visual system structure and physiology, miRNA expression analyses have revealed a remarkable diversity of miRNAs in

the vertebrate retina (Karali et al. 2007, 2010; Hackler et al. 2010; Krol et al. 2010b; Xu et al. 2007; Wang et al. 2010; Ryan et al. 2006).

miRNA transcriptome analyses provided the first clues about the importance of miRNA gene regulation in the retina. About 80 different miRNAs were initially identified in adult mouse retina by microarray, 23 of which were preferentially expressed in retina as compared to other tissues (Xu et al. 2007; Loscher et al. 2007; Karali et al. 2010).

Subsequently Karali et colleague in Banfi's lab present the first analisys of miRNA expression in ocular tissues, using both microarray and RNA in situ hybridization (ISH) procedures. Using a microarray approach, they determined the expression profiles of miRNAs in the retina, lens, cornea and retinal pigment epithelium of the adult mouse eye. Each tissue had notably distinct miRNA enrichment patterns and cluster analysis identified groups of miRNAs that showed predominant expression in specific ocular tissues or combinations of them. They also performed RNA in situ hybridization (ISH) for over 220 miRNAs, including those showing the highest expression levels by microarray, and generated a high-resolution expression atlas of miRNAs in the developing and adult wild-type mouse eye, which is accessible in the form of a publicly available web database. (Karali et al. 2010).

Studying retinal pathologies in animal models allowed the identification of miRNAs putatively involved in disease progression, and recent findings also suggest that miRNAs will be useful targets for the prevention or treatment of retinal degenerative disorders. miRNAs have been shown to promote the survival of both rod and cone photoreceptors (e.g. Zhu et al. 2011; Sanuki et al. 2011), a crucial finding as photoreceptor cell death is the primary cause of blindness in retinal degenerative diseases. These results make miRNAs and the

pathways they control attractive targets for the design of therapeutics to prevent or ameliorate various retinal degenerative disorders (Zhu et al. 2011) .

Constitutive disruption of the pre-miRNA processing enzyme Dicer leads to early death in embryonic development in mice (Bernstein et al. 2003) However, conditional knockout (CKO) of *Dicer* has become the most common technique used to assess the phenotypic consequences of miRNA gene regulation loss in selected tissues.

Effects on eye development of global perturbation of miRNA activity:

Conditional *Dicer* knockout has revealed roles for miRNAs both in retinal development and in the physiology and survival of mature retinal neurons (Damiani et al. 2008; Georgi et al. 2010; Iida et al. 2011; Pinter et al. 2010).

Recently, four different retinal Dicer CKO mouse models suggested that miRNAs play diverse roles in the development and physiology of the mammalian retina. *Dicer* CKO driven by the *Chx10*-cre transgene led to decreased electroretinogram (ERG) responses, morphological anomalies, and progressive retinal degeneration (Damiani et al. 2008). *Pax-6*cre-driven Dicer CKO resulted in abnormal differentiation of retinal cell types (Georgi et al. 2010), and *Dkk3*-cre or *Rx*-cre driven Dicer deletion led to widespread apoptosis of retinal progenitors (Iida et al. 2011; Pinter et al. 2010), a phenotype consistent with the effect of Dicer disruption in Xenopus (Decembrini et al. 2008).

Effects on eye development of perturbation of specific miRNAs:

Genetic loss-of-function studies are beginning to disclose the physiological roles of specific miRNAs or miRNA clusters in the vertebrate retina. Studies

performed in frogs, fish, and mice are beginning to identify the phenotypic and molecular consequences of specific miRNAs loss-of-functions.

Walker and Harland in 2009 reported that inhibition of miR-24a in Xenopus resulted in increased apoptosis of retinal precursors, leading to reductions in eye size. They demonstrated that miR-24a targets the pro-apoptotic factors *caspase-9* and *apoptosis protease-activating factor 1* (*apaf1*), important for the survival of neuroretinal progenitors (Walker and Harland, 2009).

Decembrini and colleagues hypothesized that miRNAs exhibiting differential expression during retinal patterning might play a role in regulating the cell fate and differentiation of retinal cell types. They demonstrated that simultaneous inhibition of a set of miRNAs (miRs -129, -155, -214, and -222) expressed early in Xenopus retinal development could, through de-repression of the homeobox genes *otx2*, and *vsx1*, promote differentiation of additional retinal bipolar cells, a late-developing retinal cell type.

Zhu et al, recently evaluated the role of the miR-183/96/182 cluster in rods. These three miRNAs are enriched in rod and cone photoreceptors, exhibit similar seed region sequences and are predicted to share common mRNA targets. Prior to this work, functional redundancy of the three miRNAs was hypothesized based on results obtained in Zebrafish. Morpholino-induced knockdown of all three miRNAs produced auditory system morphological defects that were more severe than those resulting from knockdown of miR-96 alone, or miR-182 and -183 together (Li et al. 2010). To analyse the cluster function in the retina, a miR-183 cluster sponge transgenic mouse model was developed. When the visual system of transgenic mice was stressed with intense light, they documented a dramatically increased sensitivity to light-

induced retinal degeneration causing the death of ~80 % of rods in the superior retina, due to the loss of miRNAs-cluster action on Casp2 (Zhu et al. 2011)

Using the Medakafish (*Oryzias latipes*) as a model system, Conte and colleagues, recently demonstrated that loss of miR-204 function resulted in an eye phenotype characterized by microphthalmia, abnormal lens formation, and altered dorsoventral (D-V) patterning of the retina, which is associated with optic fissure coloboma. These phonotypes were in part due to the abnormally elevated levels of the transcription factor Meis2, identified as one of the main targets of miR-204 function (Conte et al. 2010a).

As for the miR-204, another example of how a specific miRNA can regulate multiple events in eye formation is miR-124. Down regulation of this miRNA in mice cause specific apoptosis of newly differentiated cone photoreceptors and pronounced defects in the CNS. This cone cell death was partially rescues reducing the levels of a miR-124 target gene, Lhx2, a homeobox transcription factor required for eye development (Sanuki et al. 2011). More recently Baudet et al, in Holt lab, demonstrated that loss of miR-124 delayed the onset of Sema3A sensitivity and concomitant neuropilin-1 (NRP1) receptor expression and caused cell-autonomous pathfinding errors of RGC axons. CoREST, a cofactor of a NRP1 repressor, was newly identified as a miR-124 target, whose dysregulation cause the delay in RGC growth cone responsiveness. This study demonstrates miR-124 is important in regulating the intrinsic temporal changes in RGC growth cone sensitivity and suggest that miRNAs may act broadly as linear timers in vertebrate neuronal development. Moreover this represented the first report of a robust RGC axonal phenotype due to a knockdown of a single miRNA (Baudet et al. 2012).

1.7 *Oryzias latipes* as a model system to study developmental defects

Studies of individual microRNAs function is challenging for several reasons: first, microRNAs are frequently present as families of apparently redundant members that share the same seed region in which case it would be necessary to eliminate all the loci in order to dissect their global function; second, each miRNAs has numerous putative targets that have disparate functions, prediction based only on seed sequence compatibility may not be able to establish *a priori* which transcript is most meaningful and thus worthy of experimental validation; third, the degree of target down-regulation tends to be quantitatively modest, leading to a maximum of decrease of 50% of a target protein levels. This require time and high costs in mammalian species, such as mouse, whereas in a simpler vertebrate species, *Oryzias latipes* (Medakafish), it is possible to perform gain and loss of function studies in a easier way to identify the function of an individual microRNA, as already demonstrated in recent work published in Banfi's lab (Conte et al. 2010a).

Medakafish is a particularly amenable model system for this kind of analysis since its use is less time and resource consuming, as compared with mammalian systems and mouse in particular (Ishikawa, 2000). Physiology, embryology and genetics of Medakafish have been widely studied in the past 100 years. Already in 1913, the Medakafish was used to show Mendelian inheritance in vertebrates (Ishikawa, 1913; Toyama, 1916). Then, genetic studies on Medakafish, have been focused on the molecular basis of pigmentation and sex determination (Baroiler et al. 1999; Wada et al. 1998; Matsuda et al. 1998, Matsuda et al.1999, Yamamoto T. 1958). In the past few years, this model was a very useful tool to identify and/or characterize some important genes involved in the eye development (Fukada et al. 1995: Simeon

A. 1998, Zhou et al. 2000; Chaing et al.1996; Macdonald et al.1995; Ekker et al.1995; Mathers et al.2000; Conte and Bovolenta 2007; Kitambi et al. 2008; Ruiz et al. 2009; Conte et al. 2010a, 2010b; Alfano et al. 2010; Beccari et al. 2012).

In addition, the complete sequencing of its genome has greatly contributed to the use of this model to study various biological processes underlying the embryonic development. Different comparative studies among vertebrates have demonstrated a high conservation in terms of genomic sequences and molecular processes, also in model systems such as teleost (*Danio rerio* / Zebrafish and *Oryzias latipes* / Medakafish). Zebrafish and Medakafish are very close species: they separated from their last common ancestor about 110 million years ago. They are both ideal organisms for genetic studies as they display many advantages such as the simple use of different genetic engineering techniques. They have a short generation time (8-10 weeks for Zebrafish and 6-8 weeks for Medakafish). Moreover Zebrafish/Medakafish biology allows ready access to all developmental stages, and the optical clarity of embryos and larvae allow real-time imaging of developing pathologies.

In particular, unlike other teleost, Medakafish has several advantages. Medakafish is very hardy and tolerates a wide range of salinities and temperatures (10–40 ℃); it is easy to breed and hi ghly resistant to common fish diseases. For all the above-mentioned reasons, thus, Medakafish is easier to keep and maintain in aquaculture than Zebrafish and it is easier to handle. Early Medakafish development is slower than in Zebrafish: Zebrafish larvae hatch after 2–3 days, whereas Medakafish embryos are enclosed in a tough chorion that protects them in their natural habitat until they hatch as feeding young adults after 8 days. This slower development at the early phases allow to better

define and characterize developmental processes and defects. Both Zebrafish and Medakafish are considered an ideal model to study eye development (Wittbrodt et al., 2002). The eye development in Medakafish start at the end of gastrulation (stage 15, Fig. 15 B) with the determination of the eye field; in the late neurula stage (Stage 18, Fig. 15 C) the formation of the optic bud (rudimentary eye vesicle) occur; at stage 21 (Fig. 15 D) the optic vesicles differentiate to form the optic cups and the lenses begin to form; at stage 24 (Fig. 15 E) the spherical optic lenses are completed; at stage 28 the retina begins to differentiate and at stage 30 (Fig. 15 F) the plexiform layers start their differentiation, to lead finally, at stage 38 (Fig. 15 H) to an eye completely formed (Iwamatsu, 2004).

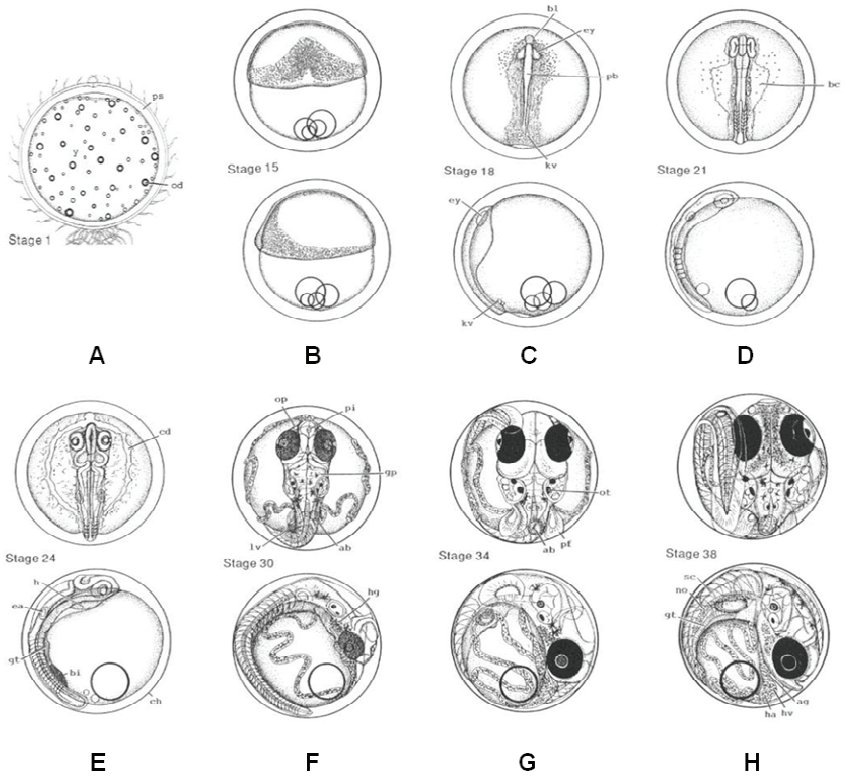

Figure15. Selected stages of Medakafish development. A) Stage 1, Fertilized eggs; B) Stage 15, Gastrula stage. C) Stage 18, Late neurula stage: eye vesicle formation; D) Stage 21, 6 somite stage: the optic vesicles differentiate to form the optic cups and the lenses begin to form. E) Stage 24, 16 somite stage: the neurocoele is formed in the fore-, mid- and hind-brains, the spherical optic lenses are completed. F) Stage 30, 35 somite stage: the retina start to differentiate. G) Stage 34. H) Stage 38 (8 days) Hatching stage.(Adapted from Iwamatsu, 2004).

From the experimental point of view, however, the two model systems are completely equivalent. In both systems, reverse-genetic analyses are also facilitated by assays of gene function using transient rather than stable misexpression, which is technically easier than in mice. Microinjection of early embryos with either mRNA or antisense morpholino oligonucleotides results in transient gene overexpression or knockdown, respectively (Wittbrodt et al., 2002).

The above reasons demonstrate that fish represent mainstream models in developmental biology. Their attributes have propelled the rise of fish as a model in developmental biology and human diseases research, allowing an enhanced understanding of the basic cell-biological processes that underlie the development and the disease phenotype of the specific genetic diseases (Lieschke and Currie, 2007; Wittbrodt et al., 2002).

AIM OF THE THESIS

My project attempted to elucidate the functional roles of microRNAs (miRNAs) in the regulatory networks necessary for the proper development of the vertebrate eye, by following these specific aims:

- Identification and characterization of miRNAs preferentially expressed in the developing vertebrate eye: a group of eye-enriched miRNAs of interest was chosen through the analysis of their sequence conservation and conserved expression profile to proceed with their functional characterization.

- Screening and functional analysis of the identified eye-enriched miRNAs by gain- and loss-of function studies using Medakafish (*Oryzias latipes*) as model system: Functional characterization was performed by manipulating the miRNAs activities in Medakafish embryos through loss- and gain-of-function screening obtained respectively by injections of morpholino (Kloosterman et al. 2007) and of miRIDIAN^{TM} Dharmacon microRNA Mimics. The possible eye developmental defects during the embryo development were analyzed by morphological inspection and detection of modification in the expression of eye developmental markers by RNA in situ hybridization analysis, qRT-PCR, immunohistochemistry and Western Blot experiments.

- Identification and functional characterization of mRNA targets for the selected eye-enriched miRNAs: the list of the predicted target genes for the miRNAs of interest, was analysed and, among them, I selected, based on previous expression and literature data, those targets that were more likely to play a part

in the genesis of the observed phenotype. Once confirmed their expression level variation in the in vivo model, by qRT-PCR and Western Blot, I proceeded with the experimental validation (Luciferase assay) needed to demonstrate the direct binding of the selected miRNA to the 3'UTR of the putative target gene. Finally, a possible phenotype rescue (morphological and/or molecular) was sought to demonstrate the functional role of the identified mRNA target in the genesis of the observed eye phenotype.

This project allowed me to gain insight into the role of miRNAs in retinal and ocular development and functions, ultimately leading to the enrichment of our understanding of retinal and ocular biology, but also of miRNA-related molecular bases of retinal and ocular diseases.

2. MATERIALS AND METHODS

2.1 Medakafish Stocks

Wild type Oryzias latipes of the cab strain were maintained in an in-house facility in a constant re-circulating system at 28°C on a 14 hours light/10 hours dark cycle. Embryos were staged according to Iwamatsu 2004 (Iwamatsu, 2004).

2.2 Morpholinos (MO), mRNAs and Mimic injections

To inhibit miR-181a and miR-181b functions, specific morpholinos (MO) (Gene Tools) were designed on the two different miR-181a/b mature sequence as follow:

Mo-miR-181a AACTCACCGACAGCGTTGAATGTTC (25b)

Mo-miR-181b AACCCACCGACAGCAATGAATGTTG (25b)

The following MOs containing five mismatches (mm-MO) with respect to the MO-miR-181a and Mo-miR-181b sequences were used as control (mismatches are in red):

mm-Mo-miR-181a AAGTCAGCGACACCGTTCAATCTTC (25b)

mm-Mo-miR-181b AAGCCACGGACACCAATCAATCTTG (25b)

MOs were injected in a range of concentrations (0,03 - 0,12 mM). Their efficiency was measured as the ability of interfering with eGFP expression using a reporter construct. The pCS2/miR-181a-GFP and pCS2/miR-181b-GFP

reporter plasmids were constructed cloning the complementary region of the MOs in the eGFP 5'UTR sequence. The PCR products for the miR-181a and miR-181b sequences were obtained with BamHI/ClaI tagged primers (miR181a/Fc 5'- GATCGAACATTCAACGCTGTCGGTGAGTT -3', miR181a/Rc 5'- TAGCAACTCACCGACAGCGTTGAATGTTC -3'; and miR181b/Fc 5'- GATC AACATTCATTGCTGTCGGTGGGTT -3', miR181b/Rc 5'- TAGCAACCCACCGACAGCAATGAATGTT -3'). The digested PCR product was inserted in the pCS2+ vector eGFP mRNA and RFP mRNA were cloned and transcribed out of pCS2+ vector using the SP6 mMessage mMachine kit (Ambion) according to manufacturer instructions. The synthesized mRNAs were quantified and re-suspended in 1x Yamamoto Ringer (Yamamoto and Yamagami, 1975). MOs were individually co-injected with the different eGFP mRNAs (25 ng/µL) and RFP mRNA (25 ng/µL).

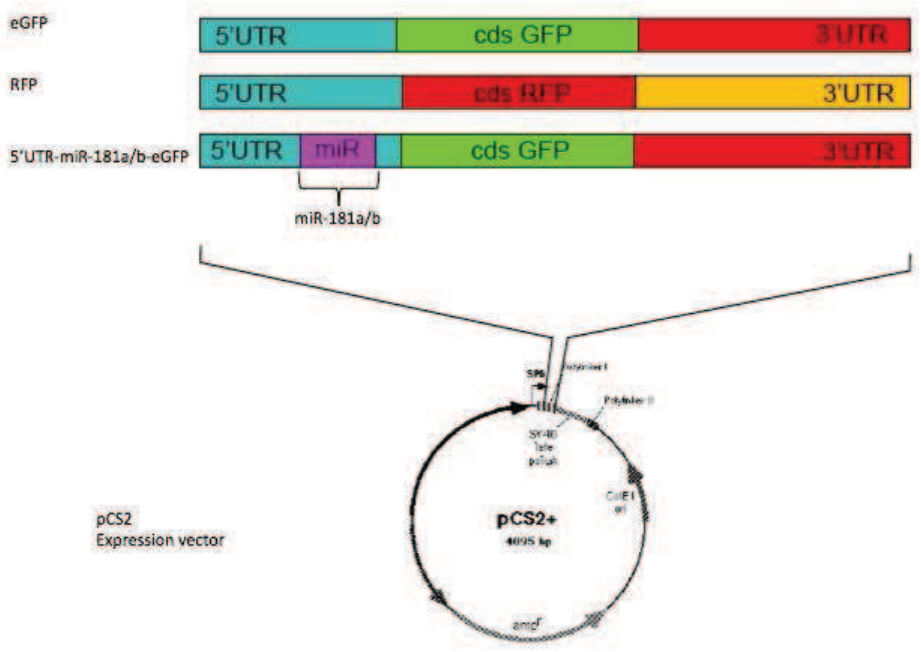

Figure 16. Schematic representation of the cloning strategy used to obtain the GFP control constructs. In the pCS2+ expressing vector were inserted the eGFP coding sequence of the RFP coding sequence, whose transcripts were injected as positive controls. For the contructs used to test the morpholino efficacy and specifity, the mature sequence of miR-181a or miR-181b was inserted in the 5'UTR region of the eGFP sequence.

The inhibitory efficiency of each MO was measured by quantification of the green/red fluorescence ratio (eGFP/RFP) intensity using Photoshop CS3 software (Adobe) to measure average pixel intensity of RFP and eGFP, as previously reported (Conte et al., 2010b; Esteve et al., 2004). Selected MO working concentrations was 0,03 mM for Mo-miR-181a and 0,03 mM for Mo-miR-181b. Control embryos were always co-injected with either eGFP mRNA or mmMOs to follow the efficiency of the injections as well as for testing possible defects associated with the injection procedures. Activation of p53 is an occasional off-targeting effect of MO injections (Robu et al., 2007), and can be counteracted by injection of a p53 Mo (Eisen and Smith, 2008). Thus possible non-specific effects of MOs were ruled out by coinjecting it with a Mo designed against Medakafish p53 (p53MO) (Conte et al., 2010b).

All the injection solutions included 25 ng/µL of eGFP mRNA as a lineage tracer. To inhibit both miR-181a/b the two morpholinos were co-injected into one blastomere of the embryos at the one-two cell stage and the optimal MOs total concentration (0.12 mM mo-miR-181a +0.12mM mo-miR-181b) were determined on the basis of morphological criteria. For the overexpression experiments miRIDIAN (Dharmacon) miRNA Mimics for miR-181 were injected. Different concentration from 0.5 µM to 2 µM were tested, and the final concentration was determined on morphological criteria. At both 1 µM and 2 µM the embryos showed the same phenotype and all the experiments were perfomed at a final concentration of 2 µM. The control embryos were injected with a Negative Mimic (Dharmacon) at the same concentration.

2.3 Transformation of E.coli with plasmid DNA

E.coli DH5α cells were prepared for transformation as follows: cells were grown to mid-log phase (A_{600}=0.6) in Luria Broth (LB: 1% bactotryptone, 1% NaCl and 0.5% Bacto-yeast extract) at 37˚C with shaking. Cells were harvested by centrifugation at 2000 x g at 4˚C, resuspended into 100ml (for each 100ml of culture) of 50% $CaCl_2$. This suspension was then centrifuged at 5000 x g for 15 min at 4˚C. The resulting pellet was resuspended into 100ml (for each 100ml of culture) of 50% $CaCl_2$ and centrifuged again. The cells were resuspended in 3 ml of ice cold 10% glycerol solution, aliquoted and stored at -80˚C. For each transformation, DNA was added to 50 µl of competent cells, and incubated in ice for 20 min; then cells were subjected to heat shock at 42˚C for 2 min and successively incubated on ice for 10 min. Cells were recovered in 1 ml of LB and incubated for 40 min at 37˚C, before plating on LB-agar containing appropriate antibiotics. Plates were incubated at 37˚C overnight to allow bacterial colonies to grow (Sambrook and Russell, 2001).

2.4 Isolation of plasmid DNA from *E. coli*

Mini-preps plasmid DNA preparations were carried out using the QIAGEN MINI prep kits. Procedure is based on the alkaline lysis method (Sambrook and Russell, 2001), but using a support column to purify isolated plasmid DNA. One aliquot of plasmid DNA was diluted in 1:200 in milliQ water, and the

concentration was determined according to the following formula: absorbance of one A_{260} unit indicates a DNA concentration of 50 µg/ml.

2.5 Whole-Mount *In Situ* Hybridization

Whole-mount *in situ* hybridization was carried out as using digoxygenin-labeled antisense RNA riboprobes. Antisense and sense cDNA templates were obtained by RT-PCR amplification of total RNA from Oryzias latipes at different stages of development with the appropriate oligonucleotide primers. These PCR products were then cloned into the Topo TA vector (Invitrogen). This vector contains two different promoter sequences (T7 and Sp6) for the expression of both the sense and antisense strands of the cloned product. The cDNA of the ol*ERK*2 gene were isolated by RT-PCR amplification with the following specific primers:

Name	Forward	Reverse
o.l.erk2 probe	F 5'- ATTTCGGTCTGGCCCGTGTG -3'	R 5'- GGTTGAGCTGATCCAGGTAG-3'
Totalcds o.l.erk2	F 5'- ATGGCGACAGCTGCGGTGTC -3'	R 5'- GGGACCTGAACCCGGGCTGAA -3'

To synthesise RNA probes the reaction mix was set up as follow:

1µg of linearized plasmid/PCR product

2 µl of 10X transcription buffer (Roche)

2 µl of DIG-labelling mix (Roche)

2 µl of appropriate RNA polymerase (T3, T7, SP6)-40 Units (Roche)

1 µl of RNase inhibitor

DEPC H_2O

The reaction mix was incubated for two hours at 37˚C, after which 2 µl (20 Units) of DNase-RNase free was added to the reaction mix and incubated for 15 minutes at 37˚C to degrade template DNA. 80 µl of H_2O were added to the reaction followed by precipitation with 0.1 volume 4M LiCl and 3x volume absolute ethanol at -20˚C for two hours. The probe was then centrifuged at 2000 x g for 30 minutes at 4˚C, washed with 70% ethanol, air-dried, dissolved in 40 µl of DEPC H_2O and stored at -20˚C.

Selected embryos were fixed in 10 ml of 4% paraformaldehyde prepared in 2X in 2X PTW (PBS containing 0.1% Tween) for 1 hour at room temperature and then 12 hours at 4℃. The embryos were dechorionate d and washed 4 times with 1X PTW. Finally, embryos were dehydrated in methanol 100% and stored at -20℃ (embryos in methanol endure to several mon ths of storage without degeneration).

Embryos were gradually rehydrated washing with 75% methanol/PTW, 50% methanol/PTW and 25%methanol/PTW. Than samples, were treated with 10mg/ml

proteinase K in PTW for a different amount of time (from 5 to 90 minutes) depending on the specific embryonic stage and washed twice with freshly prepared 2mg/ml glycine in PTW. After the embryos were refixed in 4% paraformaldehyde/PTW at room temperature for 20 minutes and washed through five changes of PTW. The embryos were pre-hybridized for at least 1 hour at 65℃ (42℃ for microRNAs LNA-DIG-probes) wi th hybridization buffer prepared as follow:

Formamide 100% 25ml

SSC 20X (pH7.0) 12.5 ml

Heparin (50mg/m) 150 µl,

Torula-RNA 250 mg

Tween20 10%.

The probes were added and the samples were hybridized overnight at 65℃ (42℃ for microRNAs LNA-DIG-probes). After the hybr idization step, embryos were washed at 65℃ (42℃ for microRNAs LNA-DIG-pro bes) with 50% formammide/2xSSCT, 2xSSCT and 0.2xSSCT. Then the embryos were incubated at room temperature with a blocking solution (5% serum/PTW) for two hours in agitation. The samples were then incubated for 12 hours at 4° with 200 µl of anti-DIG antibody (1:4000 dilution). Then the samples were washed 3 times for 10 minutes with the SB solution (0.1M Tris pH 9.5, 0.1M sodium chloride, 50 mM, Magnesium chloride, 0.1% Tween). Subsequently the embryos were placed in the appropriate colour solution with specific reagents NBT / BCIP (Boehringer).

The reaction was blocked with TE/Tween 0.1% solution, the embryos were again fixed in 4% paraformaldehyde/PTW for 20 minutes, washed with PTW1X and stored in glycerol. The embryos were embedded in a mix of BSA/Gelatine and sectioned with vibratome. Bright-field images were obtained on a Leica DM-6000 microscope. Adobe Photoshop was used to adjust image brightness and contrast. A minimum of 20 embryos, obtained from independent injections, were hybridized for each marker and condition.

2.6 Richardson Romeis staining (Histo Blue sections)

Solutions

Borax Solution: Solve 1g Borax (Borax = Sodium tetraborate decahydrate)in 100ml ddH_2O (→ 1% Borax solution) with the aid of magnetic stirrer/heater

- Filter 1% Borax solution

Blue Solution: Add 1g Methylene Blue in 100ml 1% Borax solution (→ 1% Methylene Blue in 1% Borax solution)

Azur Solution: Solve 1g Azur II in 100ml ddH_2O (→ 1% Azur II solution)

Richardson Romeis solution: Mix 1% Azur II solution and 1% Methylene Blue in 1% Borax solution at a ratio of 1:1 (→ Richardson (Romeis) staining solution)

Filter Richardson (Romeis) staining solution

Staining

- Apply the staining solution briefly on slide on heater (60℃)
- Throw it away (special waste → heavy metals!)
- Wash briefly with tap water
- Left them over night in water
- Dry slide on heater
- Coverslip

2.7 Immunofluorescence analysis

For the immunofluorescence analysis on the Medakafish sections, embryos were fixed overnight in 4% paraformaldehyde in PTW at 4℃, incubated overnight in 15% sucrose/PTW at 4℃ and than incuba ted overnight in 30% sucrose/PTW at 4℃. The cryosection of control and morphant Medakafish embryos were washed three times with PBS1x (α-Pax6, α-Calretinin, α- Otx2) or PTW 1x (α-Rhodopsin, α-Syntaxin, α-Zpr1, α-GS6). Than the slides were boiled in Citrate Buffer:

- Citric acid 1.9 mL
- Sodium Citrate 8.8 mL

- Add water to 200 mL

For each antibody were used different time of boiling, different blocking buffer and different diluite solution that are reported in the table:

Antibody	Boiling time	Blocking buffer	Diluite solution	Concentration	Secondary antibody
Rhodopsin	1'	10%FBS/PTW1x	5%FBS/PTW1x	1:5000	α -mouse
Zpr1	2'	5%GoatSerum/0.5%Triton in PBS1x	5%FBS/PTW1x	1:200	α -mouse
Syntaxin	2'	10%FBS/PTW1x	5%FBS/PTW1x	1:100	α –mouse
Otx2	10'	10%FBS/PTW1x	5%FBS/PTW1x	1:100	α –rabbit
GS6	2'	10%FBS/PTW1x	5%FBS/PTW1x	1:100	α -mouse
Pax6	8'	10%FBS/PTW1x	5%FBS/PTW1x	1:250	α –rabbit
Calretinin	5'	5%FBS/0.3%Triton/PBS1x	1%BSA/0.3%Triton/PBS1x	1:500	α –mouse
ERK1/2	5'	5%FBS/0.3%Triton/PBS1x	1%BSA/0.3%Triton/PBS1x	1:50	α –rabbit

After the overnight incubation with the primary antibodies, the slides were washed three times with PTW1x and than were incubated with the Alexa Fluor secondary antibodies (Invitrogen) 1:1000. The slides were counterstained with 4.6-diamidino-2-phenylindol, DAPI (Vector Laboratories). Slides were photographed using LSM710 Zeiss Confocal Microscopy.

2.8 Transgenic lines

The Ath5 (del Bene et al. 2007) and Six3.2 (Conte and Bovolenta, 2007) transgenic embryos were injected with mm-mo-miR-181a/b (control) and mo-miR-181a/b (morphants). The embryos were than fixed at the stages of interest overnight in 4% paraformaldehyde in PTW at 4℃, incubated overnight in 15% sucrose/PTW at 4℃ and than incubated overnight in 30% sucrose/PTW at 4℃. The cryosection of control and morphant transgenic embryos were washed three times with PTW1x and were counterstained with 4.6-diamidino-2-

phenylindol, DAPI (Vector Laboratories). Slides were photographed using and LSM710 Zeiss Confocal Microscopy.

2.9 Dissection of Medakafish tissue (eye)

To obtain RNAs or protein extracts from Medakafish embryo tissues was necessary remove the chorion (egg envelope) before dissect the tissues. To solubilize the chorion the eggs were trated with hatching enzyme.

Preparation of Hatching enzyme:

Fertilized eggs were collected in numbers ranging from hundreds to thousands, and the blastula-stage eggs were rolled between sheets of filter paper to remove the attaching filaments. The eggs were growth at 27℃ for 7-8 days. All the eggs were collected in a tube, washed 4-5- times in bidistilled water. All the water was removed and the tube were dipped into liquid nitrogen for 1' and water at 37℃ for 1'. The process was repeated thre e times. Than the eggs were homogenized with a pestle. The homogenized was centrifuged 1' at 4℃. The supernatant was transferred in a new tube. 250µL of cold PBS1x was added and homogenized with a pestle. Centrifuged 1' at 4℃. The supernatant was transferred in a new tube. Other 250µL of cold PBS1x was added, homogenized with a pestle and centrifuged 1' at 4℃ . Finally all the supernatant was collected in a new tube and centrifuged 10' at 4℃. The supernatant was transferred in a new tube and store at -80℃.

For efficient chorion solubilization on the outside of the living embryos, the eggs were incubated with Proteinase K (20 mg/mL) for 5 hours with vigorous agitation. The eggs were than treated with Pronase for 30' and subsequently with hatching anzyme at 27℃ for several hours unt il the chorions were completely digested.

2. 10 Real Time PCR

The stage 32 RNA eye tissues were obtained from control and morphants Medakafish embryos. For negative mimic and mimic-181 over-expressing analysis the RNAs were extracted from whole embryos, respectively. The RNAs were extracted and digested with DNaseI using RNeasy extraction kit according to the manufacturer's instructions.

The cDNAs were generated by the Quantitect kit for the qRT-PCR analysis. The qRT-PCR reactions were performed with nested primers and carried out with the Roche Light Cycler 480 system. The PCR reaction was performed using cDNA (200-500 ng), 10 ul of the SYBR Green Master Mix (ROCHE) and 400 nM primer, in a total volume of 20 ul. The PCR conditions for all the genes were as follows: preheating, 95℃ for 5 min; cycling, 40 cycles of 95℃ for 15 s, 60℃ for 15 s and 72℃ for 25 s. Quantification results were expressed in terms of cycle threshold (Ct). The Ct values were averaged for each triplicate. The ol*Hprt* and ol*Gapdh* genes were used as the endogenous control for the experiments. Differences between the mean Ct values of the tested genes and those of the reference gene were calculated as $\Delta Ct_{gene} = Ct_{gene} - Ct_{reference}$. Relative expression was analysed as $2^{-\Delta Ct}$. Relative fold changes in expression levels were determined as $2^{-\Delta\Delta Ct}$ (Alfano et al., 2005).

The sequences of oligonucleotide primers are summarized in Table 1.

Table 1. List of the sequences of the primers used in qRT-PCR experiments.

Name	Forward	Reverse
OI TGFBR1	F 5'- GAGTCTTTCAAGCGGGCGGA -3'	R 5'- CTCCTCCACGGACGGATCTG -3'
OI BMPR2.	F 5'- GAAACAGGGCCTGCACAACC -3'	R 5'- CTTCCAGGGAGCCGCAGTAC-3'
OI SMAD2 chr9	F 5'- GCTAAAGAAGACAGGCCAGC -3'	R 5'- CCTGATGTATCCCACTGTTC -3'
OI SMAD2 chr12	F 5'- CGATACGGCTGGCATCCTGC -3'	R 5'- GTGCACATTCTGGTTAGCTG-3'
OI SMAD3	F 5'- CTCCTCTGGATGACTACAGC-3'	R 5'- CATGCTGTGGGTCATCTGGTG-3'
OI SMAD7	F 5' -GGAGGAACCACATACTCGGC -3'	R 5'- CCGTTCCCTTGAGGTAGATC -3'
OI ERK2	F 5'- GCAGCGACAGCAGATAGTTC -3'	R 5'- GCCGAGATGTTGTCCAACAG -3'
OI AKT3	F 5'- GAAGTTGCTCACACGCTCAC -3'	R 5'- CTCCTCCGTTGACGTACTCC -3'
OI WNT11	F 5'- CCGATGCTCCCATGAAGATG -3'	R 5'- CAGGATCCAGATACACCATG -3'

2.11 Construct preparation for Luciferase assay

The PCR products for the selected human 3'UTR sequences were obtained with XbaI tagged primers (or SpeI). The sequences of oligonucleotide primers are summarized in Table 2. The digested PCR products were inserted in the pGL3-tk-LUC vector digested with XbaI.

Table 2. List of the sequences of the primers used to amplify human 3'UTR

Name	Forward	Reverse
Hsa-Erk2	F 5'-TCTAGAGTGACACGGAACAGCACCTC-3'	R 5'- TCTAGAGGAAGAAAGCAGAGACGCAG-3'
Hsa-Akt3	F 5'- TCTAGAGACATCACCAGTCCTAGCTC -3'	R 5'- TCTAGAGCTGCCTTAGTAAAATGCCC-3'

2.12 Trasfection of HeLa cells for luciferase assay

The HeLa cells were plated at the concentration of 135000 cell/mL in a 24-multi well. The cells were cultured overnight at 37℃ and 5% CO2 in DMEM supplemented with 10% FBS, penicillin (100 U/ml) and streptomycin (50 mg/ml). The cells were transfected with 370ng of DNA using PolyFect transfection

reagent (Qiagen) according to the manufacturer's instructions. For each vector the trasfection was performed in duplicate. After 7 hours the cells were trasfected with 50nM of negative mimic or mimic181 using ITERFERIN (Polyplus) according to the manufacturer's instructions. The cell were growth overnight at 37℃ and 5% CO2 in DMEM supplemented w ith 10% FBS, penicillin (100 U/ml) and streptomycin (50 mg/ml).

After 24 hours the cells were lysed using Passive Lysis Buffer 1x (Promega) and the luciferase activities were quantified using the LAR and STOP solution (Promega).

2.13 Western Blot

The stage 32 eye proteins were obtained from control and morphants Medakafish embryos. For negative mimic and mimic-181 over-expressing analysis the proteins were extracted from whole embryos. The proteins were extraxted in RIPA buffer.

The Bradford Reaction was used to detect the proteins concentration of each sample using BIO-RAD.

The protein were loaded on acrylammide gel for SDS-PAGE separation.

GEL PREPARATION:

	LOWER 12%	LOWER 15%	UPPER
H2O	3,3 mL	2,3 mL	6 mL
ACRIL 33%	4 mL	5 mL	1,25 mL
Tris HCL pH8.8	2,5 mL	2,5 mL	2,5m L (pH6.8)
SDS 10%	100uL	100uL	100uL
TEMED	10 uL	10uL	10 uL
APS 10%	100uL	100uL	100uL

For each sample was loaded a range of 15-30 ug of protein (diluited in SDS 10%, Tris HCL pH6.8, Glycerol, Bromophenol Blu, beta-mercaptoethanol).

The runs were performed for 2 hours at 100-120V. Than the proteins were transferred of a Nitrocellulose Membrane (filter BIO-RAD), for 90 minutes at 300mA.

The proteins were colored with PONCEAU-RED solution, than the filters were washed with TBS 1x, and blocked for 2 hours in MILK 5% in TBST 1x. The primary antibodies were incubated overnight. After this incubation the filters were washed 3 times in TBST 1x, than incubated with the secondary antibodies 1 hour at room temperature. The filters were washed 3 times in TBST 1x and the antibodies were revealed with ECL kit according to the manufacturer's instructions.

2. 14 Primary culture of Medakafish retinal cells

Slides treatment:

- wash 70% EtOH for 30'
- wash absolute EtOH for 30'
- Let them dry
- Sterilize them in autoclave

- Treat the slides with Poly-D-Lysine 20μg/ml in bidistilled water overnight at 37℃

- Rinse 3 or 4 times with bidistilled water

- Treat the slides with Laminin 10 μg/ml (PBS 1x) overnight at 37℃
- Rinse 3 or 4 times with bidistilled water only before adding the cells

Primary culture of Medakafish retinal cell:

- Once removed the chorion with hatching anzyme dissect the stage 28-30 eye of control or morphants embryo in cold L15 medium supplemented with 10% FBS, penicillin (100 U/ml) and streptomycin (50 mg/ml).
- Once removed the lens collect the eye in 100μL of cold complete L15 medium
- Add 20μL of Trypsin (10mg/mL in PBS1x)
- Incubate the eye 10'-15' at 37℃ (shake them perio dically)
- Add 20μL of Soybin trypsin inhibitor (20mg/mL in PBS1x)
- Up&down with syringe using a G27 needle
- Wash the slide (treated with laminin) with bidistilled water
- Add 500μL of complete L15 + 20μL N2 supplement (100x) medium pre-heated at 37 ℃ to the cells
- Add the cells to the slide
- Growth at 30℃ for 24 hours

2.15 Drug treatments

Once removed the chorion with hatching anzyme the morphant embryos were growth in 96-multi-well with

- PD98059 25μM

- DMSO 3%
- Yamamoto1x

For a minimum of 24 hours to a maximum of 6 days. For the control experiments the morphants were growth in Yamamoto1x/ DMSO3%.

For the TGF-β treatments the embryos were growth with:

- TGF-β molecule 10 ng/ml
- DMSO 3%
- Yamamoto1x

For a minimum of 24 hours to a maximum of 6 days. For the control experiments the morphants were growth in Yamamoto1x/ DMSO3%.

3. RESULTS

3.1 Identification of eye-expressed miRNAs and characterization of their expression profiles in Medakafish

To identify and select eye-enriched miRNAs, I took advantage of already published catalogs of microRNA expression profiles. In Banfi's laboratory, the expression of 13 miRNAs (miR-9, -29c, -96, -124a, -181a, -181b, -182, -183, -184, -204, -213, -216, and -217) during eye development in the mouse was previously determined (Karali et al. 2007). Their variable spatial and temporal profiles suggested their involvement in modulating diverse aspects of ocular and retinal function. Subsequently, the knowledge about microRNAs preferentially expressed in the eye was expanded with two different miRNA microarray profiling experiments which allowed us to obtain information on: 1) miRNAs enriched in the eye with respect to the rest of the embryo and 2) miRNAs showing preferential expression in each of the three main compartments that compose the eye: retina and RPE, lens and cornea (Karali et al. 2010).

Among them, I aimed at identifying a selected subset of eye-enriched microRNAs to undergo further functional characterization. My aim was to gain insight into the role of specific miRNAs in retinal and ocular development and function, with the goal not only to improve our understanding of retinal and ocular biology, but also to start uncovering the possible contribution of miRNAs to the pathogenesis of retinal and ocular diseases.

To functionally characterize these eye-enriched microRNAs, I decided to rely on Medakafish fish (*Oryzias latipes*), a particularly amenable model system to carry out gene functional studies (Ishikawa et al. 2000).

Firstly, I performed a detailed evolutionary comparison of the mature sequences of the selected eye-expressed miRNA using the information deposited in the NCBI (http://www.ncbi.nlm.nih.gov) and UCSC Genome Bioinformatics (http://genome.ucsc.edu) public databases. Moreover, I compared their expression profiles across evolution through the analysis of several gene expression public database such as EUREXPRESS (http://www.eurexpress.org), which stores RNA ISH expression profiles of miRNAs in mouse embryos at embryonic day (E)14.5; GEISHA2.0 *(*http://geisha.arizona.edu/geisha/index.jsp*),* which collects *in situ hybridization* for genes expressed in the chicken embryo during the first six days of development; and miRNEYE (www.http://mirneye.tigem.it/), which reports the previously described miRNA expression data in the mouse eye generated in our lab (Karali et al. 2010). I chose to focus my attention on the microRNAs more conserved both in terms of sequences and expression profile in the eye in vertebrates. Based on the above analysis, I finally selected the following microRNAs: miR-204, miR-29c, miR-30c, miR-30d, the miRNA cluster composed of miR-183 miR-182 and miR-96, mir-184 and the miRNA cluster composed of miR-181a and miR-181b. To evaluate their expression profile in the Medakafish eye, I perfomed RNA ISH at different developmental stages with LNA (locked-nucleic-acids) templates. Below is a summary of the results obtained (Fig. 17).

MiR-204 was found to be expressed in the optic cup since early stages of eye development. In the mature eye, miR-204 was detected in the RPE, lens epithelium cells and in INL and GCL in the retina (Fig. 17 A). The miR-29c, miR-30c and miR-30d start to be expressed during the final phases of retina maturation (stage 36) and at stage 38 they were expressed at low levels in INL,

IPL and GCL (Fig. 17 B, C, D). The miR-183, miR-182 and miR-96 are genomically organized in a cluster and present the same expression profile in all the cellular layers of the retina but with a particularly enrichment in the photoreceptor layer (Fig. 17 F, G, H). In agreement with what already described in other species (Wienholds et al. 2005; Xu et al. 2007; Karali et al. 2007; Pierce et al. 2008; Zhu et al. 2011), among the three microRNAs, the miR-183 was the most abundant one (Fig. 17 F). MiR-184 was expressed from early stages in the developing lens and at stage 38 its expression was confined to lens epithelial cells (Fig. 17 I). The two miRNAs miR-181a and miR-181b, also organized in a genomic cluster, were expressed, starting from stage 30, in the differentiating retina and at stage 38 they were both expressed in the INL and, at lower levels, in the GCL (Fig. 17 E, J).

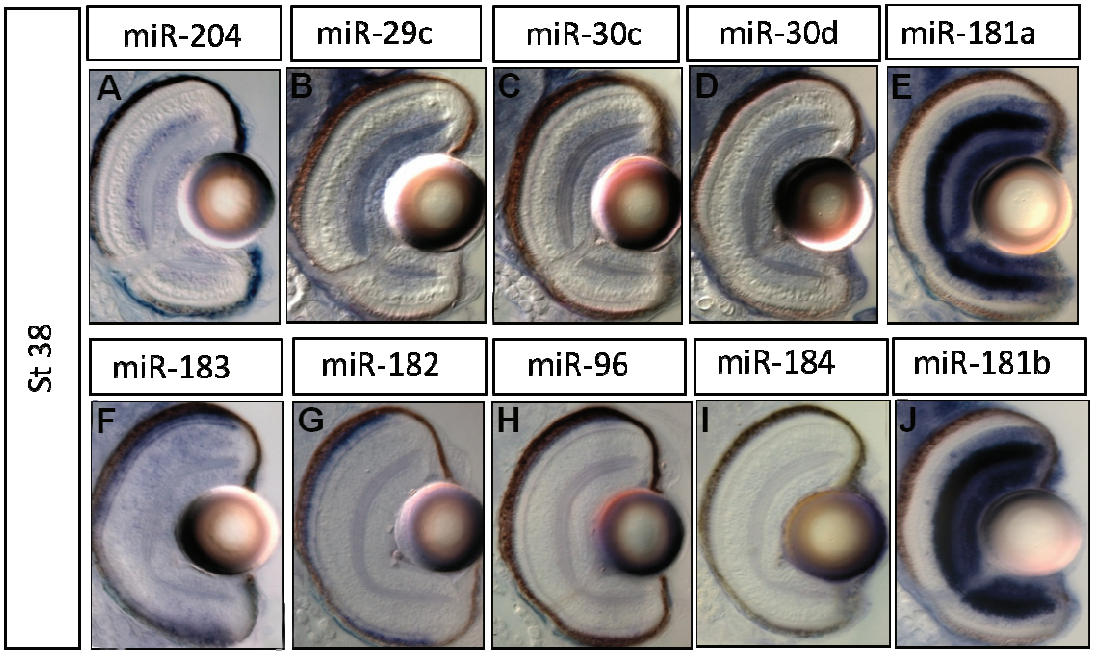

Figure 17. Expression patterns in the Medakafish mature retina of the eye-enriched miRNAs selected for the functional characterization. RNA ISH on frontal sections of wild-type medakafish embryos at stage 38 hybridized with LNA- probes for the selected miRNAs. A) miR-204 was detected in the RPE, lens epithelium cells and in INL and GCL in the retina. B-D) The miR-29c, miR-30c and miR-30d were expressed in INL, IPL and GCL. F-H) The miR-183, miR-182 and miR-96 cluster present the same expression profile in all the cellular layers of the retina but with a particularly enrichment in the photoreceptor layer. I) miR-184 was expressed in the lens epithelial cells. E, J) miR-181a and miR-181b cluster were both expressed in the INL and, at lower levels, in the GCL.

3.2 Initial functional screening for selected eye-expressed miRNAs

I performed functional characterization of a selected subset of the previously listed miRNAs by knocking-down their activity in Medakafish embryos by using a morpholino (MO)-based strategy (Kloosterman et al. 2007). Morpholinos oligos are short chains of about 25 Morpholino subunits, completely stable in cells, that act via steric blocking mechanism. I decided to focus my attention on the initial characterization of miR-184, miR-204 and the miRNA cluster formed by miR-181a and miR-181b. The morpholino injection for the miR-184 did not produce any ocular alteration at lower concentration, whereas at higher concentration it featured toxic and unspecific effects. This toxicity at higher levels was likely due to off-targeting effects, which are observed in about 15–20% of MOs used. For these reasons, I did not further pursue this miRNA.

On the other hand, the morpholino-mediated ablation of miR-204 during eye development resulted in an eye phenotype characterized by microphthalmia, abnormal lens formation, and altered dorsoventral (D-V) patterning of the retina, which is associated with optic fissure coloboma. Using different approaches for the miR-204 functional characterization, we demonstrated its role in dorso-ventral patterning of the optic cup and lens differentiation via Meis2 targeting (Conte et al. 2010a). We also demonstrated miR-204 involvement in lens migration, axon pathfinding and retina maturation (unpublished data). I was deeply involved, in the first two years of my PhD project, in the functional characterization of this miRNA. The results of this analysis are part of a publication in PNAS, in which I am a co-author, and which is enclosed to this thesis as Appendix.

The main focus of my thesis, however, has been the functional characterization of the role of the miR-181a/b cluster that displayed a very intriguing expression profile during vertebrate eye development, as also described above. The remaining part of my thesis will therefore describe the results of this characterization.

3.3 Genomic organization of the miRNA cluster miR-181a/b and detailed expression analysis in Medakafish

I started the miR-181a/b characterization by first studying their sequences and genomic organization in Medakafish, that turned out to be very conserved with respect to the mouse and human genomes. The cross-species comparison of the mature miR-181a and mature miR-181b demonstrated that their sequences are completely identical among vertebrates (Fig. 18 A). As shown in figure 18 A, the two microRNAs presented only three bases of difference, none of which is located in the seed region. This evidence strongly suggests that these two microRNAs could recognize the same set of mRNA targets.

In the human and mouse genome, two copies of the miR-181a/b mature sequences are present. In human, the miR-181a-1 and miR-181b-1 copies are located on chromosome 1, in an intron of a poorly characterized non-coding RNA gene (LOC100131234), whereas the miR-181a-2 and miR-181b-2 copies are located on chromosome 9 and overlap in opposite orientation an intronic region of the nuclear receptor subfamily 6, group A, member 1 gene (NR6A1) that encode for an orphan nuclear receptor, member of the nuclear hormone receptor family (Fig. 18 B). I found the same organization in the mouse genome: the miR-181a-1 and miR-181b-1 copies are located on chromosome 1, in an intron of a not yet classified product identified in adult male testis cDNA

(AK076660), and the miR-181a-2 and miR-181b-2 copies are on chromosome 2 in the locus of the nuclear receptor subfamily 6, group A, member 1 gene (Nr6a1) (Fig.18 B). In human and mouse it is also present a third cluster of miR-181-related sequences, which is formed by miR-181c and miR-181d that differ respectively from miR-181a and miR-181d by only one base and present the same seed sequence. In the Medakafish genome, I did not identify the miR-181c and miR-181d mature sequences, but I identified four miR-181a/b clusters (on chromosome 9, chromosome 17, chromosome 4 and on the Ultracontig 105) (Fig. 18 A), suggesting that during evolution point mutation occurred in one of this clusters thus leading to the formation of the miR-181c/d cluster.

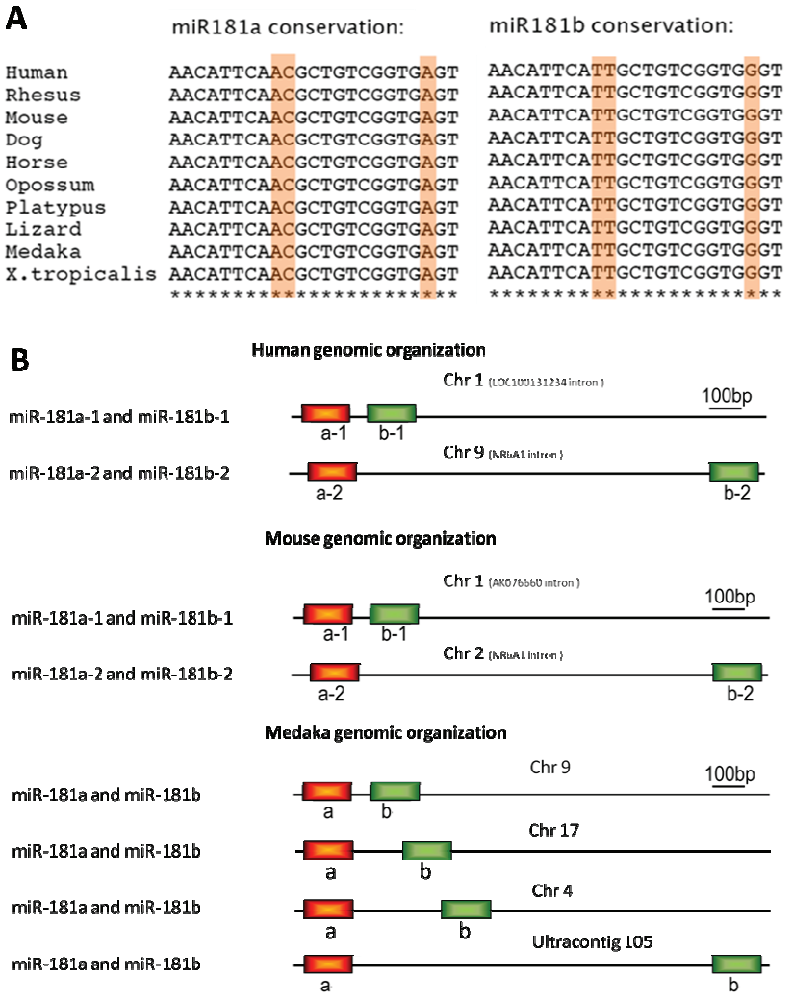

Figure 18. Characterization of miRNA-181a/b sequences and genomic organization across the vertebrate species. A) The cross-species comparison of the mature miR-181a and mature miR-181b demonstrated that are completely conserved among vertebrates. The two

microRNAs presented only three bases of difference, not located in the seed region. B) Schematic representation of human, mouse and medakafish genomic organization of miR-181a/b clusters. In human genome the two copies of miR-181a/b clusters are located on chromosome 1 in an intron of the non-coding gene LOC100131234, and on chromosome 9 overlapping in opposite orientation an intronic region of NR6A1. In mouse genome the two copies of miR-181a/b clusters are located on chromosome 1 in an intron of a not yet classified product identified in adult male testis cDNA (AK076660), and on chromosome 2 in the locus of NR6A1. In the Medakafish genome are present four miR-181a/b clusters on chromosome 9, chromosome 17, chromosome 4 and on the Ultracontig 105.

As previously mentioned, I used LNA-probes directed against miR-181a and miR-181b mature sequences to determine the expression profile of these two miRNAs in Medakafish by RNA ISH. At early stages of development, i.e., stage 24 and stage 28, it was not possible to detect a signal for neither microRNA, (Fig. 19 A a, b, f, g). However, starting from stage 30 the expression of both miRNAs was evident in the inner part of neural retina (Fig. 19 A c, h). This spatio-temporal profile suggest a miR-181a/b expression in differentiating amacrine cells. It is also to be noted that this particular stage corresponds also to the beginning of the plexiform layer formation. At later stages of eye development, stage 36 (Fig. 19 A d, i) and stage 38 (Fig. 19 A e, j) the two miRNAs were expressed at high levels in the INL and GCL, with a stronger staining in the INL in proximity of the IPL, where amacrine cells are located (see magnification in Fig. 19 A e', j'). Moreover their expression was also present in other organs and in the developing Central Nervous System (CNS). As shown in figure 19 B, at latest stage of development I detected their expression in the telencephalon, in the optic tectum and in the medulla oblongata, with a very strong staining in the optic tectum (Fig. 19 B a').

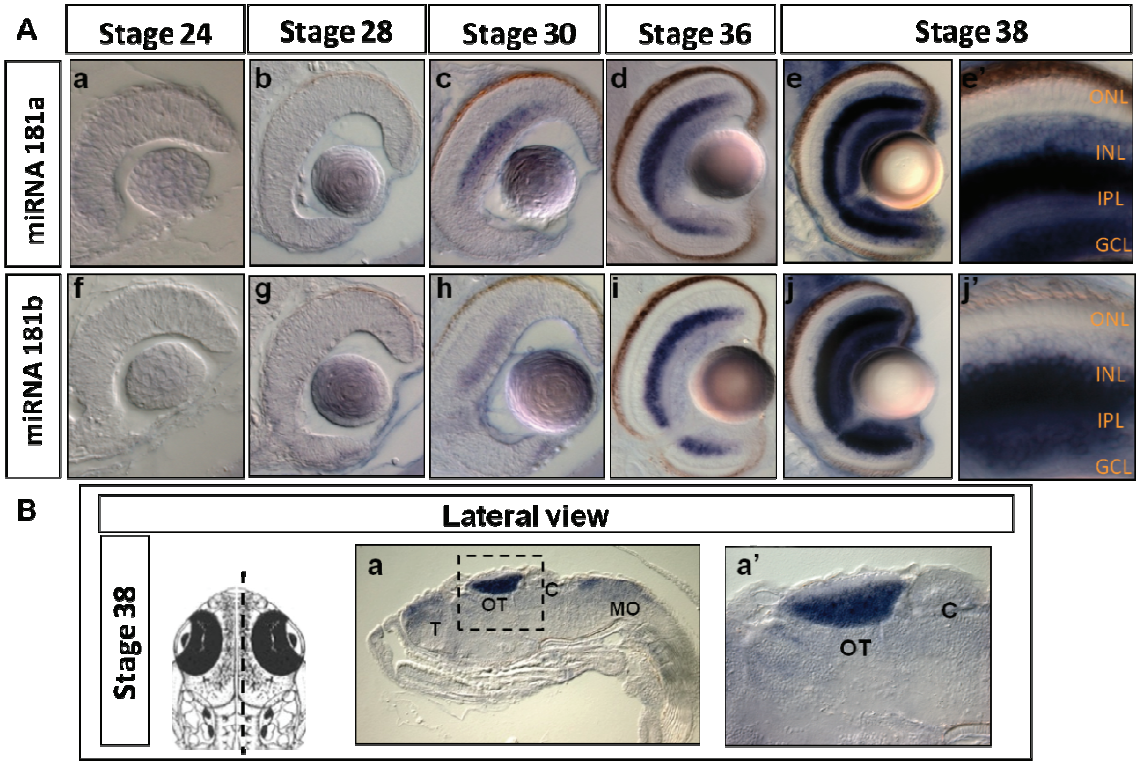

Figure 19. Expression patterns of miR-181a and miR-181b during eye development. A) RNA ISH on frontal sections of wild-type medakafish embryos hybridized with miR-181a (a-e') and miR-181b (f-j') at St 24 (a, f), St28 (b, j), St30 (c, h), St36 (d, i) and St38 (e, e', j, j'). Both miRNAs start to be detectable by ISH at stage 30 in the differentiating amacrine and gaglion cells (c, h). Note that at stage 30 starts also the plexiform layer formation. At later stages of development, st36 and st38, both miRNAs are expressed at high levels in INL and GCL (e',j'). B) On lateral section of medakafish embryos it is shown their expression in CNS, with higher levels in Optic Tectum. ONL: Outer Nuclear Layer; INL: Inner Nuclear Layer retina; IPL: Inner Plexiform Layer; GCL: Ganglion Cell Layer; T: Telencephalon; OT: Optic Tectum; C: Cerebellum; MO: Medulla Oblongata

3.4 Knockdown of miR-181a and miR-181b results in alteration of the retinal inner plexiform layer (IPL)

To determine and analyze the function of miR-181a and miR-181b during development, I employed antisense morpholinos (MO) to achieve functional gene knockdown. I used two different MOs, which were designed against the miR-181a (mo-miR-181a) and miR-181b (mo-miR-181b) mature sequences. This approach should guarantee the block of all the mature forms of these two miRNAs, regardless of their genomic origin.

To further ensure that the morpholinos were able to bind and block the miRNAs, I constructed and coinjected with the morpholinos a Green Fluorescent Protein (GFP) reporter plasmid, in the 5'UTR of which I inserted the miRNA mature sequences. In particular, I created two different constructs for the two different miRNAs (5'UTR-miR-181a-eGFP and 5'UTR-miR-181b-eGFP, see materials and methods). If the corresponding morpholino properly binds the miRNA mature sequence, it should also downregulate GFP translation which should reflect in a reduction of, green fluorescence signal. To obtain a quantitative assessment of GFP repression by the morpholinos, RNA coding for Red Fluorescent Protein (RFP) was also coinjected and the green/red fluorescence ratio was quantified, as previously described (Conte et al., 2010b; Esteve et al., 2004). As illustrated in figure 20 the reporter plasmid 5'UTR-miR-181a-eGFP (injected alone in fig. 20 A a, a') was translationally repressed when coinjected with mo-miR-181a (Fig. 20 A c, c'). However, coinjection of the same construct with a mutated form of the mo-miR-181a (mm-mo-miR-181a, see Methods), did not lead to translation downregulation of the GFP reporter (Fig. 20 A e, e') further supporting the specificity and quality of my controls.

Using the other construct 5'UTR-miR-181b-eGFP (injected alone in fig. 20 A b, b'), it was possible to assess the specificity of mo-miR-181b in binding and blocking the miR-181b mature sequence. In fact the GFP reporter plasmid was translationally repressed when coinjected with mo-miR-181b (Fig. 20 A d, d'), whereas coinjection with the mm-mo-181b was not able to repress GFP translation (Fig. 20 A f, f').

Moreover I coinjected the plasmid 5'UTR-miR-181a-eGFP with the not corresponding morpholino mo-miR-181b (Fig. 20 A g, g'), and the plasmid 5'UTR-miR-181b-eGFP with mo-miR-181a (Fig. 20 A h, h'). These co-injections

did not lead to decrease in GFP production, indicating that the three bases of difference between the two miRNAs were sufficient to avoid the binding with the not corresponding morpholino. Together these data demonstrate that the morpholinos designed against the two miR-181 mature sequences were able to bind with high efficacy the two miRNAs and to block specifically their functions.

To test if these interactions occurred also *in vivo* on the endogenous miRNAs, I performed an RNA ISH experiment on control and morphant embryos. As schematically described in figure 20 B, in control embryos, the LNA-probes were able to bind miRNAs mature sequences, whereas in morphants embryos, the binding of the morpholinos to the miRNAs mature sequences prevented the LNA-probe interaction with their complementary sequences, i.e., the miRNAs. I hybridized the LNA-probes, against miR-181a and miR-181b, separately on control and co-injected embryos (mo-miR-181a+mo-miR-181b). I did not detect any staining for each probe in co-injected embryos (Fig. 20 B a', b') compared to the control embryos (Fig. 20 B a, b), demonstrating that the morpholinos were specifically able to inhibit the miRNAs and therefore abolish their functions *in vivo*. Together, these results indicated that injecting only one morpholino I was able to specifically inhibit only the corresponding miRNA. Since miR-181a and miR-181b display the same seed region and are predicted to share their main mRNA targets, I decided to co-inject both corresponding morpholinos to block miR-181a and miR-181b together and avoid redundancy effects.

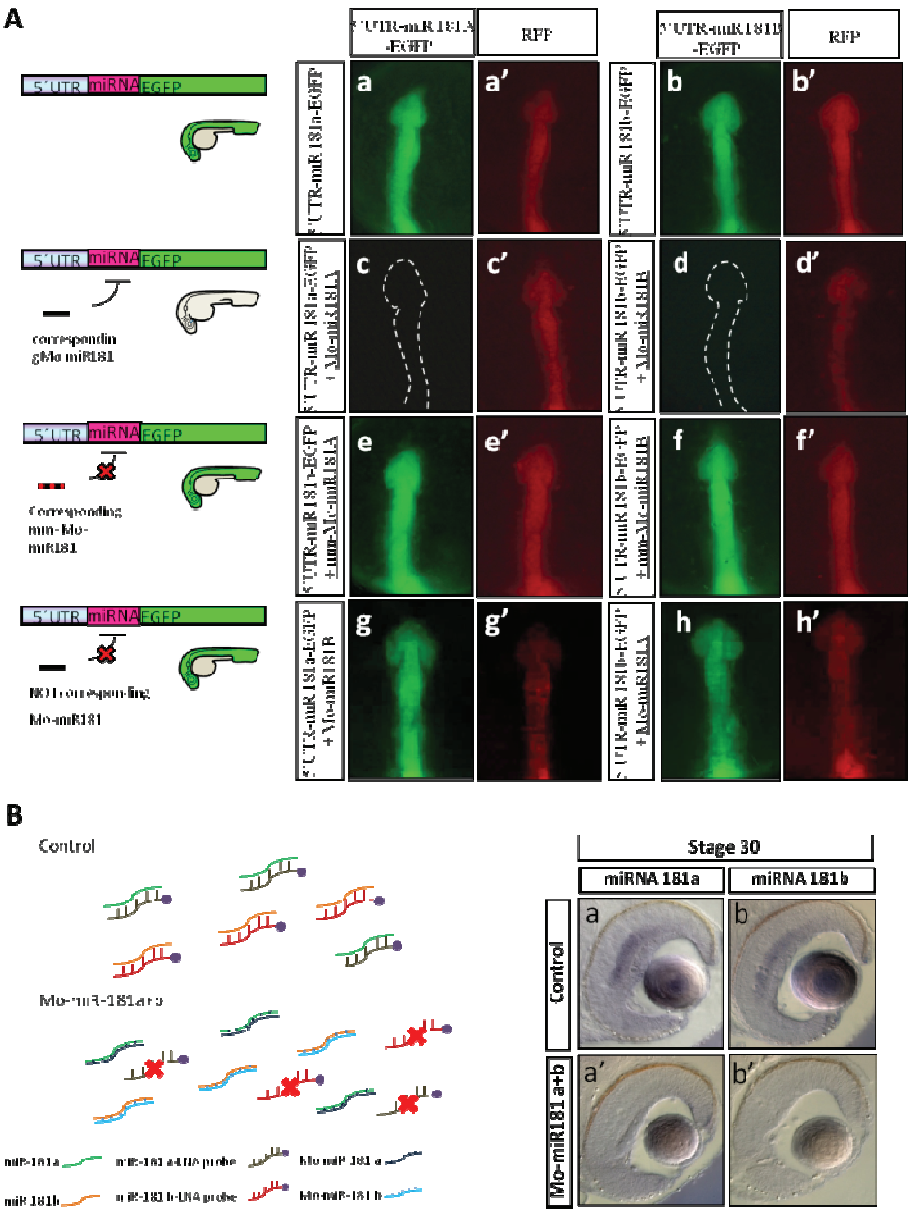

Figure 20. Mo-miR-181a and mo-miR-181b specifically bind the miR-181a and miR-181b mature sequences respectively. A) Schematic representation of the direct assay used to assess efficiency of the two Mos designed to block the miR-181a/b mature sequences. a –d') Representative embryos injected with the synthetic mRNAs encoding the reporter construct alone (a, a', b, b') or together with Mo-miR-181a/b (c, c', d, d'). Co-injection of the reporter construct 5'UTR-miR-181a-eGFP with the mo-miR-181a (c,c') and of the reporter construct 5'UTR-miR-181b-eGFP with the mo-miR-181b (d,d'), abolished the eGFP protein synthesis. Co-injection of the same constructs 5'UTR-miR-181a-eGFP with the mm-mo-miR-181a (e, e'), and of 5'UTR-miR-181b-eGFP with the mm-mo-miR-181b (f, f') did not lead to translation downregulation of the GFP reporter further supporting the specificity and quality of my controls. Moreover coinjection of the plasmid 5'UTR-miR-181a-eGFP with the not corresponding morpholino mo-miR-181b (g, g'), and the plasmid 5'UTR-miR-181b-eGFP with mo-miR-181a (h, h') did not lead to decrease in GFP production, indicating that the three bases of difference between the two miRNAs were sufficient to avoid the binding with the not corresponding morpholino. B) Frontal vibratome sections from control (a, b) and Mo-miR-181a/b-co–injected (a', b') embryos hybridized with LNA-probe for miR-181a (a, a') and miR-181b (b, b'). Both miR-181a and miR-181b expression was not detected in morphants.

The mo-miR-181a and mo-miR-181b morpholinos were co-injected at 1–2 cell stage and then the embryos were phenotypically analyzed. Morphological inspection using stereomicroscopy did not highlight gross eye defects. Indeed the co-injected embryos seemed to be quite similar to the control embryos (Fig. 21 A e B). However, by analyzing their retinal sections, it was possible to observe a specific eye phenotype, characterized by the notable thinning of the Inner Plexiform Layer (IPL) (Fig. 21 A' and B' red lines).

This phenotype was observed in 87% of injected embryos (76736 out of 88200 injected embryos). I used the Richardson-Romeis staining to mark the morphological structure of the retina in control and morphant embryos. This staining allowed me to precisely discriminate the retina cell bodies from the plexiform structures, where the nervous termination form synapses. Using the ImageJ software I could determine that the extent of thickness reduction of the IPL in morphant fish with respect to controls was of about 48%, quantified as the ratio between the IPL area and the total retina area (Fig. 21 C).

It has been reported that an activation of p53 could represent a non specific off-targeting effect of some morpholinos (Robu et al., 2007). This non specific activation can lead to activation of cell death pathways and the generation of a variety of aberrant phenotypes. In the latter scenario, the phenotype can be rescued by co-injection of the morpholino against the sequence under study and that of p53 (Eisen and Smith, 2008). Therefore, to exclude this possibility, I co-injected the (mo-miR-181a and mo-miR-181b) morpholinos with p53-MO (Conte et al., 2010b) and no amelioration of the phenotype was observed. This result indicated that the activation of p53 does not play any role in the generation of the phenotype observed after injection of mo-miR-181a/b.

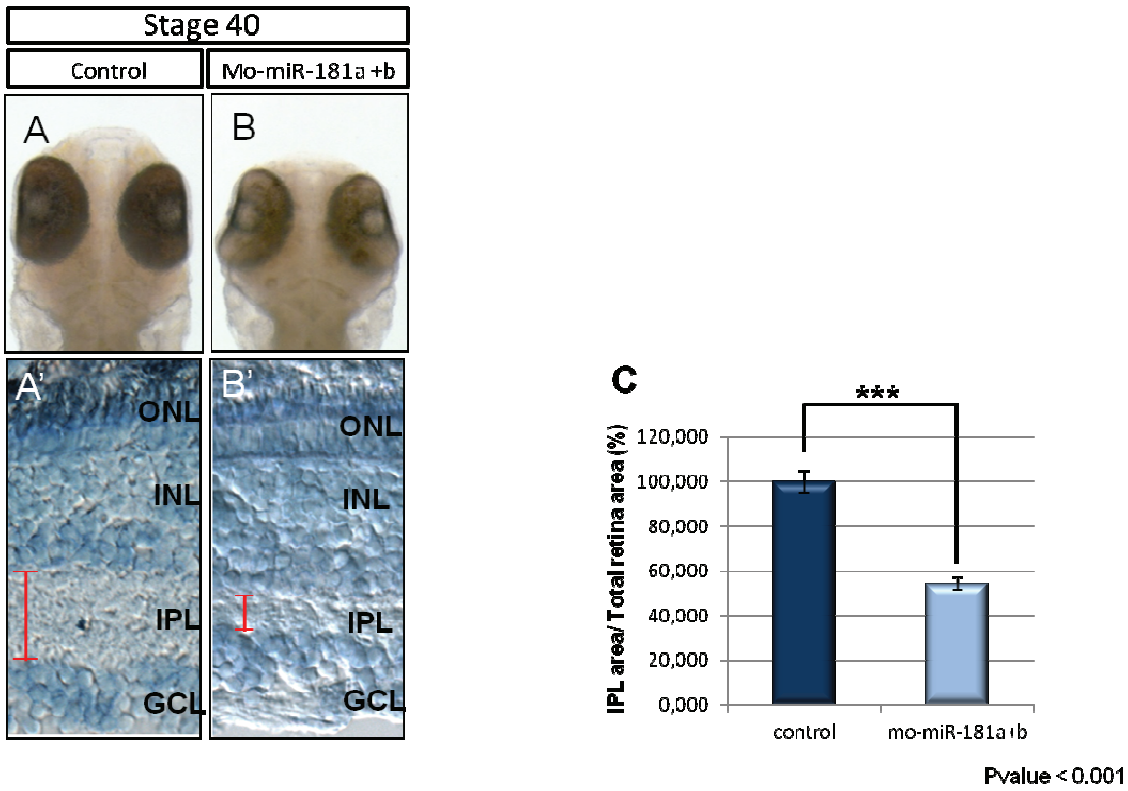

Figure 21. Knockdown of miR-181a and miR-181b results in alteration of the retinal inner plexiform layer (IPL). A-B) No morphological defects were evident analysing bright-field stereomicroscopy images of control (A) and Mo-miR-181a+b (B). A'-B') Frontal sections of st40 of control (A'), miR-181a/b-morphants (B') medakafish eye stainded with Richardson(Romeis) solution highlight Inner Plexiform Layer (IPL) (A'-B', red lines) thinning, with a reduction of 48% respect to control retinas(C).

3.5 Knockdown of miR-181a and miR-181b leads to retinal axogenesis defects

In order to verify whether the effects of the miR-181 loss-of function were restricted to the above described IPL thickness defects as well as to better dissect this retinal defects, I started to analyze the expression of several markers for the different retinal cell types. I analyzed, by immunofluorescence analysis using appropriate antibodies:

- rod and cone markers, such as Rhodopsin (Fig. 22 A, A') and Zpr1 (Fig. 22 B, B') respectively;
- Otx2 (Fig. 22 C, C'), a bipolar cells marker;
- Syntaxin (Fig. 22 D, D') a marker of amacrine and retinal ganglion cells (RGCs) synaptic terminals;
- GS6 a marker of Muller glia cells (Fig. 22 F, F');
- two markers of two different amacrine cell subtypes, i.e., Calretinin (Fig. 22 G, G') and Pax6 (Fig. 22 H, H').

This analysis was performed at two different stages, stage 38 when the retina is already mature, and stage 40, i.e., after hatching. At both stages no differences in the expression of all markers were observed between control and morphant embryos, with the exception of Syntaxin whose staining further highlighted the IPL defect in mo-miR-181a/b-injected embryos. Moreover the immunofluorescence staining for different amacrine cells type (Fig. 22 G, G', H, H') and the count of Pax6 positive cells (Fig. 22 I), indicated that there were no changes in the number of this subtype of amacrine cells morphant embryos, rejecting the hypothesis that the decrease in IPL thickness could be due to the absence of a retinal cell type whose axons and/or dendrites arborized in the IPL.

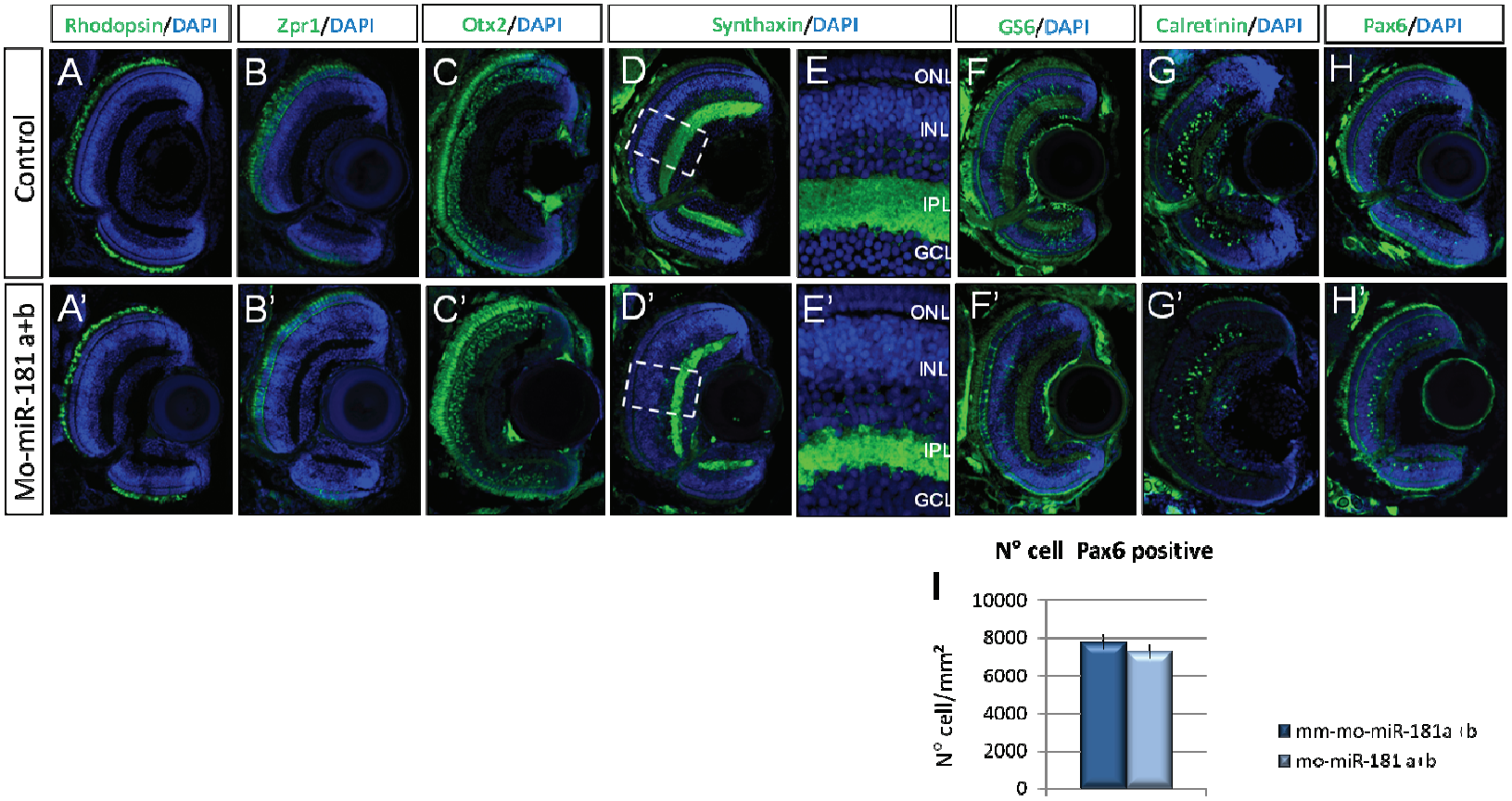

Figure 22. No differences in the expression of retinal markers were observed between control and morphant embryos. Frontal sections of St40 wild-type (A-H) and miR-181a/b-morphants (A'-H') immunostained with antibodies (green) against Rhodopsin (A, A'), Zpr1 (B, B'), Otx2 (C, C'), Synthaxin (D, E, D', E'), Glutamine Synthetase (F, F'), Calretinin (G, G') and Pax6 (H, H') and counterstained with DAPI (blue), show no alteration in the layering of retinal cells, except for Synthaxin that marks the IPL phenotype (D', E'). The number of Pax6 positive cells does not change in morphant embryos respect to control embryos (I).

Therefore, after having established that there were no differences in retina cell type generation, differentiation or organization in layered structures, I decided to investigate more deeply the IPL defects taking advantage of two different transgenic lines. In these lines, cytoplasmic eGFP was expressed under the control of retina cell type-specific promoters, which allowed the visualization of the fluorescent reporter in the axons and dendrites of a specific retina cell type.

The first line that I used was the Six3.2:eGFP line, in which the eGFP was under the control of the Six3.2 promoter, studied by Conte and Bovolenta in 2007. The Six3.2 promoter drives the eGFP expression in amacrine cells. As shown in figure 23 (A, A'), the concomitant down-regulation of miR-181a and miR-181b cause defects in the axon formation of this subtype of amacrine cells. The red arrows (Fig. 23 A') indicate different processes emerging from a single cell body, instead of one specified axon as observed in control (Fig. 23 A). Further studies are needed to establish if this processes are multiple axons or immature processes that are not correctly specified in axon or dendrites. Overall, these data allowed me to determine that miR-181a/b have a role in axogenesis of amacrine cells.

The use of the Ath5:eGFP transgenic line allowed me to characterize the effects of miR-181a/b down regulation on the axogenesis of RGCs, another retinal neuronal cell type in which the two miRNAs are expressed. In this line, developed by Del Bene and colleague (Del Bene et el. 2007) the Ath5 promoter drives the expression of eGFP in the cytoplasm of RGCs, highlighting their axonal structure bundled in the optic nerve. Using this line, it was possible to study the optic nerve formation from the eye to the optic tectum.

The down-regulation of miR-181a and miR-181b in this line caused no defects in the optic nerve bundle. I found that RGC axons crossed correctly at the optic

chiasm (Fig. 23 B, B') but along the optic tract they unbundled in a pre-tectal area, and did not correctly innervate the optic tectum (Fig. 23 C, C'). These defects were observed in 67% of the injected embryos (17728 out of 26460 Ath5:eGFP injected embryos).

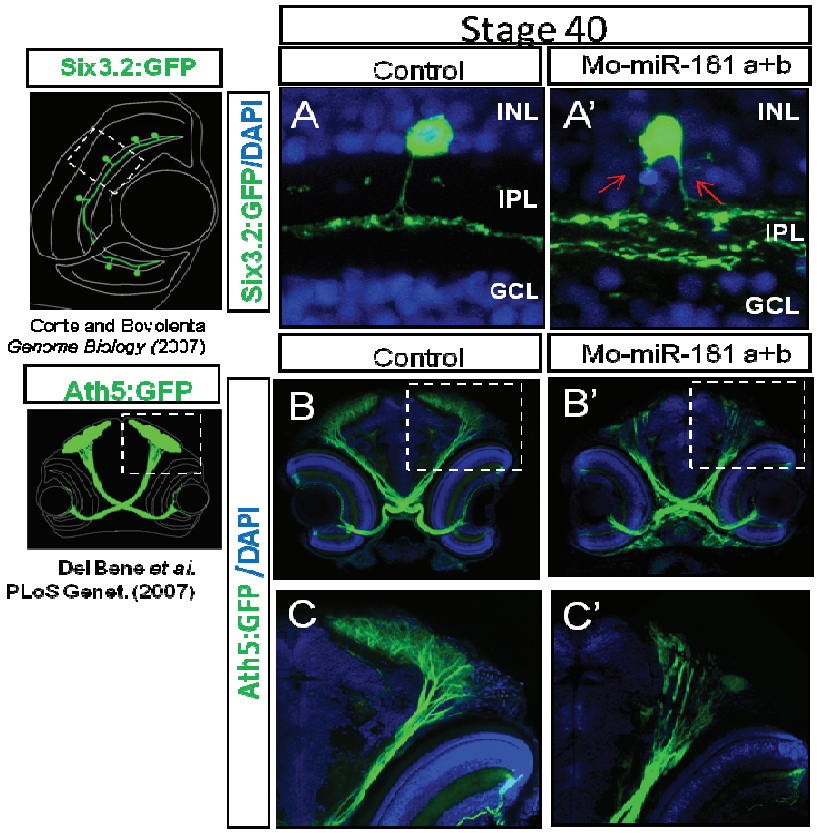

Figure 23. Knockdown of miR-181a and miR-181b leads to retinal axogenesis defects. Frontal cryostat sections of St40 control (A-B-C) and miR-181a/b-morphants (A'-B'-C') *Six3.2:EGFP* medakafish embryos (A, A') and *Ath5:EGFP* (B-C') medakafish embryos counterstained with DAPI (blue), show the axogenesis defect in amacrine and ganglion cell in morphants embryos. (A')The miR-181a/b-morphants amacrine cells, marked with GFP in *Six3.2:GFP* transgenic line, show disorganized axonal structure respect to the control amacrine cells (A), and more than one principal axon (red arrows). (B-C') The Optic Nerve formed by ganglion cells axons, marked with GFP in *Ath5:GFP* transgenic line, defasciculate earlier in the brain and does not correctly innervate the brain respect to the control embryos (C, C').

These data demonstrate that the miR-181a/b loss-of-function in Medakafish caused axogenesis defects leading to an impairment in the correct assembly of visual circuits.

3.6 Knockdown of miR-181a and miR-181b leads to RGCs axon length defects

The *in vivo* analysis allowed me to identify axogenesis defects in absence of miR-181a/b function, but to elaborate further on this observation and better define the axonal phenotype, I decided to use an in vitro system. In particular I cultured Medakafish RGCs. Since there were no previously described protocols for culturing Medakafish retinal neurons, I set up the optimal conditions in which the Medakafish cultured cells could survive and form stable neurites. To further characterize the RGCs axons phenotype, I dissociated Ath5 transgenic line eye and plated the cells onto a laminin-covered slide around stage 28-30, I.e., when RGC axons start to be bundled in the forming optic nerve. After 24 hour at 30℃, the cells were fixed, photographed at micros cope and the axon length of control and morphant cells was analyzed using the ImageJ software. I analyzed the axon length of 100 control cells and 100 morphant cells, derived from different experiments and different injections. In agreement with the *in vivo* data, analysis of primary culture of Medakafish RGCs, demonstrated axon length defects in the 80% of morphant cells. I observed a reduction in RGC axon length of about 70% in morphant RGCs with respect to controls (Fig. 24).

These data allowed me to uncover the involvement of miR-181a/b in the regulation of RGC axon growth, as assessed by the reduction in axon length

following their loss of function. These experiments also indicated that these axon defects are RGCs cell-autonomous and did not depend on altered information that could derive from the surrounding tissues. However other and different experiment will be needed to determine whether the branching defects of RGCs axons at the optic tectum are secondary effects due to these axon growth defects or are due to the loss of miR-181a/b function in optic tectum neurons.

With the *in vitro* analysis of Medakafish RGCs primary cultures, it was not possible to investigate on the miR-181a/b role in axon specification because the *in vitro* cultured RGCs have the ability to polarize intrinsically and form pseudopodia and filopodia. One of these extension soon shows a conspicuous growth cone and begin to grow faster than the others becoming the principal axon (Zolessi et al. 2006). Also in the *in vivo* condition, the developing RGC axons emerge directly from uniformly polarized cells in the absence of other neurites (Zolessi et al. 2006). This implicate the presence of a different mechanism for axon specification between the RGCs and amacrine cells. For these reasons to further investigate about the miR-181a/b role in amacrine axon specification, I will determine the best *in vitro* culture condition to analyze amacrine axon formation in control and morphant eye explantation, using a different Medakafish transgenic line (Six6).

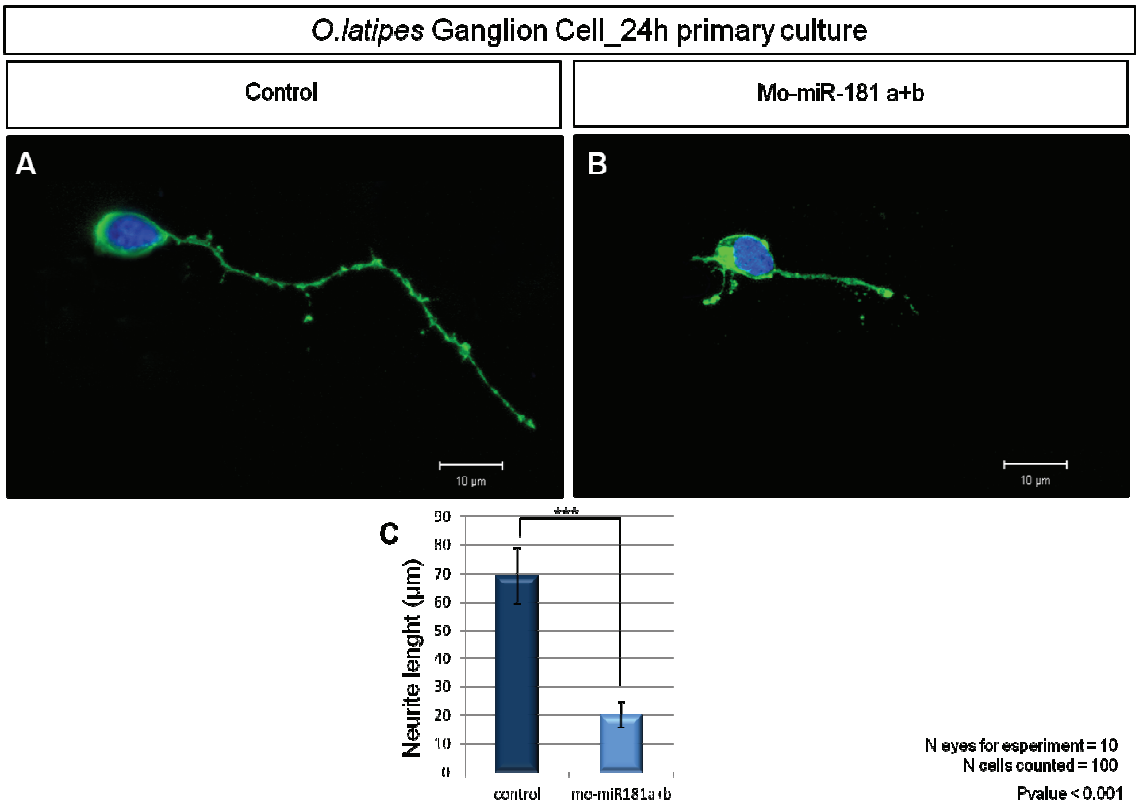

Figure 24. Knockdown of miR-181a and miR-181b leads to RGCs axon length defects. Medakafish Ganglion cell primary culture from control (A) and miR-181a/b-morphants (B) Ath5:eGFP transgenic line eyes show that miR-181a/b depletion causes retinal axon length defect with a reduction of ganglion axon length of 70% (C).

3.7 Knockdown of miR-181a and miR-181b leads to visual functional deficits

The above described defects in the wiring of IPL and axon branching of RGCs in the brain could also lead to functional defects of visual stimuli elaboration. A valid tool for the assessment of visual function is represented by the measurement of Optokinetic Response (OKR). The OKR is a stereotyped and compensatory eye movement in response to movements in the surround. The OKR serves to stabilize the visual image of an object in movement on the retina, and allows for high resolution vision. Due to its high selection value, all vertebrates display this basic behavior. When the environment is continuously moving in one direction, the OKR produces a nystagmus composed of cycles of slow eye movement in one direction and a fast resetting movement, called saccade, in the opposite direction. The OKR is triggered by a fast and directional input coming from the retina and encoded by a neural circuit involving pretectal nuclei. For these reasons this behavioral test is appropriate to determine reduced or limited vision due to defects in the assembly of retina circuits or defects in the brain elaboration of visual stimuli. In collaboration with Sara Barbato, a PhD student in our lab, and Stephan Neuhauss at the University of Zurich, I was able to demonstrate, that the morphant miR-181a/b fish had an impaired OKR. In agreement with the RGC axons defects, preliminary data indicated that morphant fish showed a statistically significant decrease in the OKR, as shown in figure 25. These data demonstrated that the loss of miR-181a/b functions not only led to morphological retinal defects, but also to impaired visual function.

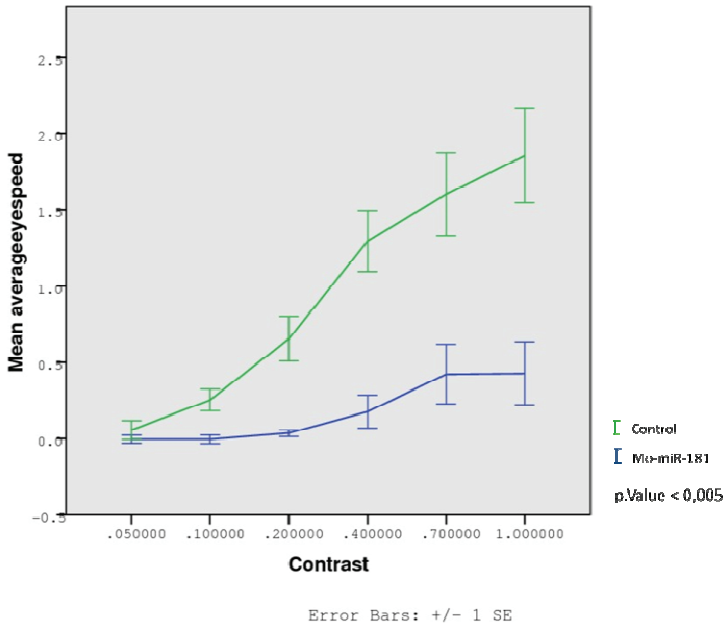

Figure 25. Knockdown of miR-181a and miR-181b leads to visual functional deficits. The Optokinetic Response (OKR) demonstrate that the miR-181a/b loss-of-function impairs visual function. In the graph are represented the mean average eye speed of control (green line) and morphant (blue line) fishes respect to the variation of stimulus contition (increased contrast). p.value <0,005.

3.8 miR-181a/b overexpression causes severe early embryonic defects

Using the above described loss-of-function approach I was able to recognize the miR-181a/b involvement in retinal cells axogenesis. In particular, inactivation of their activities led to defects in axon specification in amacrine neurons and alteration of axon growth in RGCs. To further dissect the functional role of miR-181a/b in retinal development and function, I decided to carry out gain-of-function studies. Towards this goal, I performed miR-181a/b overexpression in Medakafish embryos by injecting miRIDIAN (Dharmacon) miRNA-181 Mimics. miRIDIAN microRNA Mimics are double-stranded RNA oligonucleotides designed on the basis of miRNA sequences available in the miRBase Sequence Database. The miR-181a and miR-181b Mimics were injected at 1–2 cell stage and then the embryos were phenotypically analyzed. This approach led to the over-expression of these miRNAs since the early

stages of development and in all the tissue that derive from the first cells in which they were injected. For this reason, there was the possibility that this ectopic over-expression had strong impact on possible miR-181a/b targets, that are expressed at early stages of development. Among the different concentration tested, I observed that at both 1 μM and 2 μM concentrations the embryos showed the same phenotype and therefore all the subsequent experiments were performed at a final concentration of 2 μM. As negative control, Medakafish embryos were injected with a Negative Mimic (Dharmacon) at the same concentration used for the miRNA mimics. As shown in figure 26, the overexpression of miR-181a/b since early developmental stages caused a severe phenotype (Fig. 26 B), characterized by lethality at gastrulation (78%, 585 out of 750), with the few surviving embryos showing head defects with enlargement of otic vescicle and, in some cases, the complete absence of eye structures. Moreover the development of tail structures was severely defected resulting in shortened body. These data suggest that some of the miR-181a/b targets are already expressed at early stages of development and play important roles during gastrulation and developmental processes. Therefore, I could not use this approach to study the direct effects of miR-181a/b overexpression in the retina. An alternative strategy that could overcome the early lethality caused by miR-181a/b over-expression would be the creation of a transgenic line in which the expression of the two miR-181a/b is under the control of a tissue- specific promoter, such as Six6 that could drive their expression in same retina layer in which they are expressed.

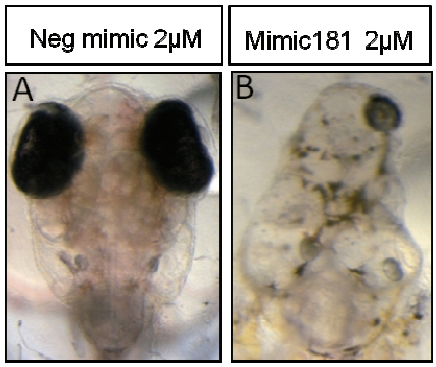

Figure 26. miR-181a/b overexpression causes severe early embryonic defects. miRIDIAN mimic heteroduplex strategy (Dharmacon) was used to overexpress miR-181a/b. B) The mimic-181a/b injected embryos show severe developmental defect compared to the control embryos (A) injected with a negative mimic heteroduplex at the same concentration.

3.9 miR-181a/b target selection and validation assay

The down-regulation of miR-181a/b function caused axogenesis defects and their over-expression altered the correct development of the entire embryo body. I hypothesized that these two phenotypes could be due to a possible role of miR-181a/b in the regulation of some signaling pathways, which are needed during early stages of development and then reused for the correct establishment of retinal axon growth processes. To dissect, at the molecular level, the roles of miR-181a and miR-181b during development it was necessary to identify their main target genes, whose dosage impairment could underlie the phenotypes observed following their knockdown and overexpression. During the past few years, the development of bioinformatic tools that allow to predict a list of possible target genes for each microRNA, facilitated the identification of the mRNAs targeted by a given microRNA. This tools, such as TargetSCAN *(*http://www.targetscan.org/*),* PicTar *(*http://pictar.mdc-berlin.de/*),* miRanda *(*http://www.microrna.org/*)*, predict the interaction between a microRNA and an mRNA target on the basis of a) miRNA seed sequence presence in the 3'UTR of a transcript, b) conservation of this sequence among species and c) strength of this possible interaction, as

assessed by evaluation of RNA secondary structure. Recently, in our laboratory, new tools were developed to increase the accuracy of these predictions, integrating the sequence-based predictions with co-expression data, such as in the case of HOCTAR (http://hoctar.tigem.it/) (Gennarino et al. 2008) and COMETA (http://cometa.tigem.it/) (Gennarino et al. 2012). In particular, using the latter tool, I obtained a list of high-confidence predicted target genes for miR-181a and miR-181b. I analyzed the list of the common predicted targets between the two miRNAs searching in particular for genes potentially able to explain the previously described morphant and overexpression phenotypes. By analyzing predicted target expression profiles, target sites conservation in Medakafish, and literature data I selected a group of ten possible miR-181a/b targets for experimental validation (Fig. 27).

I analyzed the predicted target gene expression changes in injected Medakafish (with Morpholinos or miRNA mimics) by quantitative RT-PCR. To detect the effects of miR-181a/b down-regulation on these transcripts, I extracted the RNA from eye tissues at stage 32, the first stage at which I observed the IPL phenotype, whereas to measure the over-expression effects I extracted the RNA at stage 22, when the developmental defects started to be detected.

As shown in figure 27, I analyzed the two different transcripts that encode for *SMAD2* (one located on chromosome 9, and the other on chromosome 12), *SMAD3*, *SMAD7* and *WNT11*, that did not show any significant alteration in morphant eyes with respect to control eyes. For *SMAD2* and *SMAD7*, I could not exclude that they could be real miR-181a/b targets. Indeed in the over-expressing embryos they were down-regulated with respect to controls, whereas in the morphant eyes, a little increase of these targets in the INL and GCL could not be appreciated in these experiments. In this hypothesis the

absence of increase in the morphant eye could be due to a dilution effect. Instead the *TGFB1R* and *BMPR2* transcripts alterations did not show any correlation with the miR-181a/b manipulation. Among the selected transcripts, only *ERK2* and *AKT3* levels resulted to be inversely correlated to the miR-181a/b alterations. I selected them for further characterization as putative miR-181 targets because this inverse correlation is a typical behaviour of miRNA-targeted transcripts, as also observed in the case of *PROX1*, an already validated target for miR-181a (Kazenwadel et al.2010) (Fig. 27).

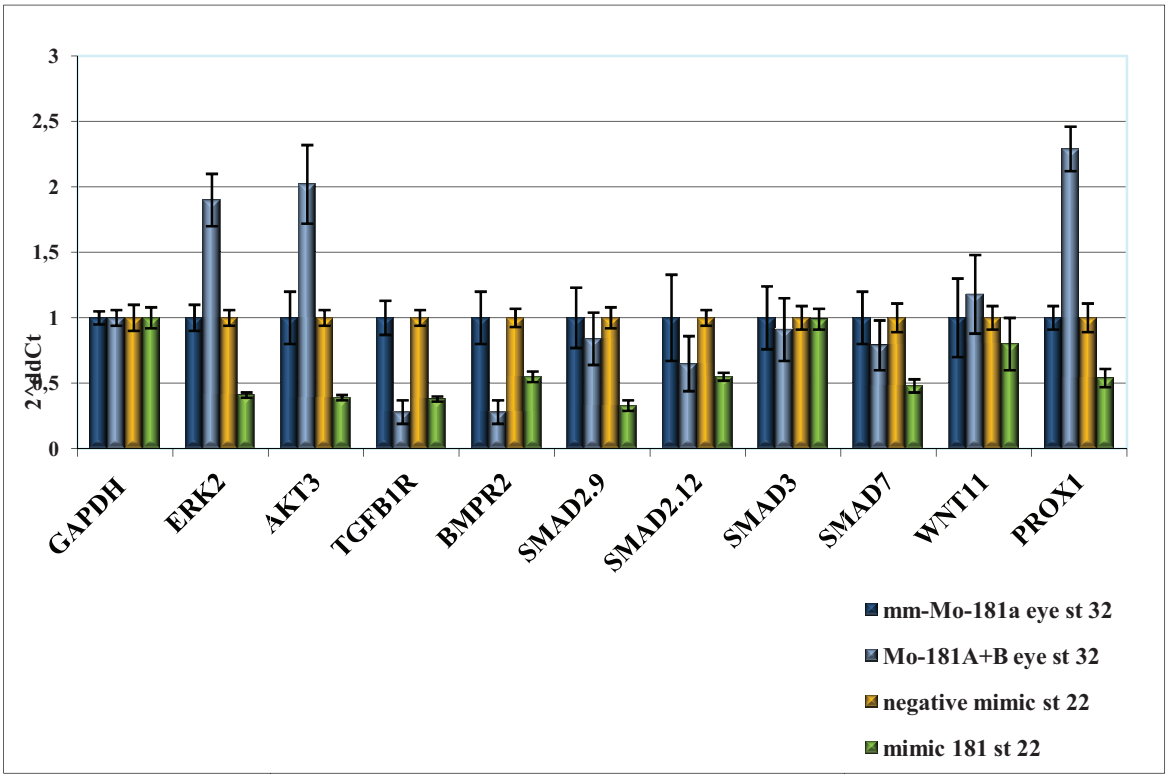

Figure 27. Analysis of miR-181a/b selected target levels. In the list of common target genes, were chosen a group of interesting genes on the basis of their expression profile, target site conservation and literature data. The selected genes were *ERK2, AKT3, TGFB1R, BMPR2, SMAD2, SMAD3, SMAD7, WNT11.*These genes were analised by qRT-PCR performed on RNA extraction from control and miR-181a/b-morphants eye (at stage 32) and control and miR-181a/b overexpression embryos (at gastrula stage).

To validate the direct binding of miR-181a/b to the 3'UTR of the *ERK2* and *AKT3* genes, I carried out luciferase assays in in vitro systems. To this purpose, I subcloned the human 3'UTR of the two genes including the predicted target

sites into a luciferase reporter construct, downstream the luciferase cassette and upstream the polyA signal. Then I co-trasfected the luciferase reporter construct with miRNA mimics duplex into HeLa cell lines that do not express neither miR-181a nor miR-181b. Luciferase activities was tested and normalized by a control luciferase activity. I observed a significant decrease of luciferase activity only in the case of the *ERK2* 3'UTR reporter construct, indicating that *ERK2* was a real and direct target of miR-181a/b (Fig. 28). On the other hand, I did not observe any significant variation of luciferase activity in the case of the *AKT3* 3'UTR reported construct indicating that the observed variation in mRNA levels, detected by RT-PCR (Fig. 27), were due to indirect effect of miR-181a/b expression alterations.

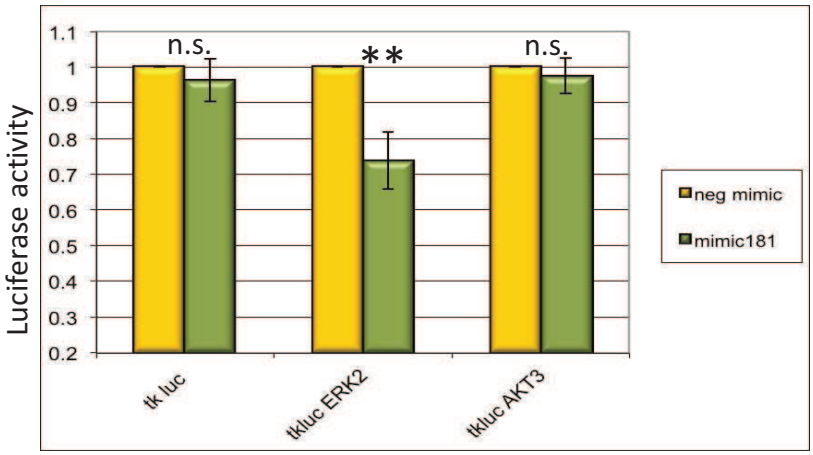

Figure 28. Luciferace validation assay. Relative Luc activities in HeLa cells as fold differences in the Luc/Renilla ratios normalized to the value of Luc reporter constructs. The construct with the *ERK2* 3'UTR or the *AKT3* 3'UTR were co-trasfected with a negative mimic or mimic-miR-181. The miR-181 addition decreases Luc activity of the construct containing 3′-UTR of *ERK2* when compared with control, whereas no significant variation of luciferase activity was detected in the case of the *AKT3* 3'UTR reported construct compared with control.

Once I established that there was a direct binding of miR-181a/b on the 3' UTR of the *ERK2* transcript, I carried out the luciferase assay using a mutagenized human *ERK2* 3' UTR. In that case I did not observe any significant variation of the luciferase activity demonstrating that the luciferase down-regulation

mediated by the human *ERK2* 3'UTR was due to the miR-181a/b binding, which did not occur in the mutagenized construct (Fig. 29 B)

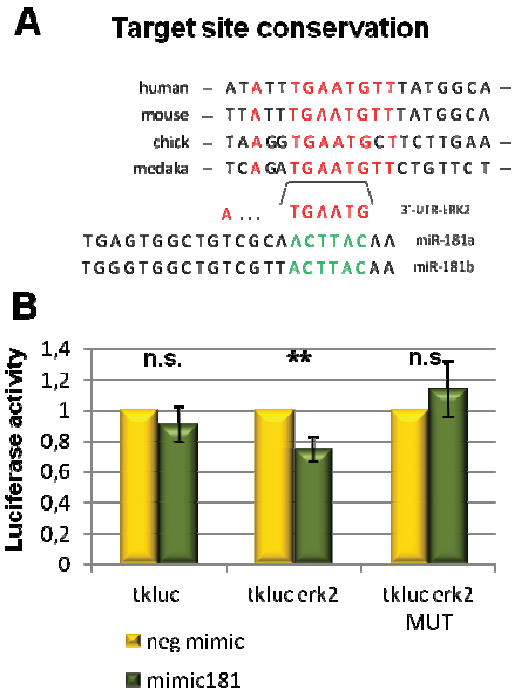

Figure 29. Luciferace assay indicate that *ERK2* is a real direct miR-181a/b target. A) Predicted target site of miR-181a/b within the 3′-UTR of the *ERK2* gene in different species, showing conserved nucleotides (red) and nonconserved nucleotides (black); in green is shown the seed region in miR-181a and miR- 181b. B) Relative Luc activities in HeLa cells as fold differences in the Luc/Renilla ratios normalized to the value of Luc reporter constructs. miR-181 addition decreases Luc activity of the construct containing 3′-UTR of *ERK2* when compared with controls. Point mutations in the predicted miR-181a/b target site in *ERK2* inhibit this effect.

As a further confirmation, not only the *ERK2* transcript levels were altered in the *in vivo* model, but also the ERK2 protein levels, as shown in western blot experiments (Fig. 30 A, B). I observed an increase of protein levels in the miR-181a/b morphant eyes and a decrease in the miR-181a/b over-expressing embryos, as already observed for the transcript levels. As shown in figure 30 C, I was also able to visualize by immunofluorescence analysis the increase of ERK2 protein levels in the retina of miR-181a/b morphant embryos at stage 32. ERK2 is catalytically inactive in its basal form. In order to become active, it requires phosphorylation events in its activation loops. This is conducted by specialized enzymes, the MEKs (MAP kinase kinase). Interestingly by western

blot analysis, using an antibody that recognize the phospho-ERK, I was able to detect the increase in morphant eyes of the phosphorylated form of ERK2 protein, and a decrease in over-expressing embryos, indicating that the alteration of ERK2 levels resulted also in an alteration of its active form, and probably of its activity (Fig. 30 A, B). ERK2 represents a very interesting target because it was already identified as a key player in different biological function including the control of axon growth in vertebrates (Biggs *et al.* 1994; Perron & Bixby 1999; Campbell & Holt 2001; Forcet *et al* 2002; Ming *et al* 2002; Carrer *et al* 2003; Campbell & Holt 2003; Althini *et al* 2004; Kim *et al* 2004; Pipet *et al* 2006). I hypothesized that the alterations of ERK2 expression levels could be the cause of the defects observed when the miR-181a/b functions were manipulated and therefore decided to gain further insight into this specific issue.

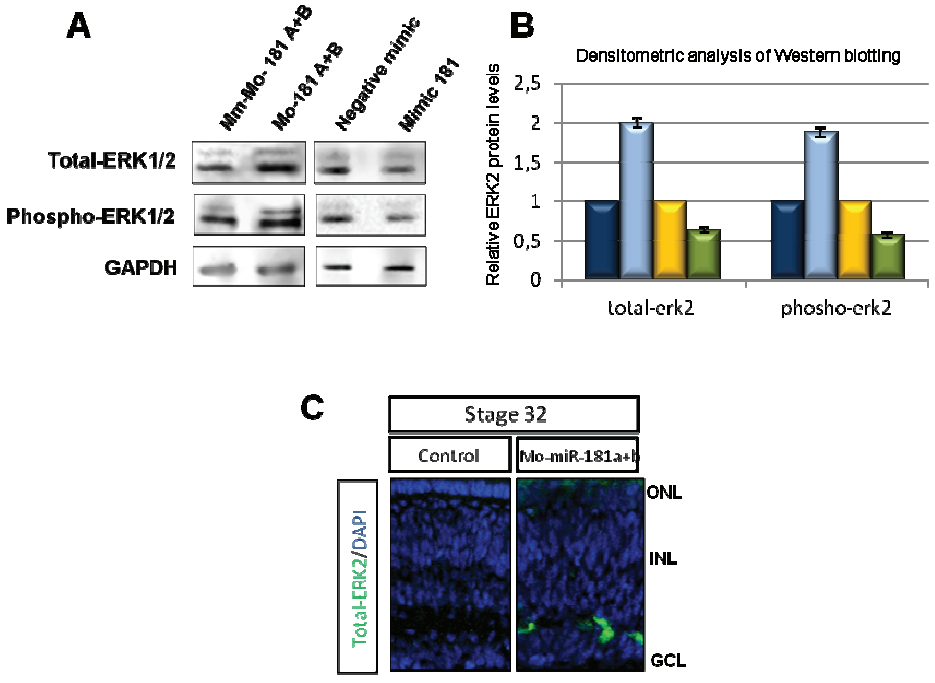

Figure 30. *In vivo* analysis of ERK2 protein levels. *In vivo* analysis of *ERK2* levels by western blot (A) show the *ERK2* increase in miR-181a/b-morphants eye and its decrease in mimic-181 overexpressing embryos. B) Densitometric analysis of western blotting shows also increased levels of phospho-ERK2 in morphants eye and decreased levels in mimic-181 overexpressing embryos. C) Frontal sections of St32 control and miR-181a/b-morphants immunostained with antibodies (green) against ERK2 and counterstained with DAPI (blue).

3.10 Interference with miR-181a/b function alters MAPK signaling via ERK2 targeting

ERK2 is a kinase member of the MAPK signaling cascade that is involved in different cellular biological functions (see for a review Kyriakis and Avruch, 2012). It was demonstrated that in Zebrafish ERK2 down-regulation causes severe developmental defects due to the absence of its activity in the regulation of actin and tubulin cytoskeletal reorganization processes, leading to the arrest of embryogenesis (Krens et al. 2008). Moreover it was demonstrated that ERK2 is involved in synaptic plasticity, learning and memory (Long-Term Potentiation) (Adams & Sweatt 2002; Satoh *et al* 2007; Satoh *et al* 2011) and in regulating neuronal processes such as responses to growth factor and morphogens. (Biggs *et al.* 1994; Perron & Bixby 1999; Campbell & Holt 2001; Forcet *et al* 2002; Ming *et al* 2002; Carrer *et al* 2003; Campbell & Holt 2003; Althini *et al* 2004; Kim *et al* 2004; Pipet *et al* 2006). To further evaluate the possible contribution of ERK2 to the phenotype caused by miR-181a/b loss- and gain-of-function, I decided to analyze its downstream targets in the signaling cascade involved in the modulation of cytoskeletal regulator molecules. This signaling cascade, under the appropriate stimuli, lead to the activation of local protein synthesis of Cofilin/ADF (Actin Depolimerization Factor) and RhoA involved in actin retraction. As reported in figure 31, I found that miR-181a/b loss-of-function, by increasing the ERK2 protein levels and ERK2 activity, increased the activation of this pathway. By western blot analysis I observed an increased phosphorylation of eiF4E, eiF4E-BP, and p70/S6K, markers of protein synthesis activation. Furthermore, I found that this activation led to increased levels of Cofilin and RhoA proteins (Fig. 31 A). To verify whether this increase in Cofilin production corresponded also to an increase in its activity, I evaluated the ratio

between its active form versus its inactive form. Cofilin protein is active in its de-phosphorylated form and inactive when phosphorylated. I found that in morphant eyes the active form of Cofilin was increased (Fig. 31 C). Increase in Cofilin activation and RhoA levels have been already described to lead to growth cone collapse or turning (Campbell & Holt 2001; Lung et al. 2006; Piper et al. 2006; Campbell & Holt 2003). Therefore, their increased levels in miR-181a/b morphant eyes could explain the axogenesis and axon length defects observed (Fig. 23 and 24).

In overexpressing miR-181a/b embryos, I observed an opposite trend, with a general decrease of the MAPK-signaling cascade, that led to a reduction of Cofilin and RhoA protein levels, whose loss of activity on cytoskeletal reorganization could explain the severe developmental defects observed in the over-expressing embryos (Fig. 31 A). With these data I demonstrated that not only ERK2 is a real target of miR-181a/b, but also that its alteration mediated by miR-181a/b manipulation, had consequences on its downstream biochemical pathway. The alteration of this pathway could be underlying in the observed phenotypes.

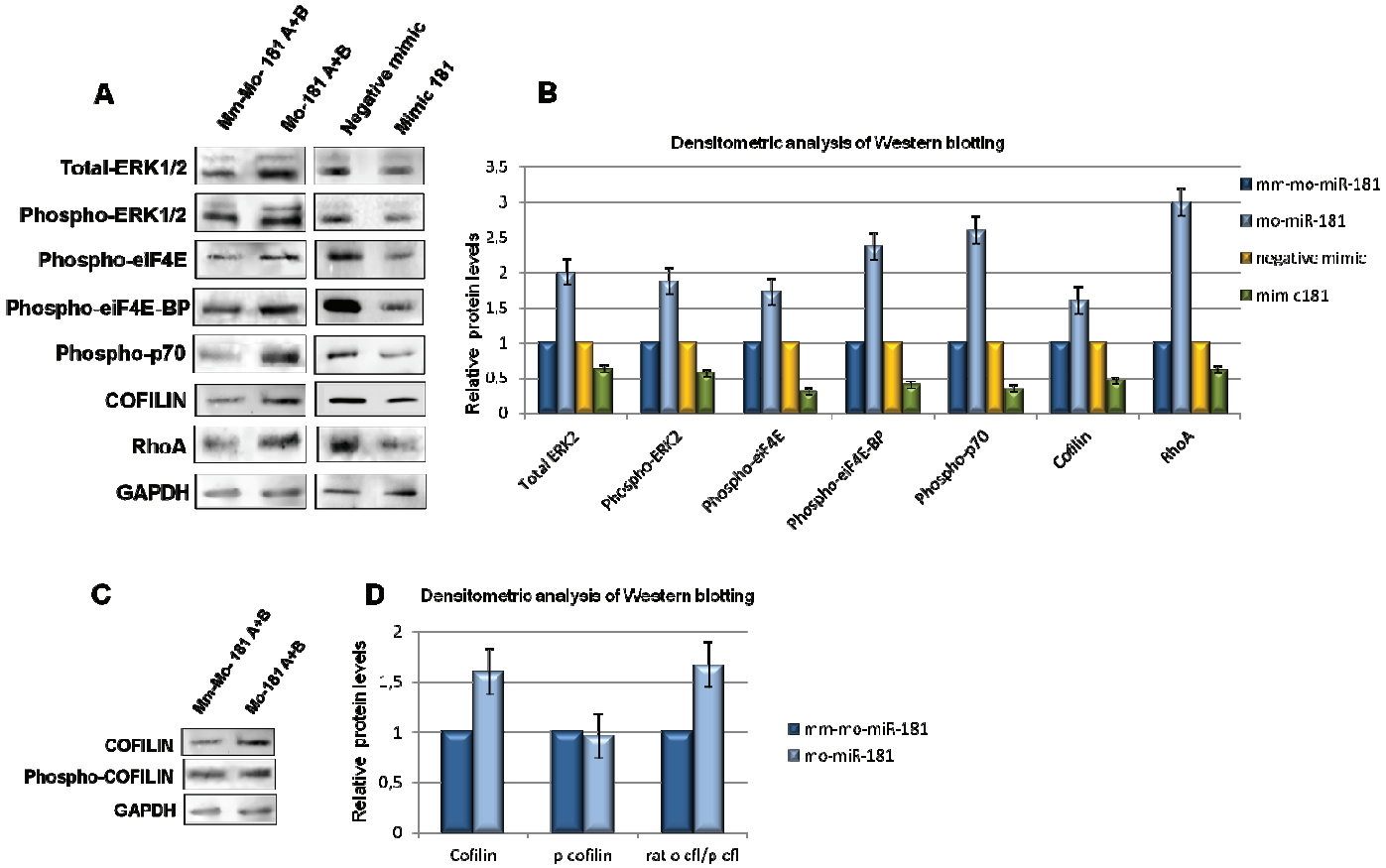

Figure 31. Interference with miR-181a/b function alters MAPK signaling via ERK2 targeting. A) Western Blot experiments showed alteration of MAPK signaling cascade involved in the modulation of cytoskeletal regulator molecules. miR-181a/b loss-of-function, by increasing the ERK2 protein levels and ERK2 activity, increased the activation of this pathway. The Western Blot and the densitometric analysis (B) showed an increased phosphorylation of eiF4E, eiF4E-BP, and p70/S6K, markers of protein synthesis activation. This activation led to increased levels of Cofilin and RhoA proteins. In overexpressing miR-181a/b embryos an opposite trend was observed with a general decrease of the signaling cascade. C) Western Blot of Cofilin (active form) and phospho-Cofilin (inactive form) and densitometric analysis (D) showed that the ratio between its active form versus its inactive form indicated the active form of Cofilin was increased in morphant eyes.

3.11 Administration of the MEK inhibitor PD98059 rescues the IPL thickness phenotype of miR-181a/b morphant embryos

If indeed the increase of ERK2 and of its downstream targets played a causative effect on the eye phenotype observed in miR-181a/b morphants, I hypothesized that by inducing their decrease I could obtain a rescue of that phenotype. Since it was not possible to down-regulate ERK2 by morpholino due to early embryonic lethality, as previously described, (Krens et al. 2008), I decided to adopt an alternative strategy based on the use of the drug PD98059. PD98059 leads to a decrease of ERK activation due to its selective inhibition of MEK1 and MEK2 kinase activity, responsible for ERK phosphorylation.

Mo-miR-181a/b injected embryos were treated with hatching enzyme to remove the egg envelop and then were grown from stage 30 in the presence of the MEK inhibitor PD98059 at a concentration of 25 μM and 3%DMSO, used to facilitate the penetrance of the drug. As negative controls, we used control and morphant embryos treated with 3% DMSO only.

The treatment with PD98059 was able to rescue the IPL defects of morphant eyes (Fig. 32 A a, b, c; red lines), quantified as the ratio between the IPL area and the total retina area (Fig. 32 B). By western blot experiments I found that this phenotypic rescue was accompanied by the rescue of the signaling pathway cascade alterations (Fig. 32 C, D). Consistent with my hypothesis, the levels of the total ERK2 protein did not change with respect to the untreated morphant embryos, and were persistently higher with respect to control embryos.

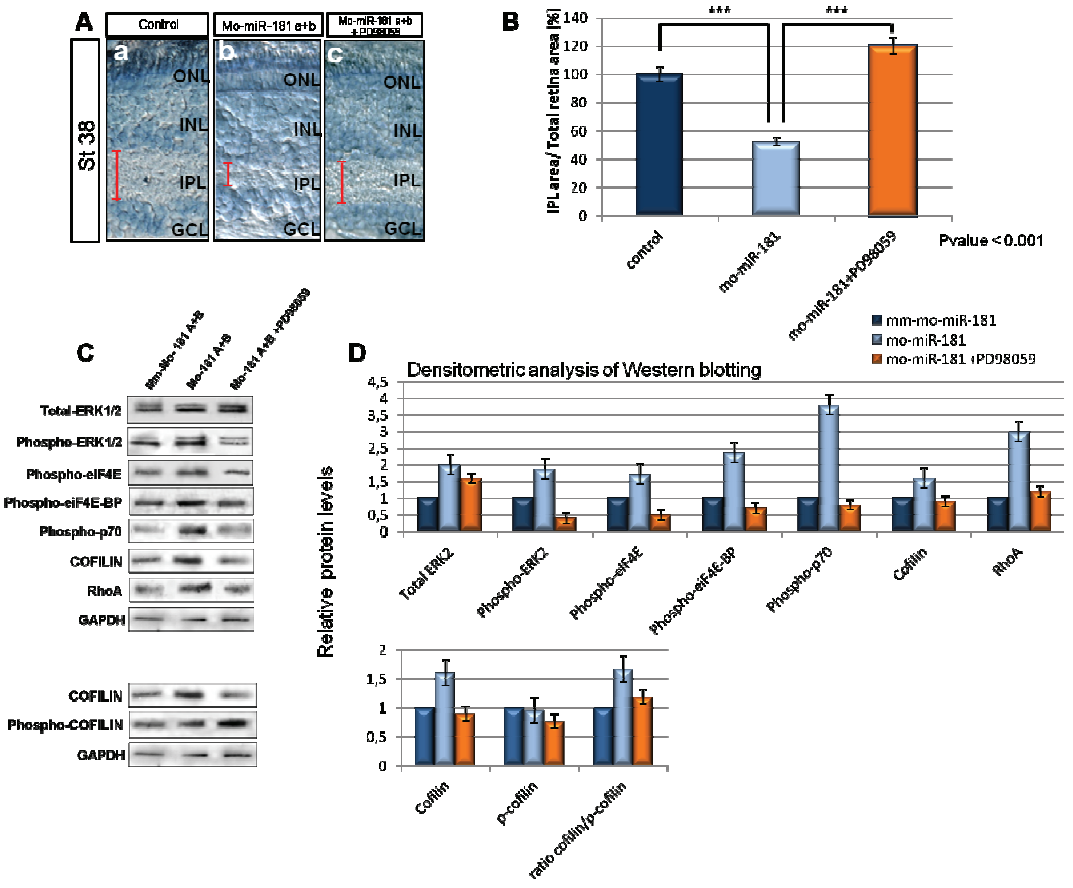

Figure 32. The ERK2-Pathway alteration in miR-181-morphants retina causes IPL phenotype (*in vivo).* A) Frontal section of st40 of control (a), miR-181a/b-morphants (b) and miR-181a/b-morphants+PD98059(c) medakafish eye stainded with Richardson(Romeis) solution show that the MEKs inhibitor PD98059 added to miR-181a/b-morphants rescues the IPL phenotype (a-c, red line; and chart B). C-D) The PD98059 inhibiting the MEKs activity decrease the phospho-ERK2 levels. (C) Western Blot demonstrate that the rescue of the phonotype is due to the rescue of correct ERK-pathway activity, quantified by densitometric analysis (D).

To demonstrate that the rescue of the IPL thickness phenotype was also accompanied by a rescue of the axogenesis defects I treated the Six3.2 mo-miR-181a/b-injected embryos with PD98059. I observed a significant rescue of amacrine processes formation, which was comparable with what present in controls (Fig. 33 C). These data allowed me to conclude not only that the IPL phenotype is indeed caused by the loss of miR-181a/b regulation on ERK2 and, as a consequence on its downstream targets, but also that miR-181a/b play a role in amacrine cell axon specification via ERK2 modulation.

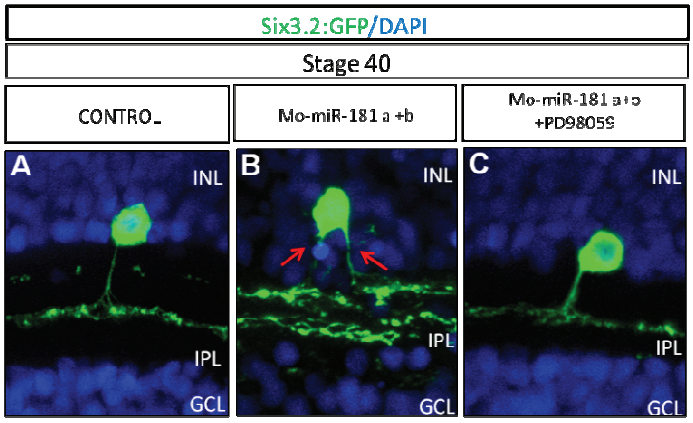

Figure 33. The PD98059 tratments rescue the amacrine axogenesis defects (*in vivo*). The rescue of the IPL thickness phenotype was accompanied by a rescue of the axogenesis defects in the PD98059 treated Six3.2 mo-miR-181a/b-injected embryos. Frontal cryostat sections of St40 control (A), mo-miR-181a/b-injected (B) and mo-miR-181a/b-injected+PD98059 (C) *Six3.2:EGFP* medakafish embryos counterstained with DAPI (blue), showed a significant rescue of amacrine processes formation, indicating a miR-181a/b role in amacrine cell axon specification via ERK2 modulation.

The above *in vivo* analysis demonstrated that by decreasing the levels of active ERK2 in morphant embryos I could obtain the rescue of the IPL phenotype and amacrine axogenesis defects. To demonstrate that the loss of miR-181a/b cause also the RGC growth defects via ERK2, I cultured miR-181a/b morphant retina neurons in presence of the PD98059 drug. I dissociated the morphant Ath5 transgenic line eye as previously described (see Chapter 3.5). After 1 hour I added PD98059 at a 10 μM concentration and 3%DMSO. After 24 hour I analyzed the axon length of 100 mo-miR-181a/b+PD98059 cells, derived from different experiments and different injections. I found that the administration of the MEKs inhibitor PD98059 on primary cultures of mo-miR-181a/b RGC rescued the axon length defect as shown in figure 34 C and 34 D. These data indicate that miR-181a/b play a role in RGC axon growth via ERK2 targeting.

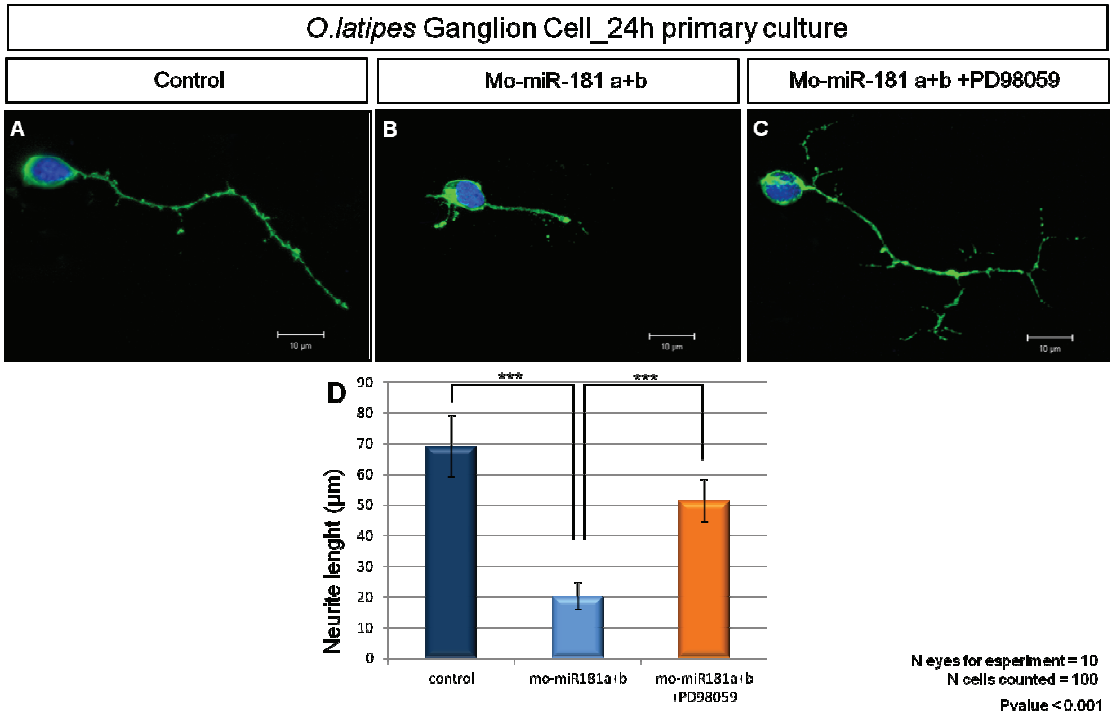

Figure 34. The PD98059 tratments rescue the RGCs axon length defects (*in vitro*). Medakafish Ganglion cell primary culture from control (A), miR-181a/b-morphants (B) and miR-181a/b-morphants+PD98059 (C) Ath5:eGFP transgenic line eyes indicate a significant rescue of the axon length defects as shown in the graph (D).

3.12 TGF-β on morphants embryos rescues the IPL thickness phenotype

The previous data demonstrated that miR-181a and miR-181b are able to modulate the MAPK signaling pathway. The miR-181-mediated ERK2 negative modulation was needed to regulate the local protein synthesis activation responsible for a correct axon specification and axon growth.

To further investigate this regulatory network involved in retinal axon specification and growth via miR-181a/b, I decided to focus my attention on the study of the role of the TGF-β pathway. It is known that this pathway regulates, through the modulation of RhoA levels, the axon specification in brain (Yi J. 2010). Moreover, recent studies demonstrated its role in the regulation of the biosynthesis of some miRNAs, including miR-181a and miR-181b (Davis et al 2008; Hata et al. 2010; Wang 2010; Wang 2011).

Therefore, I hypothesized a role for TGF-β in regulating retinal axon specification through two different mechanism: a) the first operating through the already known activation of Par6 and subsequent decrease of RhoA due to its ubiquitinization and degradation; and b) the second operating through the increase of miR-181 maturation, subsequent *ERK2* decrease and decreased protein synthesis of RhoA and Cofilin.

I first found that the *in vivo* administration of TGF-β (10ng/mL) increased miR-181a/b levels in the eye, as assessed by TaqMan RT-PCR (Fig. 35 A). The increase of both miR-181a and miR-181b was sufficient to lead to *ERK2* transcript decrease (Fig. 35 B) and ERK2 protein level decrease (Fig. 35 C).

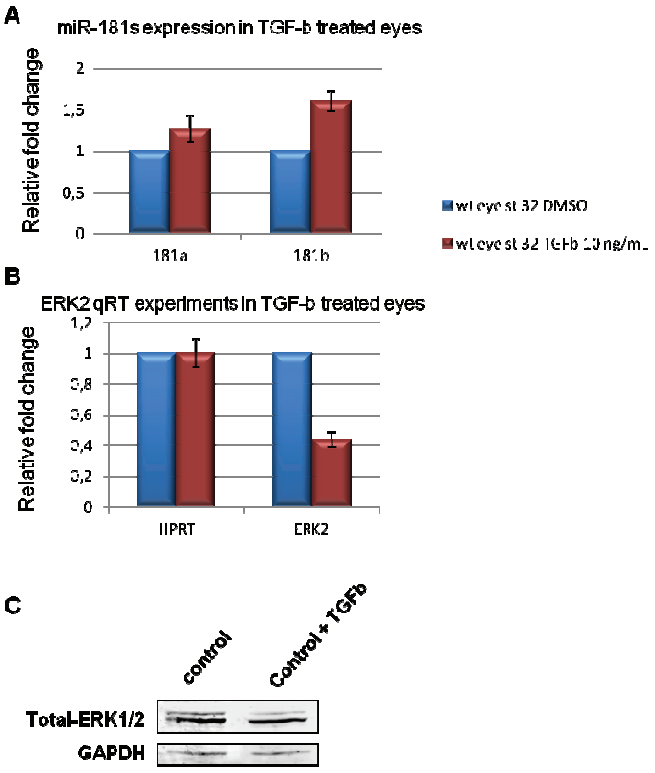

Figure 35. *in vivo* administration of TGF-β increased miR-181a/b levels in the eye. A) TaqMan RT-PCR of miR-181a and miR-181b on RNA extraction of TGF-β (10ng/mL) treated eyes compared to control eyes. B) *ERK2* qRT-PCR analysis on RNA extraction of TGF-β (10ng/mL) treated eyes compared to control eyes. C) Western Blot analysis of ERK2 RNA extraction of TGF-β (10ng/mL) treated eyes compared to control eyes.

To further confirm my hypothesis, I administered TGF-β to miR-181a/b morphant embryos from stage 30 and obtained the rescue of the IPL thickness phenotype (Fig. 36 A a, b, c; red lines), quantified as ratio between the IPL area and the total retina area (Fig. 36 B). This rescue may be due at least in part to the action of TGF-β on miR-181a/b levels, as suggested by the decrease of Total ERK2 levels (Fig. 36 C, D), that finally led to the decrease of RhoA protein levels (Fig. 36 C, D). In order to discriminate the relative contribution of the two mechanism, activated by the TGF-β ligands, in the regulation of RhoA levels and axon specification in the retina, further analysis will have to be performed in presence of the proteasomal inhibitor MG132.

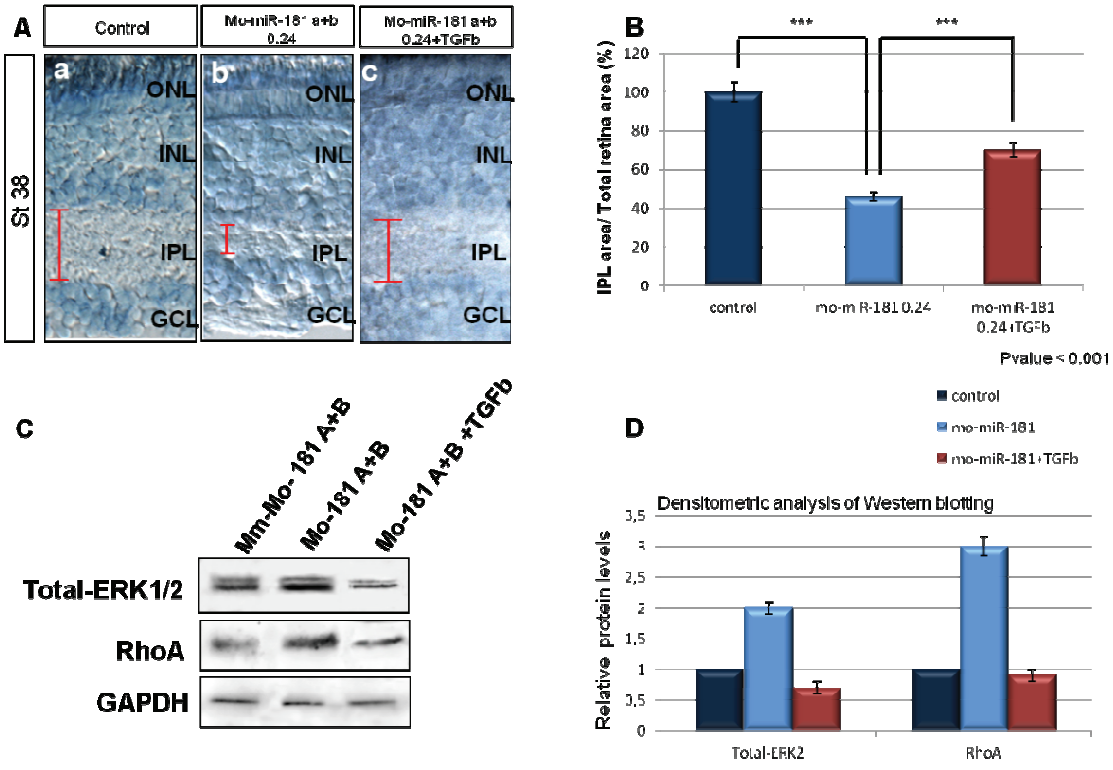

Figure 36. *in vivo* administration of TGF-β rescues the IPL thickness defect. A) Frontal section of st40 of control (a), miR-181a/b-morphants (b) and miR-181a/b-morphants+TGF-β (c) medakafish eye stainded with Richardson(Romeis) solution show that the TGF-β added to miR-181a/b-morphants rescues the IPL phenotype (a-c, red line; and chart B). C) Western Blot demonstrate that the TGF-β treatment on miR-181a/b-morphants rescue of total-ERK2 protein and RhoA levels, quantified by densitometric analysis (D).

With these data I was able to demonstrate that the TGF-β pathway and the ERK2 cascade exert an antagonist action in the regulation of retina axon specification and growth in vivo. I suggest that this antagonism is exerted via TGF- β regulation of miR-181a/b expression levels, that act in concert with the TGF- β regulation of RhoA levels. In conclusion, I propose a model in which miR-181a/b and TGF- β play a key role in the signaling network that define the correct axon specification of amacrine cells and axon growth of RGCs (Figure 37).

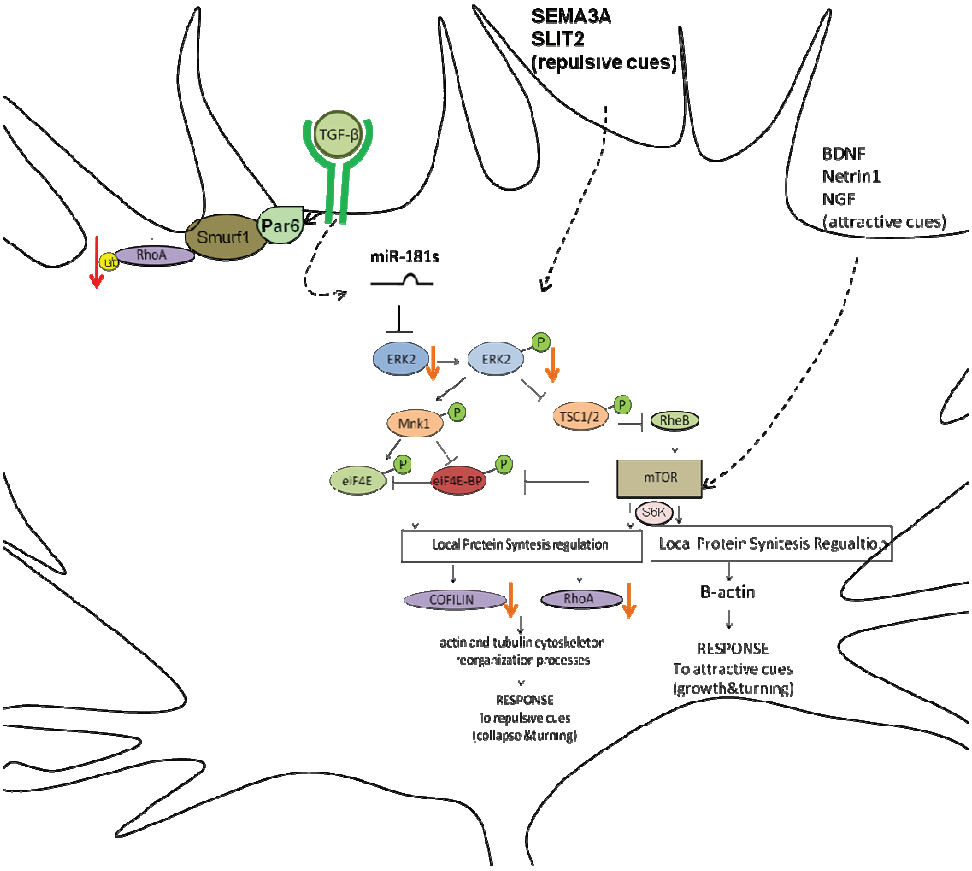

Fig. 37. Model for the regulation and function of miR-181a/b in the axon specification and growth processes. I propose that the TGF-β/MAPK signaling antagonism in the neuronal process formation is exerted via miR-181a/b. The TGF-β signaling regulates, on one hand, the RhoA degradation, and, on the other, the RhoA protein synthesis decrease via regulation of miR-181a/b levels. In fact the miR-181a/b, by regulating the *ERK2* levels, are able to modulate the MAPK signaling cascade and the protein synthesis of RhoA, allowing its physiological down-regulation, needed for neuron polarization and rapid elongation of the neurite. Then during axon elongation the miR-181a/b effect on *ERK2* levels is needed in the modulation of MAPK signaling and Protein synthesis of RhoA and Cofilin (Actin Depolimerization Factor), responsible for cytoskeletal modification involved in axon growth cone collapse and turning.

4. DISCUSSION

miRNAs appear to function as key regulators of biologically relevant molecular pathways through their ability to fine-tune gene dose (Zhao and Srivastava, 2007). Taking into account the fact that each miRNA can regulate the expression of several hundred target genes, the miRNA apparatus is expected to play a key role in controlling gene expression for a significant fraction of the vertebrate transcriptome. As a consequence, miRNAs are endowed with basic roles in the regulation of development and pathophysiology of tissues and organs in vertebrates (see for some example the reviews Guller and Russell, 2010; Bhatt, Mi and Dong, 2011; Bian and Sun, 2011; Im and Kenny, 2012).

The general importance of miRNAs in eye development and diseases is supported by the effects observed in mice after conditional inactivation of Dicer, a key enzyme in miRNAs biogenesis (Damiani et al. 2008; Georgi et al. 2010; Iida et al. 2011; Pinter et al. 2010). However, there is still little information available on the specific role of individual miRNAs contributing to the correct development and function of the eye. Genetic gain- and loss-of-function studies performed in frogs, fish, and mice are beginning to disclose the role of specific miRNAs in retinal development, physiology and disease (see for a review Sundermeier and Palczewski, 2012). These studies suggested that the role and composition of miRNA-regulated gene network in eye development is wide and is only starting to be unravelled.

The aim of my project was to identify miRNAs highly enriched in the vertebrate eye and to investigate their roles in the regulatory networks underlying eye developmental processes. To study individual microRNA functions, I took advantage of Medakafish (*Oryzias latipes*), which is considered an ideal model organism to study developmental biology processes including eye development

(Wittbrodt et al., 2002). Indeed, medakafish is a model system particularly amenable for reverse-genetic analyses. Microinjections of either mimic or antisense morpholino oligonucleotides results, respectively, in gene/miRNA overexpression or knockdown, without any laborious, time- and resource-consuming techniques (Ishikawa, 2000), as already demonstrated in recent work published in Banfi's lab (Conte et al. 2010a).

Starting from microRNA microarray profiling analysis, I first identified a group of evolutionarily conserved eye-enriched microRNAs (Fig. 17). Among them, I focused my attention on the functional characterization of the miR-181a/b cluster. I demonstrated that, besides their sequence, also their expression profile during eye development is highly conserved across vertebrate evolution (Fig. 18 and 19). The combined down-regulation of miR-181a and miR-181b, by morpholinos, caused a specific retinal phenotype characterized by the reduction of the Inner Plexiform Layer (IPL) thickness (Fig. 21), without any apparent reduction in the number of retinal cells (Fig. 22). Taking advantages of the availability of specific medakafish transgenic lines, I demonstrated that miR-181a/b loss-of-function led to defect of axogenesis in amacrine and retinal ganglion cells (RGCs) (Fig. 23).

By means of *in silico* predictions and using a variety of *in vitro* and *in vivo* experimental approaches, I have shown that ERK2 is a target of miR-181a/b activities (Fig. 29). I also demonstrated that the specific miR-181–mediated regulation of ERK2 modulates the function of the MAPK signaling cascade, which is involved in axon growth control (Fig. 37). These data indicate that miR-181a/b are essential component of the MAPK molecular pathway, and hence are important element of the molecular network that regulates axon formation during amacrine cell and RGC development.

The ERK, p38, JNK mitogen-activated protein kinases (MAPKs) are intracellular signaling pathways that play a pivotal role in many essential cellular processes, such as proliferation and differentiation (see for a review Kyriakis and Avruch, 2012). The extracellular signal-regulated kinases (ERK1/2) are among the most prominent signal transduction molecules through which extracellular stimuli are propagated from the cell surface to cytoplasmic and nuclear effectors. ERK1 (*mapk3*) and ERK2 (*mapk1*) exhibit 84% sequence identity and are activated through the sequential phosphorylation of the mitogen-activated protein kinase (MAPK) cascade. Significantly, although both ERK1 and ERK2 are expressed in the same tissues (Selcher et al., 2001; Mazzucchelli et al., 2002), genetic inactivation of ERK1 has only subtle phenotypic effects, whereas ERK2 inactivation results in early embryonic lethality (Aouadi et al., 2006). These studies strongly support our hypothesis of a regulatory cascade in which miR-181a/b are required to modulate the MAPK signaling pathway. Indeed, miR-181a/b over-expression led to a significant down-regulation of ERK2 activity, with phenotypic consequences similar to those observed after ERK2 loss-of-function, in both murine and fish models (Fig. 26). Krens and colleagues, in 2008, demonstrated that mo-*erk2* zebrafish embryos display severe developmental defects due to primary changes in gastrulation cell movements and not caused by altered cell fate specification. Their data demonstrated that the absence of phospho-ERK2 from the blastula margin blocked initiation of epiboly, actin and tubulin cytoskeleton reorganization processes and further arrested embryogenesis (Krens et al.2008). Similar to mouse, also in zebrafish ERK1 knockdown had only a mild effect on epiboly progression, defining distinct roles for ERK1 and ERK2 in developmental cell migration processes during embryogenesis. In our miR-181 over-expressing medakafish embryos, I

demonstrated that the decrease of ERK2 levels led to decreased Cofilin/ADF and RhoA protein levels, impairing actin remodeling and consequently leading to severe developmental defects.

To determine the role of ERK2 during nervous system development, a murine model in which *mapk1/*ERK2 undergoes conditional inactivation at the peak of neurogenesis was previously generated, allowing the identification of ERK2 involvement in synaptic plasticity, learning and memory (Adams & Sweatt 2002; Satoh *et al* 2007; Samuels 2008; Satoh *et al* 2011). It has been recently demonstrated that a group of genetic disorders termed neuro-cardio-facial cutaneous syndromes (including cardio-facio-cutaneous, Costello, Leopard, and Noonan syndromes) are caused by mutations in upstream elements of the ERK/MAPK signaling cascade (Bentires-Alj et al., 2006; Roberts et al., 2006) and are generally characterized by distinctive cardiac and craniofacial defects, developmental delay, and mental retardation. The mutation of downstream elements in the ERK cascade has similarly been associated with mental retardation syndromes (Weeber and Sweatt, 2002). The identification of individuals with haploinsufficiency for the ERK2 gene as a result of distal microdeletions at 22q11.2 (Shaikh et al., 2007) enabled the first analysis of humans with reduced expression levels of ERK2. These patients exhibit microcephaly and neurodevelopmental deficits, consistent with the phenotype observed in the murine models.

During nervous system development, the ERK/MAPK signaling is activated in responses to growth factor and morphogens involved in neuronal processes formation (Biggs *et al.* 1994; Perron & Bixby 1999; Campbell & Holt 2001; Forcet *et al* 2002; Ming *et al* 2002; Carrer *et al* 2003; Campbell & Holt 2003; Althini *et al* 2004; Kim *et al* 2004; Pipet *et al* 2006). The *in vitro* stimulation of

ERK/MAPK signaling activity, through the use of repulsive guidance cues such as SEMA3A and/or Slit2, led to growth cone collapse or turning and inhibition of neurite growth (Campbell & Holt 2003; Piper et al. 2006). This inhibition is due to the Cofilin/ADF and RhoA protein synthesis, via phosphorylation of eiF4E and mTOR pathway activation (Campbell & Holt 2001; Lung et al. 2006; Piper et al. 2006; Campbell & Holt 2003). These observations suggest that perturbations in ERK/MAPK signaling, in both positive or negative directions, underlie a diverse range of neurodevelopmental defects.

In agreement with these data, in medakafish embryos, expression levels of ERK2 and, concomitantly, the activation of its downstream targets (Fig. 31) are increased in miR-181a/b knock-down eyes. Furthermore, the axon growth alterations observed in miR-181a/b morphants (Fig. 24) strongly resembled those reported for ERK2 activation in *Xenopus* axon growth cone upon repulsive cues stimulation (Campbell & Holt 2003).

I found that concomitant knockdown of miR-181a/b and decrease of ERK2 phosphorylation, using PD98059, significantly rescued levels of phospho-ERK2 and its downstream targets, phospho-eiF4E, phospho-eiF4E-BP, phospho-p70, Cofilin and RhoA levels in the eyes (Fig. 32), leading to the rescue of axon defects (Fig. 33 and 34). The above observations are consistent with a pathway in which miR-181a/b control local protein synthesis activation and axon growth through regulation of ERK2 levels. In summary, these data demonstrated, at least in RGCs, that miR-181a/b play an important role in axon growth via ERK2 modulation, and that the loss of their functions caused a decrease in axon length. The *in vitro* primary culture experiments (Fig. 24 and 34) gave also the indication that these axon defects are RGC cell-autonomous and did not depend on altered information that could derive from surrounding tissues.

Additional experiments are needed to determine if the branching defects of RGCs axons at optic tectum are secondary effects due to these axon growth defects or are due to the loss of miR-181a/b function in the optic tectum neurons. Using the cell transplantation technique it will be possible to isolate the eye precursor cells or optic tectum precursor cells from mo-miR-181s-injected embryos and transplant them in a control embryos. In that way, it will be possible to discriminate between the defects due to the miR-181s ablation in the retina cells and the defects due to the miR-181s ablation in the optic tectum.

The experiment carried out in the Six3.2:eGFP transgenic line (Fig. 23) highlighted another axonal phenotype characterized by the presence of different processes emerging from a single amacrine cell body, instead of one specified axon as in controls. One explanation for this phenotype could be that the miR-181a/b loss-of-function led not only to RGC axonal defects but, during amacrine cells development, also caused the trans-differentiation of one amacrine subtype to another. Indeed there is a strong variability in the amacrine structure of the different and numerous amacrine subtypes. However, the first analysis of amacrine cell markers to identify the different subtype, did not highlight an increased number of one subtype at the expense of others. The use of additional other markers will be helpful to complete this analysis. However, the other and more likely explanation would be that the different processes, observed in mo-miR-181a/b Six3.2:eGFP amacrine cells, correspond to multiple specified axons or immature processes that are not correctly specified in axon or dendrites. Dotti and colleagues demonstrated that the axon specification process starts with neuronal polarization that occurs when one of the neurites emerging from the cell body elongates rapidly; this neurite becomes the axon, whereas the remaining neurites become dendrites (Dotti et al. 1988). In 1999,

Bradke and Dotti also demonstrated that the neurite with the most active growth cone became the cell's axon (Bradke and Dotti, 1999). Furthermore, they showed that inactivation of RhoA produced the loss of F-actin and the growth of multiple axons, concluding that the remodelling of growth cone actin is a physiological requirement for neuronal polarization and that the Rho family of GTPases is involved in the control of neuronal polarization (Bradke and Dotti, 1999).

In the mo-miR-181a/b-injected eyes, I observed the increase of RhoA levels and Cofilin/ADF, as final result of the increased activation of the MAPK signaling cascade. Supported by the rescue experiments in both *in vitro* and *in vivo* conditions, I demonstrated that the ERK2 increased activity is the cause of the axon growth defects in RGCs, and the axon specification defects of amacrine cells (Fig. 33 and 34). The physiological down-regulation of RhoA, needed for neuron polarization and rapid elongation of one neurite, did not occur in amacrine cells following miR-181a/b function ablation. This could explain why, even if partially polarized, amacrine cells of miR-181a/b morphant embryos did not correctly specify the axon. With the *in vitro* analysis of medakafish RGCs primary cultures, it was not possible to further investigate this axon specification phenotype because the *in vitro* cultured RGCs have the ability to polarize intrinsically, with the immediate and fast growth of one extension that becomes the principal axon (Zolessi et al. 2006). The presence of two different phenotype for RGCs and amacrine cells could be explained analyzing the onset of miR-181s expression (Fig. 19). Indeed miR-181a/b started to be detected by ISH at stage 30 when the RGCs have already specified their axons whereas the amacrine cells are differentiating and do not have yet specified the axons. This implicated a RGC axon specification

mechanism independent from the miR-181a/b activity, whereas their functions are needed in the other phases of RGC axon growth. The presence of a different mechanism for axon specification in the RGCs is in agreement with previous *in vivo* data which report that the developing RGC axons emerge directly from uniformly polarized cells in the absence of other neurites (Zolessi et al. 2006).

On the contrary, in amacrine cells, the loss of miR-181a/b function in a pre-axon-specification stage determined firstly an axon specification defect. To further investigate and elaborate these observations, I will determine the best *in vitro* culture condition to analyze amacrine axon formation in control and morphant eye explants. I will use a medakafish transgenic line in which the GFP is expressed under the control of an amacrine-specific promoter, such as the Six6 promoter. In *in vitro* condition it will be possible to use axon specific marker (Tau1), and/or dendrites specific marker (Map2), in order to determine if the multiple observed processes are multiple specified axons (Tau1 positive), dendrites (MAP2 positive) or unspecified processes.

As previously mentioned, Bradke and Dotti identified a mechanism by which the neurite with the most active actin filament dynamics becomes the axon, and that the RhoA GTPase is implicated in this mechanism. Moreover they hypothesized that the selection of the neurite to become axon depends on the contact with a factor, or different concentration of it, that activate a signaling cascade leading finally to actin remodeling and process elongation. Only recently it was demonstrated that, at least in the brain, this signaling cascade is mediated by the TGF-β molecules (Yi et al. 2010). In this study, the authors demonstrated that the TGF-β-dependent axon specification in brain is a Smad- independent mechanism, mediated by site specific phosphorylation of Par6. The latter, by

recruiting the ubiquitin ligase Smurf1, promotes the proteasomal degradation of RhoA (Ozdamar et al. 2005). In their model, in the neurite nearest the TGF-β gradient area, the local levels of RhoA result to be decreased and altered the actin dynamics, allowing the process elongation and axon specification.

At present, a similar mechanism is not yet described for the retinal amacrine cells axon specification. To further investigate on the regulatory network involved in amacrine axon specification via miR-181a/b, I decided to focus my attention on the TGF-β pathway.

Different studies, reported in literature, identified an antagonistic effect between the TGF-β/BMP pathways and ERK2 in the regulation of axon/dendrites specification and growth (Kerrinson et al. 2005; Hocking at al. 2007; Walshe et al. 2011; Kim et al. 2004). In these studies the authors demonstrated that members of BMP family increase neurite number, length and complexity (Kerrinson et al.2005). Developing similar analysis on retinal neurons, Hocking et al, from McFarlane group, addressed the role of TGF-β ligands in promoting RGC dendrites *in vivo* and *in vitro* (Hocking et al. 2007). Interestingly in the study of Walshe and colleagues, a crosstalk between TGF-β and the MAPK signaling was identified in the RGC-5 cell line (Walshe et al. 2011). Kim and colleagues analyzed the crosstalk between TGF-β/BMP and ERK/MAPK pathways in *in vitro* rat sympathetic neurons, demonstrating that inhibition of ERK1/2 functions potentiates dendritic versus axonal growth in the presence of BMPs, whereas its FGF-mediated activation inhibits the TGF-β/BMP-stimulated dendritic growth in sympathetic neurons (Kim et al. 2004).

Even if a conspicuous number of studies indicated that these two signaling pathways act in an antagonistic manner in the neuronal processes formation, it was not yet identified the molecular mechanism through which this antagonism

was exerted. I investigated about a possible role for TGF-β in the regulation of retina axon specification, hypothesizing two different mechanism: the first, as in the brain, consisting in the activation of Par6 and subsequent decrease of RhoA due to its ubiquitination and degradation (Yi et al. 2010); the second, through the increase of miR-181a/b maturation (Davis et al. 2008; Hata et al. 2010), subsequent *ERK2* decrease and decreased protein synthesis of RhoA. This hypothesized mechanism is represented in figure 37, in the schematic model for miR-181a/b action in neuronal process formation. My data demonstrated that *in vivo* administration of TGF-β caused an increase of miR-181a and miR-181b mature levels in the medakafish eye, and that this increase was sufficient to lead to *ERK2* decrease, at both transcript and protein levels (Fig. 35). The possible role of TGF-β in retinal axon specification and growth, exerted via miR-181a/b, was validated through the rescue of IPL defects obtained upon TGF-β administration on morphant embryos (Fig. 36 A, B). The reduction of the Total-ERK2 levels indicated that this rescue may be due, at least in part, to the action of TGF-β on miR-181a/b levels, which by modulating the ERK2 levels, finally led to the decrease of RhoA protein levels (Fig. 36 C, D). Further experiments, using the proteasomal inhibitor MG132, will be necessary in order to determine the amount of RhoA decrease due to the decrease of its protein synthesis, via miR-181a/b-mediated modulation of the MAPK cascade, rather than to its degradation, via Par6 induced proteasomal degradation (Fig. 37). With these experiment I will be able to discriminate the relative contribution of the two TGF-β-mediated mechanism in the regulation of RhoA levels and axon specification in the retina.

4.1 Conclusions

I begun the functional characterization of miRNAs with a role in eye development by first using a high-resolution expression screening to identify those with the most significant expression levels in the vertebrate eye. Among them, the functional characterization of miR-204 and of the miR-181a/b cluster gave important results, with a strong impact on the knowledge of the miRNA regulatory networks underlying the vertebrate eye development. The analysis of miR-181a/b ablated medakafish embryos revaled the role of these two miRNAs in the axon specification and growth of amacrine and ganglion cell axons. The morphological retinal axon defects in miR-181a/b- ablated embryos, led to impaired retinal circuits assembly responsible of visual function defects. I demonstrated that the functions of miR-181a/b during eye development are largely mediated by *ERK2* targeting and by the modulation of its downstream signaling cascade involved in the growth cone cytoskeleton remodeling. For the first time I provide *in vivo* evidences of an antagonism between the TGF-β pathway and the ERK2 cascade in the regulation of retina axon specification and growth. My data demonstrated that this antagonism is exerted via miR-181a/b activity regulation. The TGF-β-activated miR-181a/b, targeting *ERK2* and modulating the MAPK cascade, play a key role in the signaling network that define the correct axon specification and growth needed for the development and the assembly of a functional retina neural circuits.

5. ACKNOWLEDGEMENTS

I wish to thank in particular Dr. Ivan Conte for scientific and critical discussions, Francesco Giuseppe Salierno for technical support, Dr. Ylenia D'Agostino that worked with me on these data during her degree thesis period, Dr. Sara Barbato for the OKR behavioral test. I wish also to thank my tutor Prof. Sandro Banfi and the Telethon Institute of Genetics and Medicine (TIGEM), my internal supervisor Prof. Antonio Simeone and my external supervisor Prof. Paola Bovolenta.

6. REFERENCES

- Abdelmohsen, K., E. R. Hutchison, E. K. Lee, Y. Kuwano, M. M. Kim, K. Masuda, S. Srikantan, S. S. Subaran, B. S. Marasa, M. P. Mattson and M. Gorospe (2010). "miR-375 inhibits differentiation of neurites by lowering HuD levels." Mol Cell Biol 30(17): 4197-4210.
- Adams, J. P. and J. D. Sweatt (2002). "Molecular psychology: roles for the ERK MAP kinase cascade in memory." Annu Rev Pharmacol Toxicol 42: 135-163.
- Agostini, M., P. Tucci, J. R. Steinert, R. Shalom-Feuerstein, M. Rouleau, D. Aberdam, I. D. Forsythe, K. W. Young, A. Ventura, C. P. Concepcion, Y. C. Han, E. Candi, R. A. Knight, T. W. Mak and G. Melino (2011). "microRNA-34a regulates neurite outgrowth, spinal morphology, and function." Proc Natl Acad Sci U S A 108(52): 21099-21104.
- Agostini, M., P. Tucci, R. Killick, E. Candi, B. S. Sayan, P. Rivetti di Val Cervo, P. Nicotera, F. McKeon, R. A. Knight, T. W. Mak and G. Melino (2011). "Neuronal differentiation by TAp73 is mediated by microRNA-34a regulation of synaptic protein targets." Proc Natl Acad Sci U S A 108(52): 21093-21098.
- Alfano, G., C. Vitiello, C. Caccioppoli, T. Caramico, A. Carola, M. J. Szego, R. R. McInnes, A. Auricchio and S. Banfi (2005). "Natural antisense transcripts associated with genes involved in eye development." Hum Mol Genet 14(7): 913-923.
- Alfano, G., I. Conte, T. Caramico, R. Avellino, B. Arno, M. T. Pizzo, N. Tanimoto, S. C. Beck, G. Huber, P. Dolle, M. W. Seeliger and S. Banfi (2011). "Vax2 regulates retinoic acid distribution and cone opsin expression in the vertebrate eye." Development 138(2): 261-271.

- Althini, S., D. Usoskin, A. Kylberg, P. L. Kaplan and T. Ebendal (2004). "Blocked MAP kinase activity selectively enhances neurotrophic growth responses." Mol Cell Neurosci 25(2): 345-354.
- Altshuler, D., Lo Turco, J.J., Rush, J., and Cepko, C. (1993). Taurine promotes the differentiation of a vertebrate retinal cell type in vitro. Development 119, 1317-1328.
- Ammermuller, J. and H. Kolb (1995). "The organization of the turtle inner retina. I. ON- and OFF-center pathways." J Comp Neurol 358(1): 1-34.
- Aouadi, M., B. Binetruy, L. Caron, Y. Le Marchand-Brustel and F. Bost (2006). "Role of MAPKs in development and differentiation: lessons from knockout mice." Biochimie 88(9): 1091-1098. striatal-mediated learning and memory." Neuron 34(5): 807-820.
- Augsburger, A., A. Schuchardt, S. Hoskins, J. Dodd and S. Butler (1999). "BMPs as mediators of roof plate repulsion of commissural neurons." Neuron 24(1): 127-141.
- Austin, C.P., Feldman, D.E., Ida, J.A., Jr., and Cepko, C.L. (1995). Vertebrate retinal ganglion cells are selected from competent progenitors by the action of Notch. Development 121, 3637-3650.
- Bartel, D. P. (2009). "MicroRNAs: target recognition and regulatory functions." Cell 136(2): 215-233.
- Baudet, M. L., A. Bellon and C. E. Holt (2012). "Role of microRNAs in Semaphorin function and neural circuit formation." Semin Cell Dev Biol.
- Beccari, L., I. Conte, E. Cisneros and P. Bovolenta (2012). "Sox2-mediated differential activation of Six3.2 contributes to forebrain patterning." Development 139(1): 151-164.

- Beebe, D. C. (1986). "Development of the ciliary body: a brief review." Trans Ophthalmol Soc U K 105 (Pt 2): 123-130.
- Belecky-Adams, T., B. Cook and R. Adler (1996). "Correlations between terminal mitosis and differentiated fate of retinal precursor cells in vivo and in vitro: analysis with the "window-labeling" technique." Dev Biol 178(2): 304-315.
- Belliveau, M.J., and Cepko, C.L. (1999). Extrinsic and intrinsic factors control the genesis of amacrine and cone cells in the rat retina. Development 126, 555-566.
- Belliveau, M.J., Young, T.L., and Cepko, C.L. (2000). Late retinal progenitor cells show intrinsic limitations in the production of cell types and the kinetics of opsin synthesis. J Neurosci 20, 2247-2254.
- Bentires-Alj, M., M. I. Kontaridis and B. G. Neel (2006). "Stops along the RAS pathway in human genetic disease." Nat Med 12(3): 283-285.
- Bernstein, E., S. Y. Kim, M. A. Carmell, E. P. Murchison, H. Alcorn, M. Z. Li, A. A. Mills, S. J. Elledge, K. V. Anderson and G. J. Hannon (2003). "Dicer is essential for mouse development." Nat Genet 35(3): 215-217.
- Bhatt, K., Q. S. Mi and Z. Dong (2011). "microRNAs in kidneys: biogenesis, regulation, and pathophysiological roles." Am J Physiol Renal Physiol 300(3): F602-610.
- Bian, S. and T. Sun (2011). "Functions of noncoding RNAs in neural development and neurological diseases." Mol Neurobiol 44(3): 359-373.
- Biggs WH 3rd, Zavitz KH, Dickson B, van der Straten A, Brunner D, Hafen E, Zipursky SL. The Drosophila rolled locus encodes a MAP kinase required in the sevenless signal transduction pathway.EMBO J. 1994 Apr 1;13(7):1628-35

- Bodnarenko, S. R., G. Jeyarasasingam and L. M. Chalupa (1995). "Development and regulation of dendritic stratification in retinal ganglion cells by glutamate-mediated afferent activity." J Neurosci 15(11): 7037-7045.
- Bodnarenko, S. R., G. Yeung, L. Thomas and M. McCarthy (1999). "The development of retinal ganglion cell dendritic stratification in ferrets." Neuroreport 10(14): 2955-2959.
- Bohnsack, M. T., K. Czaplinski and D. Gorlich (2004). "Exportin 5 is a RanGTP-dependent dsRNA-binding protein that mediates nuclear export of pre-miRNAs." RNA 10(2): 185-191.
- Bovolenta, P. (2005). "Morphogen signaling at the vertebrate growth cone: a few cases or a general strategy?" J Neurobiol 64(4): 405-416.
- Bovolenta P. Marco-Ferreres, R and Conte I. (2010) Retinal development: Embryology and early patterning. In: Darlene A. Dartt, editor. Encyclopedia of the Eye, Vol 2. Oxford:Academic Press; p.69-75
- Bradke, F. and C. G. Dotti (1999). "The role of local actin instability in axon formation." Science 283(5409): 1931-1934.
- Bramblett, D. E., M. E. Pennesi, S. M. Wu and M. J. Tsai (2004). "The transcription factor Bhlhb4 is required for rod bipolar cell maturation." Neuron 43(6): 779-793.
- Brown, N.L., Patel, S., Brzezinski, J., and Glaser, T. (2001). Math5 is required for retinal ganglion cell and optic nerve formation. Development 128, 2497-2508.
- Burmeister, M., Novak, J., Liang, M.Y., Basu, S., Ploder, L., Hawes, N.L., Vidgen, D., Hoover, F., Goldman, D., Kalnins, V.I., et al. (1996). Ocular retardation mouse caused by Chx10 homeobox null allele: impaired retinal progenitor proliferation and bipolar cell differentiation. Nat Genet 12, 376-384.

- Burridge, K. and M. Chrzanowska-Wodnicka (1996). "Focal adhesions, contractility, and signaling." Annu Rev Cell Dev Biol 12: 463-518.
- Butler, S. J. and J. Dodd (2003). "A role for BMP heterodimers in roof plate-mediated repulsion of commissural axons." Neuron 38(3): 389-401.
- Cai, X., C. H. Hagedorn and B. R. Cullen (2004). "Human microRNAs are processed from capped, polyadenylated transcripts that can also function as mRNAs." RNA 10(12): 1957-1966.
- Cajal, S. R. (1972). The Structure of the Retina, ed. S. A. Thorpe and M. Glickstein. Springfield: Charles C Thomas, pp. 17–132
- Campbell, D. S. and C. E. Holt (2001). "Chemotropic responses of retinal growth cones mediated by rapid local protein synthesis and degradation." Neuron 32(6): 1013-1026.
- Campbell, D. S. and C. E. Holt (2003). "Apoptotic pathway and MAPKs differentially regulate chemotropic responses of retinal growth cones." Neuron 37(6): 939-952.
- Carrer, H. F., M. J. Cambiasso, V. Brito and S. Gorosito (2003). "Neurotrophic factors and estradiol interact to control axogenic growth in hypothalamic neurons." Ann N Y Acad Sci 1007: 306-316.
- Carter-Dawson, L. D. and M. M. LaVail (1979). "Rods and cones in the mouse retina. II. Autoradiographic analysis of cell generation using tritiated thymidine." J Comp Neurol 188(2): 263-272.
- Carthew, R. W. and E. J. Sontheimer (2009). "Origins and Mechanisms of miRNAs and siRNAs." Cell 136(4): 642-655.
- Ceman, S. and J. Saugstad (2011). "MicroRNAs: Meta-controllers of gene expression in synaptic activity emerge as genetic and diagnostic markers of human disease." Pharmacol Ther 130(1): 26-37.

- Cepko, C. L., C. P. Austin, X. Yang, M. Alexiades and D. Ezzeddine (1996). "Cell fate determination in the vertebrate retina." Proc Natl Acad Sci U S A 93(2): 589-595
- Chalupa, L. M. and E. Gunhan (2004). "Development of On and Off retinal pathways and retinogeniculate projections." Prog Retin Eye Res 23(1): 31-51.
- Chendrimada, T. P., R. I. Gregory, E. Kumaraswamy, J. Norman, N. Cooch, K. Nishikura and R. Shiekhattar (2005). "TRBP recruits the Dicer complex to Ago2 for microRNA processing and gene silencing." Nature 436(7051): 740-744.
- Cheng, H. J., M. Nakamoto, A. D. Bergemann and J. G. Flanagan (1995). "Complementary gradients in expression and binding of ELF-1 and Mek4 in development of the topographic retinotectal projection map." Cell 82(3): 371-381.
- Chow, R. L. and R. A. Lang (2001). "Early eye development in vertebrates." Annu Rev Cell Dev Biol 17: 255-296.
- Conte, I. and P. Bovolenta (2007). "Comprehensive characterization of the cis-regulatory code responsible for the spatio-temporal expression of olSix3.2 in the developing medaka forebrain." Genome Biol 8(7): R137.
- Conte, I., S. Carrella, R. Avellino, M. Karali, R. Marco-Ferreres, P. Bovolenta and S. Banfi (2010a). "miR-204 is required for lens and retinal development via Meis2 targeting." Proc Natl Acad Sci U S A 107(35): 15491-15496.
- Conte, I., R. Marco-Ferreres, L. Beccari, E. Cisneros, J. M. Ruiz, N. Tabanera and P. Bovolenta (2010b). "Proper differentiation of photoreceptors and amacrine cells depends on a regulatory loop between NeuroD and Six6." Development 137(14): 2307-2317.
- Damiani, D., J. J. Alexander, J. R. O'Rourke, M. McManus, A. P. Jadhav, C. L. Cepko, W. W. Hauswirth, B. D. Harfe and E. Strettoi (2008). "Dicer inactivation

leads to progressive functional and structural degeneration of the mouse retina." J Neurosci 28(19): 4878-4887.

- Davis, B. N., A. C. Hilyard, G. Lagna and A. Hata (2008). "SMAD proteins control DROSHA-mediated microRNA maturation." Nature 454(7200): 56-61.
- de la Torre, J. R., V. H. Hopker, G. L. Ming, M. M. Poo, M. Tessier-Lavigne, A. Hemmati-Brivanlou and C. E. Holt (1997). "Turning of retinal growth cones in a netrin-1 gradient mediated by the netrin receptor DCC." Neuron 19(6): 1211-1224.
- Dotti, C. G. and G. A. Banker (1987). "Experimentally induced alteration in the polarity of developing neurons." Nature 330(6145): 254-256.
- Drenhaus, U., P. Morino and G. Rager (2004). "Expression of axonin-1 in developing amacrine cells in the chick retina." J Comp Neurol 468(4): 496-508.
- Drenhaus, U., P. Morino and R. W. Veh (2003). "On the development of the stratification of the inner plexiform layer in the chick retina." J Comp Neurol 460(1): 1-12.
- Drescher, U., C. Kremoser, C. Handwerker, J. Loschinger, M. Noda and F. Bonhoeffer (1995). "In vitro guidance of retinal ganglion cell axons by RAGS, a 25 kDa tectal protein related to ligands for Eph receptor tyrosine kinases." Cell 82(3): 359-370.
- Dyer, M.A., Livesey, F.J., Cepko, C.L., and Oliver, G. (2003). Prox1 function controls progenitor cell proliferation and horizontal cell genesis in the mammalian retina. Nat Genet 34, 53-58.
- Edbauer, D., J. R. Neilson, K. A. Foster, C. F. Wang, D. P. Seeburg, M. N. Batterton, T. Tada, B. M. Dolan, P. A. Sharp and M. Sheng (2010). "Regulation of synaptic structure and function by FMRP-associated microRNAs miR-125b and miR-132." Neuron 65(3): 373-384.

- Eisen, J.S., and Smith, J.C. (2008). Controlling morpholino experiments: don't stop making antisense. Development 135, 1735-1743.
- Ekker SC, Ungar AR, Greenstein P, von Kessler DP, Porter JA, Moon RT, Beachy PA. Patterning activities of vertebrate hedgehog proteins in the developing eye and brain. Curr Biol. 1995 Aug 1;5(8):944-55
- Esteve, P., J. Lopez-Rios and P. Bovolenta (2004). "SFRP1 is required for the proper establishment of the eye field in the medaka fish." Mech Dev 121(7-8): 687-701.
- Ezzeddine, Z.D., Yang, X., DeChiara, T., Yancopoulos, G., and Cepko, C.L. (1997). Postmitotic cells fated to become rod photoreceptors can be respecified by CNTF treatment of the retina. Development 124, 1055-1067.
- Famiglietti, E. V., Jr. and H. Kolb (1976). "Structural basis for ON-and OFF-center responses in retinal ganglion cells." Science 194(4261): 193-195.
- Famiglietti, E. V., Jr., A. Kaneko and M. Tachibana (1977). "Neuronal architecture of on and off pathways to ganglion cells in carp retina." Science 198(4323): 1267-1269.
- Fish, J. E., M. M. Santoro, S. U. Morton, S. Yu, R. F. Yeh, J. D. Wythe, K. N. Ivey, B. G. Bruneau, D. Y. Stainier and D. Srivastava (2008). "miR-126 regulates angiogenic signaling and vascular integrity." Dev Cell 15(2): 272-284.
- Forcet, C., E. Stein, L. Pays, V. Corset, F. Llambi, M. Tessier-Lavigne and P. Mehlen (2002). "Netrin-1-mediated axon outgrowth requires deleted in colorectal cancer-dependent MAPK activation." Nature 417(6887): 443-447.
- Fukata, Y., T. Kimura and K. Kaibuchi (2002). "Axon specification in hippocampal neurons." Neurosci Res 43(4): 305-315.

- Furukawa, T., Mukherjee, S., Bao, Z.Z., Morrow, E.M., and Cepko, C.L. (2000). rax, Hes1, and notch1 promote the formation of Muller glia by postnatal retinal progenitor cells. Neuron 26, 383-394.
- Gebauer, F. and M. W. Hentze (2004). "Molecular mechanisms of translational control." Nat Rev Mol Cell Biol 5(10): 827-835.
- Georgi, S. A. and T. A. Reh (2010). "Dicer is required for the transition from early to late progenitor state in the developing mouse retina." J Neurosci 30(11): 4048-4061.
- Giancotti, F. G. and E. Ruoslahti (1999). "Integrin signaling." Science 285(5430): 1028-1032.
- Giraldez, A. J., R. M. Cinalli, M. E. Glasner, A. J. Enright, J. M. Thomson, S. Baskerville, S. M. Hammond, D. P. Bartel and A. F. Schier (2005). "MicroRNAs regulate brain morphogenesis in zebrafish." Science 308(5723): 833-838.
- Godinho, L., J. S. Mumm, P. R. Williams, E. H. Schroeter, A. Koerber, S. W. Park, S. D. Leach and R. O. Wong (2005). "Targeting of amacrine cell neurites to appropriate synaptic laminae in the developing zebrafish retina." Development 132(22): 5069-5079.
- Goldberg, J. L., Espinosa, J. S., Xu, Y. *et al*. (2002a). Retinal ganglion cells do not extend axons by default: promotion by neurotrophic signaling and electrical activity. Neuron, 33, 689–702
- Goslin, K. and G. Banker (1989). "Experimental observations on the development of polarity by hippocampal neurons in culture." J Cell Biol 108(4): 1507-1516.
- Gregory, R. I., K. P. Yan, G. Amuthan, T. Chendrimada, B. Doratotaj, N. Cooch and R. Shiekhattar (2004). "The Microprocessor complex mediates the genesis of microRNAs." Nature 432(7014): 235-240.

- Gregory, R. I., T. P. Chendrimada, N. Cooch and R. Shiekhattar (2005). "Human RISC couples microRNA biogenesis and posttranscriptional gene silencing." Cell 123(4): 631-640.
- Grishok, A., A. E. Pasquinelli, D. Conte, N. Li, S. Parrish, I. Ha, D. L. Baillie, A. Fire, G. Ruvkun and C. C. Mello (2001). "Genes and mechanisms related to RNA interference regulate expression of the small temporal RNAs that control C. elegans developmental timing." Cell 106(1): 23-34.
- Guillemot, F., and Cepko, C.L. (1992). Retinal fate and ganglion cell differentiation are potentiated by acidic FGF in an in vitro assay of early retinal development. Development 114, 743-754.
- Guller, I. and A. P. Russell (2010). "MicroRNAs in skeletal muscle: their role and regulation in development, disease and function." J Physiol 588(Pt 21): 4075-4087.
- Haase, A. D., L. Jaskiewicz, H. Zhang, S. Laine, R. Sack, A. Gatignol and W. Filipowicz (2005). "TRBP, a regulator of cellular PKR and HIV-1 virus expression, interacts with Dicer and functions in RNA silencing." EMBO Rep 6(10): 961-967.
- Hackler L Jr, Wan J, Swaroop A, Qian J, Zack DJ. MicroRNA profile of the developing mouse retina. Invest Ophthalmol Vis Sci. 2010; 51(4):1823–1831.
- Han, J., Y. Lee, K. H. Yeom, J. W. Nam, I. Heo, J. K. Rhee, S. Y. Sohn, Y. Cho, B. T. Zhang and V. N. Kim (2006). "Molecular basis for the recognition of primary microRNAs by the Drosha-DGCR8 complex." Cell 125(5): 887-901.
- Han, L., Z. Wen, R. C. Lynn, M. L. Baudet, C. E. Holt, Y. Sasaki, G. J. Bassell and J. Q. Zheng (2011). "Regulation of chemotropic guidance of nerve growth cones by microRNA." Mol Brain 4: 40.

- Harris, W. A., C. E. Holt and F. Bonhoeffer (1987). "Retinal axons with and without their somata, growing to and arborizing in the tectum of Xenopus embryos: a time-lapse video study of single fibres in vivo." Development 101(1): 123-133.
- Harris, W.A. (1997). Cellular diversification in the vertebrate retina. Curr Opin Genet Dev 7, 651-658.
- Hata, A. and B. N. Davis (2010). "Regulation of pri-miRNA processing through Smads." Adv Exp Med Biol 700: 15-27.
- Hinds, J. W. and P. L. Hinds (1974). "Early ganglion cell differentiation in the mouse retina: an electron microscopic analysis utilizing serial sections." Dev Biol 37(2): 381-416.
- Hocking, J. C., C. L. Hehr, R. Y. Chang, J. Johnston and S. McFarlane (2008). "TGFbeta ligands promote the initiation of retinal ganglion cell dendrites in vitro and in vivo." Mol Cell Neurosci 37(2): 247-260.
- Hollander, J. A., H. I. Im, A. L. Amelio, J. Kocerha, P. Bali, Q. Lu, D. Willoughby, C. Wahlestedt, M. D. Conkright and P. J. Kenny (2010). "Striatal microRNA controls cocaine intake through CREB signalling." Nature 466(7303): 197-202.
- Holt, C. E. (1989). "A single-cell analysis of early retinal ganglion cell differentiation in Xenopus: from soma to axon tip." J Neurosci 9(9): 3123-3145.
- Holt, C.E., Bertsch, T.W., Ellis, H.M., and Harris, W.A. (1988). Cellular determination in the Xenopus retina is independent of lineage and birth date. Neuron 1, 15-26.
- Honjo, M., Tanihara, H., Suzuki, S. *et al*. (2000). Differential expression of cadherin adhesion receptors in neural retina of the postnatal mouse. Invest. Opthamol. Vis. Sci., 41, 546–51

- Horton, A. C. and M. D. Ehlers (2003). "Neuronal polarity and trafficking." Neuron 40(2): 277-295.
- Hu, M. and S. S. Easter (1999). "Retinal neurogenesis: the formation of the initial central patch of postmitotic cells." Dev Biol 207(2): 309-321.
- Huntzinger, E. and E. Izaurralde (2011). "Gene silencing by microRNAs: contributions of translational repression and mRNA decay." Nat Rev Genet 12(2): 99-110.
- Huse, J. T., C. Brennan, D. Hambardzumyan, B. Wee, J. Pena, S. H. Rouhanifard, C. Sohn-Lee, C. le Sage, R. Agami, T. Tuschl and E. C. Holland (2009). "The PTEN-regulating microRNA miR-26a is amplified in high-grade glioma and facilitates gliomagenesis in vivo." Genes Dev 23(11): 1327-1337.
- Hynes, R. O. and A. D. Lander (1992). "Contact and adhesive specificities in the associations, migrations, and targeting of cells and axons." Cell 68(2): 303-322.
- Iida, A., T. Shinoe, Y. Baba, H. Mano and S. Watanabe (2011). "Dicer plays essential roles for retinal development by regulation of survival and differentiation." Invest Ophthalmol Vis Sci 52(6): 3008-3017.
- Im, H. I. and P. J. Kenny (2012). "MicroRNAs in neuronal function and dysfunction." Trends Neurosci 35(5): 325-334.
- Im, H. I., J. A. Hollander, P. Bali and P. J. Kenny (2010). "MeCP2 controls BDNF expression and cocaine intake through homeostatic interactions with microRNA-212." Nat Neurosci 13(9): 1120-1127.
- Inoue, T., Hojo, M., Bessho, Y., Tano, Y., Lee, J.E., and Kageyama, R. (2002). Math3 and NeuroD regulate amacrine cell fate specification in the retina. Development 129, 831-842.
- Inui, M., G. Martello and S. Piccolo (2010). "MicroRNA control of signal transduction." Nat Rev Mol Cell Biol 11(4): 252-263.

- Inui, M., M. Montagner and S. Piccolo (2012). "miRNAs and morphogen gradients." Curr Opin Cell Biol 24(2): 194-201.
- Ishikawa, Y. (2000). Medakafish as a model system for vertebrate developmental genetics. Bioessays 22, 487-495.
- Iwamatsu, T. (2004). Stages of normal development in the medaka Oryzias latipes. Mech Dev 121, 605-618.
- Jiang, H., Guo, W., Liang, X. and Rao, Y (2005). Both the establishment and the maintenance of neuronal polarity require active mechanisms: critical roles of GSK-3beta and its upstream regulators. Cell, 120, 123–35
- Jung, H., B. C. Yoon and C. E. Holt (2012). "Axonal mRNA localization and local protein synthesis in nervous system assembly, maintenance and repair." Nat Rev Neurosci 13(5): 308-324.
- Jung, H., C. M. O'Hare and C. E. Holt (2011). "Translational regulation in growth cones." Curr Opin Genet Dev 21(4): 458-464.
- Karali, M., I. Peluso, V. A. Gennarino, M. Bilio, R. Verde, G. Lago, P. Dolle and S. Banfi (2010). "miRNeye: a microRNA expression atlas of the mouse eye." BMC Genomics 11: 715.
- Karali, M., I. Peluso, V. Marigo and S. Banfi (2007). "Identification and characterization of microRNAs expressed in the mouse eye." Invest Ophthalmol Vis Sci 48(2): 509-515.
- Kay, J. N., T. Roeser, J. S. Mumm, L. Godinho, A. Mrejeru, R. O. Wong and H. Baier (2004). "Transient requirement for ganglion cells during assembly of retinal synaptic layers." Development 131(6): 1331-1342.
- Kazenwadel, J., M. Z. Michael and N. L. Harvey (2010). "Prox1 expression is negatively regulated by miR-181 in endothelial cells." Blood 116(13): 2395-2401.

- Kelley, M.W., Turner, J.K., and Reh, T.A. (1994). Retinoic acid promotes differentiation of photoreceptors in vitro. Development 120, 2091-2102.
- Kerrison, J. B., R. N. Lewis, D. C. Otteson and D. J. Zack (2005). "Bone morphogenetic proteins promote neurite outgrowth in retinal ganglion cells." Mol Vis 11: 208-215.
- Khvorova, A., A. Reynolds and S. D. Jayasena (2003). "Functional siRNAs and miRNAs exhibit strand bias." Cell 115(2): 209-216.
- Kitambi, S. S. and J. J. Malicki (2008). "Spatiotemporal features of neurogenesis in the retina of medaka, Oryzias latipes." Dev Dyn 237(12): 3870-3881.
- Kloosterman, W. P., A. K. Lagendijk, R. F. Ketting, J. D. Moulton and R. H. Plasterk (2007). "Targeted inhibition of miRNA maturation with morpholinos reveals a role for miR-375 in pancreatic islet development." PLoS Biol 5(8): e203.
- Krens, S. F., S. He, G. E. Lamers, A. H. Meijer, J. Bakkers, T. Schmidt, H. P. Spaink and B. E. Snaar-Jagalska (2008). "Distinct functions for ERK1 and ERK2 in cell migration processes during zebrafish gastrulation." Dev Biol 319(2): 370-383.
- Krol, J., I. Loedige and W. Filipowicz (2010a). "The widespread regulation of microRNA biogenesis, function and decay." Nat Rev Genet 11(9): 597-610.
- Krol, J., V. Busskamp, I. Markiewicz, M. B. Stadler, S. Ribi, J. Richter, J. Duebel, S. Bicker, H. J. Fehling, D. Schubeler, T. G. Oertner, G. Schratt, M. Bibel, B. Roska and W. Filipowicz (2010b). "Characterizing light-regulated retinal microRNAs reveals rapid turnover as a common property of neuronal microRNAs." Cell 141(4): 618-631.

- Krutzfeldt, J., N. Rajewsky, R. Braich, K. G. Rajeev, T. Tuschl, M. Manoharan and M. Stoffel (2005). "Silencing of microRNAs in vivo with 'antagomirs'." Nature 438(7068): 685-689.
- Kuhnert, F., M. R. Mancuso, J. Hampton, K. Stankunas, T. Asano, C. Z. Chen and C. J. Kuo (2008). "Attribution of vascular phenotypes of the murine Egfl7 locus to the microRNA miR-126." Development 135(24): 3989-3993.
- Kyriakis, J. M. and J. Avruch (2012). "Mammalian MAPK signal transduction pathways activated by stress and inflammation: a 10-year update." Physiol Rev 92(2): 689-737.
- La Vail, M. M., D. H. Rapaport and P. Rakic (1991). "Cytogenesis in the monkey retina." J Comp Neurol 309(1): 86-114.
- Lagos-Quintana, M., R. Rauhut, W. Lendeckel and T. Tuschl (2001). "Identification of novel genes coding for small expressed RNAs." Science 294(5543): 853-858.
- Lanford, R. E., E. S. Hildebrandt-Eriksen, A. Petri, R. Persson, M. Lindow, M. E. Munk, S. Kauppinen and H. Orum (2010). "Therapeutic silencing of microRNA-122 in primates with chronic hepatitis C virus infection." Science 327(5962): 198-201.
- Lau, N. C., L. P. Lim, E. G. Weinstein and D. P. Bartel (2001). "An abundant class of tiny RNAs with probable regulatory roles in Caenorhabditis elegans." Science 294(5543): 858-862.
- Leaman, D., P. Y. Chen, J. Fak, A. Yalcin, M. Pearce, U. Unnerstall, D. S. Marks, C. Sander, T. Tuschl and U. Gaul (2005). "Antisense-mediated depletion reveals essential and specific functions of microRNAs in Drosophila development." Cell 121(7): 1097-1108.

- Lee, K., J. H. Kim, O. B. Kwon, K. An, J. Ryu, K. Cho, Y. H. Suh and H. S. Kim (2012). "An activity-regulated microRNA, miR-188, controls dendritic plasticity and synaptic transmission by downregulating neuropilin-2." J Neurosci 32(16): 5678-5687.
- Lee, R. C. and V. Ambros (2001). "An extensive class of small RNAs in Caenorhabditis elegans." Science 294(5543): 862-864.
- Lee, R. C., R. L. Feinbaum and V. Ambros (1993). "The C. elegans heterochronic gene lin-4 encodes small RNAs with antisense complementarity to lin-14." Cell 75(5): 843-854.
- Lee, Y., M. Kim, J. Han, K. H. Yeom, S. Lee, S. H. Baek and V. N. Kim (2004). "MicroRNA genes are transcribed by RNA polymerase II." EMBO J 23(20): 4051-4060.
- Li, S., Mo, Z., Yang, X., Price, S.M., Shen, M.M., and Xiang, M. (2004). Foxn4 controls the genesis of amacrine and horizontal cells by retinal progenitors. Neuron 43, 795-807.
- Lieschke, G.J., and Currie, P.D. (2007). Animal models of human disease: zebrafish swim into view. Nat Rev Genet 8, 353-367.
- Lillien, L. and D. Wancio (1998). "Changes in Epidermal Growth Factor Receptor Expression and Competence to Generate Glia Regulate Timing and Choice of Differentiation in the Retina." Mol Cell Neurosci 10(5/6): 296-308.
- Lim, L. P., N. C. Lau, P. Garrett-Engele, A. Grimson, J. M. Schelter, J. Castle, D. P. Bartel, P. S. Linsley and J. M. Johnson (2005). "Microarray analysis shows that some microRNAs downregulate large numbers of target mRNAs." Nature 433(7027): 769-773.
- Lin, A. C. and C. E. Holt (2007). "Local translation and directional steering in axons." EMBO J 26(16): 3729-3736.

- Lin, A. C. and C. E. Holt (2008). "Function and regulation of local axonal translation." Curr Opin Neurobiol 18(1): 60-68.
- Livesey, F.J., and Cepko, C.L. (2001). Vertebrate neural cell-fate determination: lessons from the retina. Nat Rev Neurosci 2, 109-118.
- Lohmann, C. and R. O. Wong (2001). "Cell-type specific dendritic contacts between retinal ganglion cells during development." J Neurobiol 48(2): 150-162.
- Lom, B. and S. Cohen-Cory (1999). "Brain-derived neurotrophic factor differentially regulates retinal ganglion cell dendritic and axonal arborization in vivo." J Neurosci 19(22): 9928-9938.
- Lom, B., J. Cogen, A. L. Sanchez, T. Vu and S. Cohen-Cory (2002). "Local and target-derived brain-derived neurotrophic factor exert opposing effects on the dendritic arborization of retinal ganglion cells in vivo." J Neurosci 22(17): 7639-7649.
- Loscher, C. J., K. Hokamp, P. F. Kenna, A. C. Ivens, P. Humphries, A. Palfi and G. J. Farrar (2007). "Altered retinal microRNA expression profile in a mouse model of retinitis pigmentosa." Genome Biol 8(11): R248.
- Lund, E., S. Guttinger, A. Calado, J. E. Dahlberg and U. Kutay (2004). "Nuclear export of microRNA precursors." Science 303(5654): 95-98.
- Luo, L., L. Y. Jan and Y. N. Jan (1997). "Rho family GTP-binding proteins in growth cone signalling." Curr Opin Neurobiol 7(1): 81-86.
- Macrae, I. J., K. Zhou, F. Li, A. Repic, A. N. Brooks, W. Z. Cande, P. D. Adams and J. A. Doudna (2006). "Structural basis for double-stranded RNA processing by Dicer." Science 311(5758): 195-198.
- Magill, S. T., X. A. Cambronne, B. W. Luikart, D. T. Lioy, B. H. Leighton, G. L. Westbrook, G. Mandel and R. H. Goodman (2010). "microRNA-132 regulates

dendritic growth and arborization of newborn neurons in the adult hippocampus." Proc Natl Acad Sci U S A 107(47): 20382-20387.

- Mann, F., E. Miranda, C. Weinl, E. Harmer and C. E. Holt (2003). "B-type Eph receptors and ephrins induce growth cone collapse through distinct intracellular pathways." J Neurobiol 57(3): 323-336.
- Marquardt, T., and Gruss, P. (2002). Generating neuronal diversity in the retina: one for nearly all. Trends Neurosci 25, 32-38.
- Marquardt, T., Ashery-Padan, R., Andrejewski, N., Scardigli, R., Guillemot, F., and Gruss, P. (2001). Pax6 is required for the multipotent state of retinal progenitor cells. Cell 105, 43-55.
- Masai, I., Lele, Z., Yamaguchi, M. *et al*. (2003). N-cadherin mediates retinal lamination, maintenance of forebrain compartments and patterning of retinal neurites. Development, 130, 2479–94
- Maslim, J. and J. Stone (1988). "Time course of stratification of the dendritic fields of ganglion cells in the retina of the cat." Brain Res Dev Brain Res 44(1): 87-93.
- Maslim, J., M. Webster and J. Stone (1986). "Stages in the structural differentiation of retinal ganglion cells." J Comp Neurol 254(3): 382-402.
- Mathers PH, Jamrich M. Regulation of eye formation by the Rx and pax6 homeobox genes. Cell Mol Life Sci. 2000 Feb;57(2):186-94. Review.
- Mathers, P.H., Grinberg, A., Mahon, K.A., and Jamrich, M. (1997). The Rx homeobox gene is essential for vertebrate eye development. Nature 387, 603-607.

- Matsuda, M., C. Matsuda, S. Hamaguchi and M. Sakaizumi (1998). "Identification of the sex chromosomes of the medaka, Oryzias latipes, by fluorescence in situ hybridization." Cytogenet Cell Genet 82(3-4): 257-262.
- Mazzucchelli, C., C. Vantaggiato, A. Ciamei, S. Fasano, P. Pakhotin, W. Krezel, H. Welzl, D. P. Wolfer, G. Pages, O. Valverde, A. Marowsky, A. Porrazzo, P. C. Orban, R. Maldonado, M. U. Ehrengruber, V. Cestari, H. P. Lipp, P. F. Chapman, J. Pouyssegur and R. Brambilla (2002). "Knockout of ERK1 MAP kinase enhances synaptic plasticity in the striatum and facilitates
- McNeill, E. and D. Van Vactor (2012). "MicroRNAs shape the neuronal landscape." Neuron 75(3): 363-379.
- Meng, F., R. Henson, H. Wehbe-Janek, K. Ghoshal, S. T. Jacob and T. Patel (2007). "MicroRNA-21 regulates expression of the PTEN tumor suppressor gene in human hepatocellular cancer." Gastroenterology 133(2): 647-658.
- Ming, G. L., S. T. Wong, J. Henley, X. B. Yuan, H. J. Song, N. C. Spitzer and M. M. Poo (2002). "Adaptation in the chemotactic guidance of nerve growth cones." Nature 417(6887): 411-418.
- Morrow, E.M., Furukawa, T., Lee, J.E., and Cepko, C.L. (1999). NeuroD regulates multiple functions in the developing neural retina in rodent. Development 126, 23-36.
- Muddashetty, R. S., V. C. Nalavadi, C. Gross, X. Yao, L. Xing, O. Laur, S. T. Warren and G. J. Bassell (2011). "Reversible inhibition of PSD-95 mRNA translation by miR-125a, FMRP phosphorylation, and mGluR signaling." Mol Cell 42(5): 673- 688.
- Nelson, R., Famigletti, E. V. J. and Kolb, H. (1978). Intracellular staining reveals different levels of stratification for on- and off-center ganglion cells in the cat retina. J. Neurophysiol. 41, 472–83

- Newman, M. A. and S. M. Hammond (2010). "Emerging paradigms of regulated microRNA processing." Genes Dev 24(11): 1086-1092.
- Ng, J. (2008). "TGF-beta signals regulate axonal development through distinct Smad-independent mechanisms." Development 135(24): 4025-4035.
- Nguyen, M. and H. Arnheiter (2000). "Signaling and transcriptional regulation in early mammalian eye development: a link between FGF and MITF." Development 127(16): 3581-3591.
- Ohta, K., S. Takagi, H. Asou and H. Fujisawa (1992). "Involvement of neuronal cell surface molecule B2 in the formation of retinal plexiform layers." Neuron 9(1): 151-161.
- Orom, U. A., F. C. Nielsen and A. H. Lund (2008). "MicroRNA-10a binds the 5'UTR of ribosomal protein mRNAs and enhances their translation." Mol Cell 30(4): 460-471.
- Ozdamar, B., R. Bose, M. Barrios-Rodiles, H. R. Wang, Y. Zhang and J. L. Wrana (2005). "Regulation of the polarity protein Par6 by TGFbeta receptors controls epithelial cell plasticity." Science 307(5715): 1603-1609.
- Pasquinelli, A. E., B. J. Reinhart, F. Slack, M. Q. Martindale, M. I. Kuroda, B. Maller, D. C. Hayward, E. E. Ball, B. Degnan, P. Muller, J. Spring, A. Srinivasan, M. Fishman, J. Finnerty, J. Corbo, M. Levine, P. Leahy, E. Davidson and G. Ruvkun (2000). "Conservation of the sequence and temporal expression of let-7 heterochronic regulatory RNA." Nature 408(6808): 86-89.
- Perron, J. C. and J. L. Bixby (1999). "Distinct neurite outgrowth signaling pathways converge on ERK activation." Mol Cell Neurosci 13(5): 362-378.
- Pierce, M. L., M. D. Weston, B. Fritzsch, H. W. Gabel, G. Ruvkun and G. A. Soukup (2008). "MicroRNA-183 family conservation and ciliated neurosensory organ expression." Evol Dev 10(1): 106-113.

- Pillai, R. S., S. N. Bhattacharyya and W. Filipowicz (2007). "Repression of protein synthesis by miRNAs: how many mechanisms?" Trends Cell Biol 17(3): 118-126.
- Pinter, R. and R. Hindges (2010). "Perturbations of microRNA function in mouse dicer mutants produce retinal defects and lead to aberrant axon pathfinding at the optic chiasm." PLoS One 5(4): e10021.
- Piper, M., R. Anderson, A. Dwivedy, C. Weinl, F. van Horck, K. M. Leung, E. Cogill and C. Holt (2006). "Signaling mechanisms underlying Slit2-induced collapse of Xenopus retinal growth cones." Neuron 49(2): 215-228.
- Rajasethupathy, P., F. Fiumara, R. Sheridan, D. Betel, S. V. Puthanveettil, J. J. Russo, C. Sander, T. Tuschl and E. Kandel (2009). "Characterization of small RNAs in Aplysia reveals a role for miR-124 in constraining synaptic plasticity through CREB." Neuron 63(6): 803-817.
- Reese, B. E., M. A. Raven, K. A. Giannotti and P. T. Johnson (2001). "Development of cholinergic amacrine cell stratification in the ferret retina and the effects of early excitotoxic ablation." Vis Neurosci 18(4): 559-570.

REFERENCES

- Roberts, A. E., T. Araki, K. D. Swanson, K. T. Montgomery, T. A. Schiripo, V. A. Joshi, L. Li, Y. Yassin, A. M. Tamburino, B. G. Neel and R. S. Kucherlapati (2007). "Germline gain-of-function mutations in SOS1 cause Noonan syndrome." Nat Genet 39(1): 70-74.
- Robu, M.E., Larson, J.D., Nasevicius, A., Beiraghi, S., Brenner, C., Farber, S.A., and Ekker, S.C. (2007). p53 activation by knockdown technologies. PLoS Genet 3, e78.

- Ruiz, J. M., J. Rodriguez and P. Bovolenta (2009). "Growth and differentiation of the retina and the optic tectum in the medaka fish requires olSfrp5." Dev Neurobiol 69(10): 617-6
- Ryan, D. G., M. Oliveira-Fernandes and R. M. Lavker (2006). "MicroRNAs of the mammalian eye display distinct and overlapping tissue specificity." Mol Vis 12: 1175-1184.
- Saba, R., P. H. Storchel, A. Aksoy-Aksel, F. Kepura, G. Lippi, T. D. Plant and G. M. Schratt (2012). "Dopamine-regulated microRNA MiR-181a controls GluA2 surface expression in hippocampal neurons." Mol Cell Biol 32(3): 619-632.
- Sanchez-Camacho, C. and P. Bovolenta (2009). "Emerging mechanisms in morphogen-mediated axon guidance." Bioessays 31(10): 1013-1025.
- Sanuki, R., A. Onishi, C. Koike, R. Muramatsu, S. Watanabe, Y. Muranishi, S. Irie, S. Uneo, T. Koyasu, R. Matsui, Y. Cherasse, Y. Urade, D. Watanabe, M. Kondo, T. Yamashita and T. Furukawa (2011). "miR-124a is required for hippocampal axogenesis and retinal cone survival through Lhx2 suppression." Nat Neurosci 14(9): 1125-1134.
- Satoh, Y., S. Endo, T. Ikeda, K. Yamada, M. Ito, M. Kuroki, T. Hiramoto, O. Imamura, Y. Kobayashi, Y. Watanabe, S. Itohara and K. Takishima (2007). "Extracellular signal-regulated kinase 2 (ERK2) knockdown mice show deficits in long-term memory; ERK2 has a specific function in learning and memory." J Neurosci 27(40): 10765-10776.
- Satoh, Y., Y. Kobayashi, A. Takeuchi, G. Pages, J. Pouyssegur and T. Kazama (2011). "Deletion of ERK1 and ERK2 in the CNS causes cortical abnormalities and neonatal lethality: Erk1 deficiency enhances the impairment of neurogenesis in Erk2-deficient mice." J Neurosci 31(3): 1149-1155.

- Satow, T., Bae, S.K., Inoue, T., Inoue, C., Miyoshi, G., Tomita, K., Bessho, Y., Hashimoto, N., and Kageyama, R. (2001). The basic helix-loop-helix gene hesr2 promotes gliogenesis in mouse retina. J Neurosci 21, 1265-1273.
- Schratt, G. M., F. Tuebing, E. A. Nigh, C. G. Kane, M. E. Sabatini, M. Kiebler and M. E. Greenberg (2006). "A brain-specific microRNA regulates dendritic spine development." Nature 439(7074): 283-289.
- Schwarz, D. S., G. Hutvagner, T. Du, Z. Xu, N. Aronin and P. D. Zamore (2003). "Asymmetry in the assembly of the RNAi enzyme complex." Cell 115(2): 199-208.
- Selcher, J. C., T. Nekrasova, R. Paylor, G. E. Landreth and J. D. Sweatt (2001). "Mice lacking the ERK1 isoform of MAP kinase are unimpaired in emotional learning." Learn Mem 8(1): 11-19.
- Shaikh, T. H., R. J. O'Connor, M. E. Pierpont, J. McGrath, A. M. Hacker, M. Nimmakayalu, E. Geiger, B. S. Emanuel and S. C. Saitta (2007). "Low copy repeats mediate distal chromosome 22q11.2 deletions: sequence analysis predicts breakpoint mechanisms." Genome Res 17(4): 482-491.
- Shi, S. H., Cheng, T. Jan, L. Y. and Jan, Y. N. (2004). APC and GSK-3beta are involved in mPar3 targeting to the nascent axon and establishment of neuronal polarity. Curr. Biol., 14, 2025–32
- Siegel, G., G. Obernosterer, R. Fiore, M. Oehmen, S. Bicker, M. Christensen, S. Khudayberdiev, P. F. Leuschner, C. J. Busch, C. Kane, K. Hubel, F. Dekker, C. Hedberg, B. Rengarajan, C. Drepper, H. Waldmann, S. Kauppinen, M. E. Greenberg, A. Draguhn, M. Rehmsmeier, J. Martinez and G. M. Schratt (2009). "A functional screen implicates microRNA-138-dependent regulation of the depalmitoylation enzyme APT1 in dendritic spine morphogenesis." Nat Cell Biol 11(6): 705-716.

- Silber, J., D. A. Lim, C. Petritsch, A. I. Persson, A. K. Maunakea, M. Yu, S. R. Vandenberg, D. G. Ginzinger, C. D. James, J. F. Costello, G. Bergers, W. A. Weiss, A. Alvarez-Buylla and J. G. Hodgson (2008). "miR-124 and miR-137 inhibit proliferation of glioblastoma multiforme cells and induce differentiation of brain tumor stem cells." BMC Med 6: 14.
- Siomi, H. and M. C. Siomi (2010). "Posttranscriptional regulation of microRNA biogenesis in animals." Mol Cell 38(3): 323-332.
- Smrt, R. D., K. E. Szulwach, R. L. Pfeiffer, X. Li, W. Guo, M. Pathania, Z. Q. Teng, Y. Luo, J. Peng, A. Bordey, P. Jin and X. Zhao (2010). "MicroRNA miR-137 regulates neuronal maturation by targeting ubiquitin ligase mind bomb-1." Stem Cells 28(6): 1060-1070.
- Stacy, R. C. and R. O. Wong (2003). "Developmental relationship between cholinergic amacrine cell processes and ganglion cell dendrites of the mouse retina." J Comp Neurol 456(2): 154-166.
- Stell, W. K., A. T. Ishida and D. O. Lightfoot (1977). "Structural basis for on-and off-center responses in retinal bipolar cells." Science 198(4323): 1269-1271.
- Stiemke, M. M. and J. G. Hollyfield (1995). "Cell birthdays in Xenopus laevis retina." Differentiation 58(3): 189-193.
- Sundermeier, T. R. and K. Palczewski (2012). "The physiological impact of microRNA gene regulation in the retina." Cell Mol Life Sci 69(16): 2739-2750.
- Szulwach, K. E., X. Li, R. D. Smrt, Y. Li, Y. Luo, L. Lin, N. J. Santistevan, W. Li, X. Zhao and P. Jin (2010). "Cross talk between microRNA and epigenetic regulation in adult neurogenesis." J Cell Biol 189(1): 127-141.
- Tay, Y., J. Zhang, A. M. Thomson, B. Lim and I. Rigoutsos (2008). "MicroRNAs to Nanog, Oct4 and Sox2 coding regions modulate embryonic stem cell differentiation." Nature 455(7216): 1124-1128.

- Tessier-Lavigne, M. and C. S. Goodman (1996). "The molecular biology of axon guidance." Science 274(5290): 1123-1133.
- Thum, T., C. Gross, J. Fiedler, T. Fischer, S. Kissler, M. Bussen, P. Galuppo, S. Just, W. Rottbauer, S. Frantz, M. Castoldi, J. Soutschek, V. Koteliansky, A. Rosenwald, M. A. Basson, J. D. Licht, J. T. Pena, S. H. Rouhanifard, M. U. Muckenthaler, T. Tuschl, G. R. Martin, J. Bauersachs and S. Engelhardt (2008). "MicroRNA-21 contributes to myocardial disease by stimulating MAP kinase signalling in fibroblasts." Nature 456(7224): 980-984.
- Tomita, K., Moriyoshi, K., Nakanishi, S., Guillemot, F., and Kageyama, R. (2000). Mammalian achaete-scute and atonal homologs regulate neuronal versus glial fate determination in the central nervous system. EMBO J 19, 5460-5472.
- Turner, D.L., and Cepko, C.L. (1987). A common progenitor for neurons and glia persists in rat retina late in development. Nature 328, 131-136.
- Turner, D.L., Snyder, E.Y., and Cepko, C.L. (1990). Lineage-independent determination of cell type in the embryonic mouse retina. Neuron 4, 833-845.
- Wada H, Shimada A, Fukamachi S, Naruse K, Shima A. Sex-Linked Inheritance of the lf Locus in the Medaka Fish (Oryzias latipes). Zoolog Sci. 1998 Jan 1;15(1):123-6. doi: 10.2108/zsj.15.123.
- Wada, H., A. Shimada, S. Fukamachi, K. Naruse and A. Shima (1998). "Sex-Linked Inheritance of the lf Locus in the Medaka Fish (Oryzias latipes)." Zoolog Sci 15(1): 123-126.
- Walker, J. C. and R. M. Harland (2009). "microRNA-24a is required to repress apoptosis in the developing neural retina." Genes Dev 23(9): 1046-1051.

- Wang FE, et al. MicroRNA-204/211 alters epithelial physiology. FASEB J. 2010; 24(5):1552–1571.
- Wang, B., S. H. Hsu, S. Majumder, H. Kutay, W. Huang, S. T. Jacob and K. Ghoshal (2010). "TGFbeta-mediated upregulation of hepatic miR-181b promotes hepatocarcinogenesis by targeting TIMP3." Oncogene 29(12): 1787-1797.
- Wang, Y., Y. Yu, A. Tsuyada, X. Ren, X. Wu, K. Stubblefield, E. K. Rankin-Gee and S. E. Wang (2011). "Transforming growth factor-beta regulates the sphere-initiating stem cell-like feature in breast cancer through miRNA-181 and ATM." Oncogene 30(12): 1470-1480.
- Wassle, H. (2004). "Parallel processing in the mammalian retina." Nat Rev Neurosci 5(10): 747-757.
- Wassle, H. and B. B. Boycott (1991). "Functional architecture of the mammalian retina." Physiol Rev 71(2): 447-480.
- Weeber, E. J. and J. D. Sweatt (2002). "Molecular neurobiology of human cognition." Neuron 33(6): 845-848.
- Wen, Z., L. Han, J. R. Bamburg, S. Shim, G. L. Ming and J. Q. Zheng (2007). "BMP gradients steer nerve growth cones by a balancing act of LIM kinase and Slingshot phosphatase on ADF/cofilin." J Cell Biol 178(1): 107-119.
- Werblin, F., B. Roska and D. Balya (2001). "Parallel processing in the mammalian retina: lateral and vertical interactions across stacked representations." Prog Brain Res 131: 229-238.
- Wienholds, E. and R. H. Plasterk (2005). "MicroRNA function in animal development." FEBS Lett 579(26): 5911-5922.

- Wightman, B., I. Ha and G. Ruvkun (1993). "Posttranscriptional regulation of the heterochronic gene lin-14 by lin-4 mediates temporal pattern formation in C. elegans." Cell 75(5): 855-862.
- Wightman, B., T. R. Burglin, J. Gatto, P. Arasu and G. Ruvkun (1991). "Negative regulatory sequences in the lin-14 3'-untranslated region are necessary to generate a temporal switch during Caenorhabditis elegans development." Genes Dev 5(10): 1813-1824.
- Williams, S. E., F. Mann, L. Erskine, T. Sakurai, S. Wei, D. J. Rossi, N. W. Gale, C. E. Holt, C. A. Mason and M. Henkemeyer (2003). "Ephrin-B2 and EphB1 mediate retinal axon divergence at the optic chiasm." Neuron 39(6): 919-935.
- Wittbrodt, J., Shima, A., and Schartl, M. (2002). Medaka--a model organism from the far East. Nat Rev Genet 3, 53-64.
- Wodarz, A. (2002). Establishing cell polarity in development. Nat. Cell Biol., 4, E39–E44
- Wohrn, J. C., L. Puelles, S. Nakagawa, M. Takeichi and C. Redies (1998). "Cadherin expression in the retina and retinofugal pathways of the chicken embryo." J Comp Neurol 396(1): 20-38.
- Xu, S., P. D. Witmer, S. Lumayag, B. Kovacs and D. Valle (2007). "MicroRNA (miRNA) transcriptome of mouse retina and identification of a sensory organ-specific miRNA cluster." J Biol Chem 282(34): 25053-25066.
- Yamagata, M., J. A. Weiner and J. R. Sanes (2002). "Sidekicks: synaptic adhesion molecules that promote lamina-specific connectivity in the retina." Cell 110(5): 649-660.
- Yamamoto, M. and K. Yamagami (1975). "Electron microscopic studies on choriolysis by the hatching enzyme of the teleost, Oryzias latipes." Dev Biol 43(2): 313-321.

- Yamamoto, T. (1958). "Artificial induction of functional sex-reversal in genotypic females of the medaka (Oryzias latipes)." J Exp Zool 137(2): 227-263.
- Yang, M., J. E. Lee, R. W. Padgett and I. Edery (2008). "Circadian regulation of a limited set of conserved microRNAs in Drosophila." BMC Genomics 9: 83.
- Yao, J., Y. Sasaki, Z. Wen, G. J. Bassell and J. Q. Zheng (2006). "An essential role for beta-actin mRNA localization and translation in Ca2+-dependent growth cone guidance." Nat Neurosci 9(10): 1265-1273.
- Yi, J. J., A. P. Barnes, R. Hand, F. Polleux and M. D. Ehlers (2010). "TGF-beta signaling specifies axons during brain development." Cell 142(1): 144-157.
- Yi, R., Y. Qin, I. G. Macara and B. R. Cullen (2003). "Exportin-5 mediates the nuclear export of pre-microRNAs and short hairpin RNAs." Genes Dev 17(24): 3011-3016.
- Yoshimura, T., Kawano, Y., Arimura, N. *et al*. (2005). GSK-3beta regulates phosphorylation of CRMP-2 and neuronal polarity. Cell, 120, 137–49
- Young, R.W. (1985). Cell differentiation in the retina of the mouse. Anat Rec 212, 199-205.
- Zhang, H., F. A. Kolb, L. Jaskiewicz, E. Westhof and W. Filipowicz (2004). "Single processing center models for human Dicer and bacterial RNase III." Cell 118(1): 57-68.
- Zhang, X.M., and Yang, X.J. (2001). Regulation of retinal ganglion cell production by Sonic hedgehog. Development 128, 943-957.
- Zhao, Y. and D. Srivastava (2007). "A developmental view of microRNA function." Trends Biochem Sci 32(4): 189-197.
- Zhou, X., T. Hollemann, T. Pieler and P. Gruss (2000). "Cloning and expression of xSix3, the Xenopus homologue of murine Six3." Mech Dev 91(1-2): 327-330.

- Zhu, Q., W. Sun, K. Okano, Y. Chen, N. Zhang, T. Maeda and K. Palczewski (2011). "Sponge transgenic mouse model reveals important roles for the microRNA-183 (miR-183)/96/182 cluster in postmitotic photoreceptors of the retina." J Biol Chem 286(36): 31749-31760.
- Zolessi, F. R., L. Poggi, C. J. Wilkinson, C. B. Chien and W. A. Harris (2006). "Polarization and orientation of retinal ganglion cells in vivo." Neural Dev 1: 2.

APPENDIX

miR-204 is required for lens and retinal development via Meis2 targeting

Ivan Conte, Sabrina Carrella, Raffaella Avellino, Marianthi Karali, Raquel Marco-Ferreres, Paola Bovolenta, and Sandro Banfi.

MicroRNAs (miRNAs) are small noncoding RNAs that have important roles in the regulation of gene expression. The roles of individual miRNAs in controlling vertebrate eye development remain, however, largely unexplored. Here, we show that a single miRNA, miR-204, regulates multiple aspects of eye development in the medaka fish (Oryzias latipes). Morpholino-mediated ablation of miR-204 expression resulted in an eye phenotype characterized by microphthalmia, abnormal lens formation, and altered dorsoventral (D-V) patterning of the retina, which is associated with optic fissure coloboma. Using a variety of in vivo and in vitro approaches, we identified the transcription factor Meis2 as one of the main targets of miR-204 function. We show that, together with altered regulation of the Pax6 pathway, the abnormally elevated levels of Meis2 resulting from miR-204 inactivation are largely responsible for the observed phenotype. These data provide an example of how a specific miRNA can regulate multiple events in eye formation; at the same time, they uncover an as yet unreported function of Meis2 in the specification of D-V patterning of the retina.

miR-204 is required for lens and retinal development via *Meis2* targeting

Ivan Conte[a,b], Sabrina Carrella[a], Raffaella Avellino[a], Marianthi Karali[a], Raquel Marco-Ferreres[c], Paola Bovolenta[c], and Sandro Banfi[a,1]

[a]Telethon Institute of Genetics and Medicine, 80131 Naples, Italy; [b]Institute of Genetics and Biophysics Adriano Buzzati Traverso, Consiglio Nazionale delle Ricerche, 80131 Naples, Italy; and [c]Departamento de Neurobiología Molecular Celular y del Desarrollo, Instituto Cajal, Consejo Superior de Investigaciones Cientificas, and Centro de investigaciònes Biomédica en Red de Enfermedades Raras, 28002 Madrid, Spain

Edited* by Huda Y. Zoghbi, Baylor College of Medicine, Houston, TX, and approved July 16, 2010 (received for review December 30, 2009)

MicroRNAs (miRNAs) are small noncoding RNAs that have important roles in the regulation of gene expression. The roles of individual miRNAs in controlling vertebrate eye development remain, however, largely unexplored. Here, we show that a single miRNA, miR-204, regulates multiple aspects of eye development in the medaka fish (*Oryzias latipes*). Morpholino-mediated ablation of miR-204 expression resulted in an eye phenotype characterized by microphthalmia, abnormal lens formation, and altered dorsoventral (D-V) patterning of the retina, which is associated with optic fissure coloboma. Using a variety of in vivo and in vitro approaches, we identified the transcription factor *Meis2* as one of the main targets of miR-204 function. We show that, together with altered regulation of the Pax6 pathway, the abnormally elevated levels of *Meis2* resulting from miR-204 inactivation are largely responsible for the observed phenotype. These data provide an example of how a specific miRNA can regulate multiple events in eye formation; at the same time, they uncover an as yet unreported function of Meis2 in the specification of D-V patterning of the retina.

microRNA | eye development | medaka fish

Development of the vertebrate eye takes place through a series of morphogenetic events that are controlled by molecular networks in which transcription factors and signaling pathways have major roles (1). Specific components of these networks are reiteratively exploited in space and time to pattern eye tissues and to control the subsequent cellular programs, such as cell proliferation, differentiation, migration, and programmed cell death (2, 3). Most of these developmental processes are critically sensitive to gene dose, and variations in the normal levels of regulatory proteins appear to result in a variety of eye anomalies (4, 5). Posttranscriptional regulatory mechanisms maintain the appropriate levels of expression of these proteins and enable rapid changes in the cellular proteome; thus, they have fundamental roles in the development of the nervous system (6).

MicroRNAs (miRNAs) are a class of 20- to 25-nucleotide noncoding RNA molecules that mediate a newly recognized level of posttranscriptional control of gene expression. Indeed, miRNAs can impair either mRNA translation or stability by binding through imperfect base pairing to specific sites in the 3′-UTR of target mRNAs (7). Recently, many miRNAs have been shown to be required for vertebrate developmental processes, such as cell fate determination and patterning as well as cell death and proliferation (8).

A number of miRNAs show restricted expression patterns in the developing lens, retinal pigment epithelium (RPE), neural retina, and other ocular tissues, which suggests their potential relevance to eye development and function (9, 10). However, the precise roles of individual miRNAs and their specific influences on given mRNA targets that are important for vertebrate eye development remain unclear.

In the present study, we show that miR-204, which is highly expressed in the presumptive RPE, lens, ciliary body, and neural retina (11, 12), is required for correct lens and optic cup development. Using a variety of gain- and loss-of-function approaches in the medaka fish [*Oryzias latipes* (ol)], we demonstrate that miR-204–mediated modulation of the *Meis2* gene dose has a significant impact on regulation of the genetic pathways controlling eye morphogenesis and differentiation.

Results

miR-204 Knockdown Causes Lens Abnormalities, Microphthalmia, and Eye Coloboma. We found that during early medaka development [stage (St) 23], ol-miR-204 was expressed in the lens placode and in the presumptive RPE, with an apparent dorsal^{high}-to-ventral^{low} gradient (Fig. S1*A*). At later stages, ol-miR-204 expression was also detected in the ciliary marginal zone, ciliary body, and presumed migratory neural crest cells (Fig. 1 *A*–*A*′). This expression pattern suggested that miR-204 might modulate different aspects of eye development.

To investigate this further, we interfered with miR-204 processing and activity using a multiblocking morpholino (Mo)-based knockdown approach (13). To this end, we designed two Mos, Mo-miR-204- and Mo-miR-204-2, against the two ol-miR-204-1 and ol-miR-204-2 precursor sequences present in the medaka genome, which give rise to an identical mature miR-204 sequence. Embryos injected with either of these two Mos at the one-cell stage were morphologically indistinguishable from control embryos up to the optic-vesicle stage. In contrast, from St24 onward, an aberrant eye phenotype was clearly visible in most of the Mo-miR-204–injected embryos (65 ± 5% of 3,000 injected embryos). Growth of the eye cup was significantly impaired and culminated in evident microphthalmia at St40 (Fig. S2 *A* and *D*). In 90% of the microphthalmic embryos, lens development was also impaired. Specifically, at St24, the monolayer of lens epithelial cells was positioned in the dorsal region of the lens vesicle instead of lining its distal surface in morphants (Fig. 2 *A*–*F*, Fig. S3 *H*, *H*′, *J*, and *J*′, and Fig. S4 *A*, *B*, *G*, and *H*). Furthermore, the primary fiber cells that are located in the center of the lens vesicle were misplaced and disorganized, whereas those of the control embryos had begun to elongate to form the organized concentrical layers (Fig. 2 *A*–*F* and Fig. S4 *A*, *B*, *G*, and *H*). This altered cellular organization was also evident at later stages, when abnormal ventral-distal herniations of the lens were also evident (Fig. S2*E*). Finally, a significant number of the microphthalmic morphant embryos (30%) were characterized by a ventral coloboma, through failure of optic fissure closure (Fig. S2 *C* and *F*).

We did not observe any qualitative and quantitative phenotypic differences following the injection of Mo-miR-204-1 or Mo-miR-204-2; hence, subsequent studies were performed only with

Author contributions: I.C., P.B., and S.B. designed research; I.C., S.C., R.A., M.K., R.M.-F., and S.B. performed research; I.C. analyzed data; and I.C., P.B., and S.B. wrote the paper.

The authors declare no conflict of interest.

*This Direct Submission article had a prearranged editor.

[1]To whom correspondence should be addressed. E-mail: banfi@tigem.it.

This article contains supporting information online at www.pnas.org/lookup/suppl/doi:10.1073/pnas.0914785107/-/DCSupplemental.

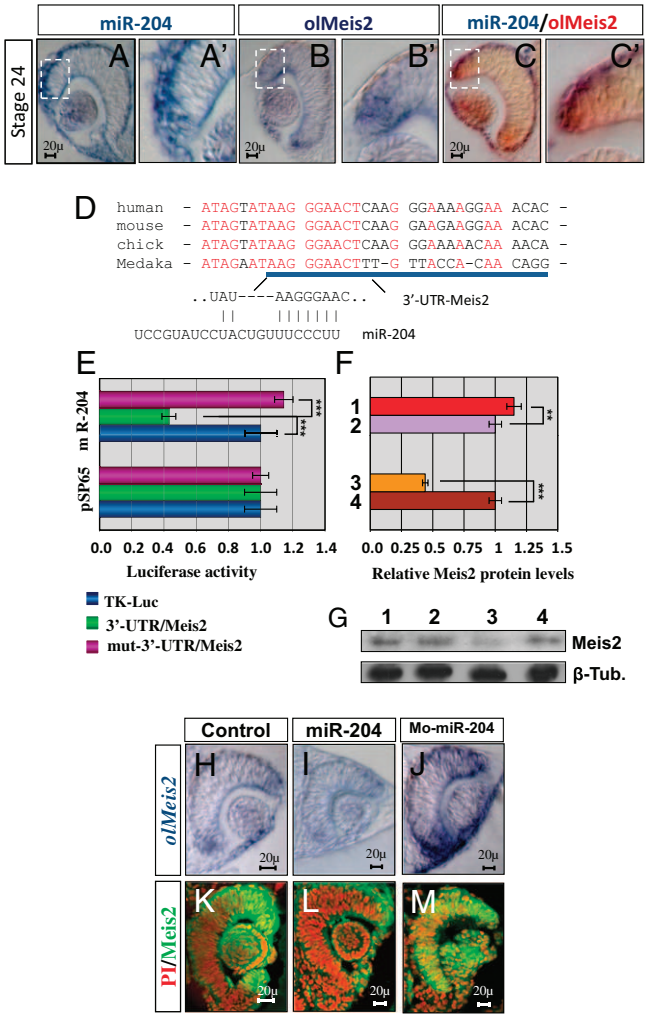

Fig. 1. miR-204 directly targets *Meis2*. (*A*–*C*′) Frontal sections of St24 WT medaka embryos hybridized in both single (*A*–*B*′) and double (*C* and *C*′) whole-mount RNA ISH with probes against *olMeis2* (red) and miR-204 (blue). miR-204 (A and A′) and *olMeis2* (blue) (*B*–*B*′) colocalize in the lens placode and ciliary marginal zone (*C*–*C*′). Boxed areas are magnified in *A*′–*C*′. (*D*) Predicted target site of miR-204 within the 3′-UTR of the *Meis2* gene in different species, showing conserved nucleotides (red) and nonconserved nucleotides (black). The blue line represents the sequence against which Meis2-TPmiR-204 Mo was designed. (*E*) Relative Luc activities in H36CE cells as fold differences in the Luc/Renilla ratios normalized to the value of Luc reporter constructs. miR-204 addition significantly decreases Luc activity of the construct containing 3′-UTR of *MEIS2* when compared with controls. ***$P < 0.0001$ (*t* tests). Three point mutations in the predicted miR-204 target site in *Meis2* inhibit this effect (no significant variation when compared with the thymidine kinase (TK)-Luc control). Densitometric analysis (*F*) of Western blotting (*G*) shows reduction of Meis2 protein levels in the presence of miR-204 duplexes and increase after miR-204 depletion when compared with cel-miR-67 control transfections. **$P < 0.001$; ***$P < 0.0001$ (*t* tests). 1, inhibitor hsa-miR-204; 2, inhibitor cel-miR-67; 3, mimic hsa-miR-204; 4, mimic cel-miR-67. Relative levels of the Meis2 protein measured 48 h after transfection of H36CE cells. (*H*–*M*) Frontal sections of St24 control (*H* and *K*), miR-204–overexpressing (*I* and *L*), and Mo-miR-204–injected (*J* and *M*) embryos treated for whole-mount RNA ISH with an *olMeis2* probe (*H*–*J*) or immunostained with an anti-Meis2 antibody (green) (*K*–*M*). Sections are counterstained with propidium iodide (PI, red). Both *olMeis2* mRNA and protein are down-regulated in lens placode and retina of miR-204–overexpressing embryos (*I* and *L*) but up-regulated in miR-204 morphants (*J* and *M*). (Scale bars: 20 µm.).

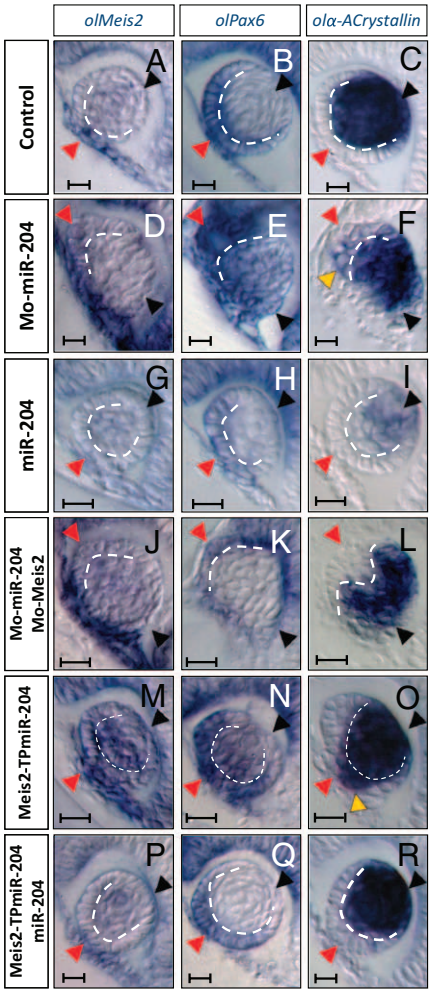

Fig. 2. Interference with miR-204 expression modifies lens cell differentiation via *Meis2* targeting. Frontal sections of St24 control (*A*–*C*), Mo-miR-204 (*D*–*F*), miR-204 (*G*–*I*), Mo-Meis2/Mo-miR-204 (*J*–*L*), Meis2-TPmiR-204 (*M*–*O*), and Meis2-TPmiR-204/miR-204 (*P*–*R*)–injected medaka embryos processed for whole-mount RNA ISH with probes specific for *olMeis2* (*A*, *D*, *G*, *J*, *M*, and *P*), *olPax6* (*B*, *E*, *H*, *K*, *N*, and *Q*), and *olα-ACrystallin* (*C*, *F*, *I*, *L*, *O*, and *R*). Expression of *olMeis2* (*D* and *M*) and *olPax6* (*E* and *N*) is up-regulated in lens of miR-204 and Meis2-TPmiR-204 morphant embryos, whereas that of *olα-ACrystallin* is increased in the lens placode and ectopically expressed in the epithelial lens monolayer (*F* and *O*, yellow arrowheads). Lens epithelial (*D*–*F* and *J*–*L*, red arrowheads) and primary fiber (*D*–*F* and *J*–*L*, black arrowheads) cells are displaced. (*J*) MOs act at the translational level; thus, Mo-Meis2/Mo-miR-204 coinjection does not rescue *olMeis2* mRNA expression. miR-204 gain-of-function has opposite effects in lens gene expression, without affecting lens epithelial monolayer (*G*–*I*, red arrowheads) and the primary fibers (*G*–*I*, black arrowheads). Mo-Meis2/Mo-miR-204 and Meis2-TPmiR-204/miR-204 coinjections restore correct expression of lens differentiation markers (*J*–*L* and *P*–*R*). Mo-Meis2/Mo-miR-204 coinjections do not rescue cell displacement (*J*–*L*, red and black arrowheads). Broken lines mark boundaries between the lens epithelial monolayer and the primary fiber cells. (Scale bars: 20 µm.)

Mo-miR-204-1. The Mo blocking efficiency and the specificity of the eye phenotype were verified through a series of experiments described in *SI Text* (Fig. S1 and Tables S1 and S2). These included RNA in situ hybridization (ISH) using the miR-204-locked nucleic acid antisense probe and injections of 6-bp–mismatched Mo (mm-Mo-miR-204), which gave no aberrant phenotype at any concentration (Table S2). To rule out off-targeting Mo effects, we coinjected Mo-miR-204-1 and a Mo against p53 (Mo-p53). We did not observe any modifications of the phenotype, which further confirmed the specificity of Mo-miR-204 targeting (14) (*SI Text* and Fig. S2 *V*–*X*).

***Meis2* Gene Is a Direct Target of miR-204.** Given the specificity of this miR-204 loss-of-function phenotype, we searched for its

potential mRNA targets using the recently developed host-gene oppositely correlated target (HOCTAR) tool, which integrates expression profiling and sequence-based miRNA target recognition software (15). Among the predicted miR-204 targets, the homeobox transcription factors *Meis1* and *Meis2* appeared particularly attractive to explain the observed eye defects because they had been previously shown to regulate vertebrate eye development by modulating *Pax6* expression (16). Furthermore, the predicted target site of miR-204 within the 3′-UTR of *Meis2* (but not of *Meis1*) was highly conserved across all vertebrate species analyzed, including medaka (Fig. 1*D*). To validate this prediction, we cloned the 3′-UTR of the human *MEIS2* gene containing the miR-204 target site downstream of the coding region of the *Luciferase* (Luc) reporter gene, and tested the ability of miR-204 to affect reporter expression in vitro. The presence of the *MEIS2* 3′-UTR sequence specifically inhibited Luc activity in response to miR-204 (Fig. 1*E*). In addition, point mutations in the miR-204 binding site of the *MEIS2* 3′-UTR abolished this repression, indicating that miR-204 directly and specifically targets *MEIS2* (Fig. 1*E*). In agreement with these observations, the levels of MEIS2 protein in H36CE human lens epithelial cells were decreased in the presence of miR-204 duplexes and elevated on miR-204 inhibition (Fig. 1 *F* and *G*). The specificity of this repression was confirmed by additional controls described in *SI Text* (i.e., a Luc construct containing the 3′-UTR of *PAX6* and miR-182, an unrelated miRNA expressed in the eye) (Fig. S3 *K–N*).

The miR-204 targeting of *Meis2* was also confirmed in vivo. miR-204 and *Meis2* showed overlapping expression patterns in the lens and in the peripheral optic cup (Fig. 1 *A–C′*). Moreover, injections of miR-204 duplexes resulted in a decrease in endogenous *Meis2* mRNA and protein levels, whereas injections of Mo-miR-204 led to an increase in the optic cup of medaka embryos (Fig. 1 *H–M*). The expansion of the *Meis2* domain in the miR-204 morphants was not caused by a generalized delay of eye development because (*i*) *Meis2* was correctly expressed at early stages of lens and retinal development in the morphants (Fig. S3 *G–J′*) and (*ii*) *Ath5*, an early marker of retinal ganglion cell differentiation, was expressed normally at St26, when the retina begins to differentiate (Fig. S3 *O* and *P*). Altogether, these data strongly indicate that *Meis2* is a bona fide miR-204 target.

miR-204 Controls Lens Differentiation by Targeting *Meis2* and Modulating the *Pax6* Transcriptional Pathway. We next sought to determine whether the miR-204 morphant phenotype was indeed related to abnormal activation of *olMeis2* expression. *Meis2* has been reported to regulate Pax6 activity in the lens in a direct and positive way (16). *Pax6*, in turn, controls the expression of genes involved in lens differentiation, including *Sox2*, *Prox1*, and α-*ACrystallin* (17, 18). With the exception of *Meis2*, none of these genes are predicted to contain miR-204 target sites. We thus reasoned that if miR-204 directly controls expression of *Meis2* in vivo, the levels of expression of all these genes should be increased in the miR-204 morphant as a consequence of alterations in *Meis2* expression.

Indeed, RNA ISH demonstrated that in the morphant optic cup, *olPax6*, *olSox2*, *olProx1*, and *olα-ACrystallin* showed up-regulated expression and/or were misexpressed in both lens ectoderm and primary lens fiber cells when compared with control embryos (Fig. 2 *A–F* and Fig. S4 *A*, *B*, *G*, and *H*). To demonstrate a direct interaction between miR-204 and *Meis2* further, and to dissect out the role of this interaction in lens development, we increased the levels of miR-204 by injecting miR-204 duplexes. From St20 onward, duplex-injected embryos were severely microphthalmic, with small lenses (Fig. S2 *J–L*), which strongly resembled the phenotype reported for *Meis2.2* zebrafish morphant embryos (19). Consistent with the hypothesis that *olMeis2* is an important miR-204 target, expression of the *olMeis2*, *olPax6*, *olSox2, olProx1*, and *olα-ACrystallin* genes was significantly reduced in the lens placode of all the duplex-injected embryos (Fig. 2 *G–I* and Fig. S4 *C* and *I*), as confirmed by quantitative real-time qRT (PCR) (Fig. S4*M*). Of note, inhibition of miR-204 activity by Mo-miR-204 injections was accompanied by an opposite trend in the relative transcript levels (Fig. S4*N*). Interestingly, both the lens epithelial monolayer and the primary fiber cells were normally localized in duplex-injected embryos (Fig. 2 *G–I* and Fig. S4 *C* and *I*).

If most of the changes in lens differentiation marker expression caused by miR-204 knockdown are mediated by *Meis2*, coinjection of a Mo against *olMeis2* (Mo-Meis2) should reestablish normal expression levels in miR-204 morphants. Consistent with this, Mo-Meis2 injection was sufficient to rescue the normal expression of lens differentiation markers in a substantial proportion of miR-204 morphants (Fig. 2 *J–L*, Fig. S4 *D* and *J*, and Table S2), although defects in epithelial and lens fiber cell organization were not rescued (Fig. 2 *J–L* and Fig. S4 *D* and *J*). This suggests that miR-204 regulates additional, and as yet unidentified, genes that are important for correct lens development.

To obtain additional support for the importance of miR-204–mediated regulation of *olMeis2*, we disrupted the interaction of miR-204 with its target site in *olMeis2* 3′-UTR by injecting a *Meis2* "target protector" (20) Mo (Meis2-TPmiR-204) in WT embryos (*SI Text* and Fig. S3 *A–F*). A significant percentage of Meis2-TPmiR-204–injected embryos were morphologically indistinguishable from miR-204 morphants and characterized by similar defects in the lens, optic cup size, and optic fissure coloboma (Fig. S2 *G–I* and Table S2). Moreover, protection of the miR-204 target site within *Meis2* mRNA resulted in expansion of the lens placode expression domains of *olMeis2*, *olPax6*, and *olSox2* and mislocalization of *olProx1* and *olα-ACrystallin*, the mRNAs of which were ectopically detected in the epithelial cell monolayer (Fig. 2 *M–O* and Fig. S4 *E* and *K*). Unlike our observations in miR-204 morphant embryos, these changes were not associated with defects in epithelial and lens fiber cell organization (Fig. 2 *M–O* and Fig. S4 *E* and *K*), further supporting the possibility that these alterations are mediated by other mRNA targets. Finally, protection of *Meis2* targeting was sufficient to rescue the correct expression of lens differentiation markers in miR-204–overexpressing embryos (Fig. 2 *P–R* and Fig. S4 *F* and *L*).

Altogether, these data indicate that miR-204 controls lens cell differentiation by modulating the expression of lens placode differentiation genes via the Meis2/Pax6 pathway.

miR-204 Has an Active Role in Establishment of Dorsoventral Polarity of the Optic Cup. Defects in optic fissure closure were observed in both the Mo-miR-204 and Meis2-TPmiR-204 morphants (Fig. S2 *D–I*). Colobomas have been frequently described as a consequence of impaired dorsoventral (D-V) polarity of the optic cup (21). As observed in the lens, this defect was associated with concomitant up-regulation of *olMeis2* (Fig. 1 *H*, *J*, *K*, and *M* and Fig. S5*B*) and *olPax6* expression. In particular, *olPax6* expression extended to the ventral retina, where it is normally expressed at relatively low levels (Fig. 3 *A*, *D*, and *M*). Previous studies have shown that expansion of *Pax6* expression in the ventral retina results in alterations in D-V polarity of the optic cup (22, 23). Therefore, we asked whether expression of D-V optic cup markers was modified in Mo-miR-204 and Meis2-TPmiR-204 morphants. In all the injected embryos, the expression domain of the ventral marker *olVax2* and the ventral expression domain of *olPax2* (24) were reduced or absent (Fig. 3 *B*, *E*, and *N* and Fig. S5 *E* and *H*), whereas the expression domains of the dorsal markers *olBmp4* and *olTbx5* were ventrally expanded (Fig. 3 *C*, *F*, and *O* and Fig. S5 *K* and *N*). A reciprocal molecular phenotype was observed after miR-204 overexpression: The *olBmp4* and *olTbx5* domains were largely reduced, whereas those of *olPax2* and *olVax2* were dorsally expanded (Fig. 3 *H* and *I* and Fig. S5 *F* and *L*). Furthermore, coinjection of Mo-Meis2 with Mo-miR-204 (Fig. S2 *M–O*,

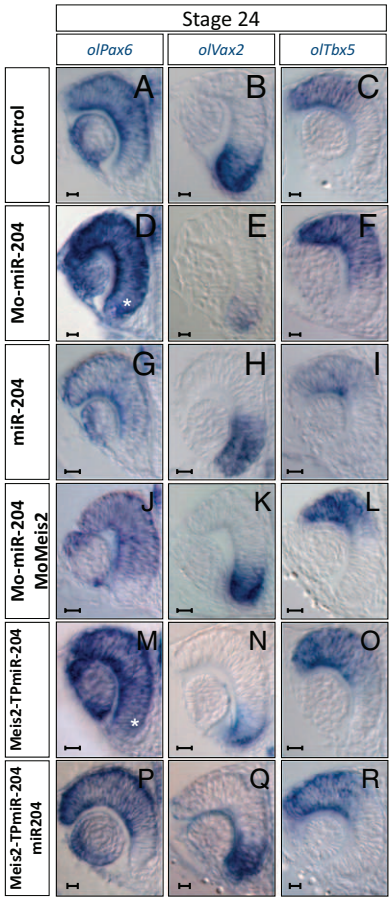

Fig. 3. miR-204 is required for establishment of D-V polarity of the optic cup. Frontal vibratome sections of control (*A–C*), Mo-miR-204 (*D–F*), miR-204 (*G–I*), Mo-Meis2/Mo-miR-204 (*J–L*), Meis2-TPmiR-204 (*M–O*), and Meis2-TPmiR-204/miR-204 (*P–R*)–injected embryos processed for whole-mount RNA ISH with probes specific for *olPax6* (*A*, *D*, *G*, *J*, *M*, and *P*), *olVax2* (*B*, *E*, *H*, *K*, *N*, and *Q*), and *olTbx5* (*C*, *F*, *I*, *L*, *O*, and *R*). *olPax6* is up-regulated and ectopically expressed in ventral retina of morphant embryos (*D* and *M*, asterisk). Expression of ventral gene *olVax2* is reduced, whereas that of dorsal marker *olTbx5* is expanded ventrally in morphant embryos (*E*, *F*, *N*, and *O*) when compared with control embryos (*B* and *C*). miR-204–overexpressing embryos show reciprocal alterations in *Pax6* and D-V marker expression (*G–I*). Defects in D-V optic cup polarity are completely rescued by coinjection of Mo-miR-204 with Mo-Meis2 (*J–L*) and Meis2-TPmiR-204 with miR-204 (*P–R*). (Scale bars: 20 μm.)

Fig. S5*A*, and Table S2) or that of miR-204 with the Meis2-TPmiR-204 target protector (Fig. S2 *S–U*, Fig. S5*C*, and Table S2) fully rescued the coloboma phenotype and the normal levels of D-V markers and *Pax6* expression (Fig. 3 *J–L*, *P–R* and Fig. S5 *G*, *I*, *M*, and *O*).

Altogether, these data demonstrate that miR-204–mediated control of the Meis2/Pax6 pathway contributes to D-V patterning of the optic cup. Moreover, our findings reveal a previously unidentified role for *Meis2* in this morphogenetic event.

Discussion

MiRNAs appear to function as "master regulators" of key molecular pathways through their ability to fine-tune gene dose (25); consequently, they have basic roles in vertebrate organogenesis and pathogenesis. The general importance of this class of molecule in eye development is supported by effects observed in mice after genetic inactivation of Dicer, a key enzyme of miRNA biogenesis (26). However, there is little information available on individual miRNAs that contribute to the correct development and function of the eye. Examples exist with miR-24a, miR-124, and miR-26a for the regulation of apoptotic pathways, retinogenesis, and circadian rhythms of mRNAs in the retina, respectively (27–29). Here, we showed that a single miRNA can regulate multiple aspects of eye development. Indeed, miR-204 is required for lens differentiation, optic cup development, and optic fissure closure.

Starting from in silico predictions and using a variety of in vitro and in vivo experimental approaches, we have shown that *Meis2* is a bona fide target of miR-204 activity. Our data also show that the specific miR-204–mediated regulation of *Meis2* modulates the function of the *Pax6* transcriptional network. These data indicate that miR-204 is an essential component of the Meis2/Pax6 molecular pathway, and hence is an important element of the molecular network that regulates eye development in vertebrates (Fig. 4). This regulatory cascade is strongly supported by a number of observations. *Meis2* directly activates *Pax6* expression during lens and retina development in the zebrafish, chick, and mouse (16, 19, 30). In medaka fish embryos, expression levels of *olMeis2* and, concomitantly, those of *olPax6* and its downstream targets are up-regulated on miR-204 knock-down or inhibition of the miR-204 interaction with its specific target site in the *Meis2* 3′-UTR. Furthermore, the phenotypic alterations observed in miR-204 morphants strongly resembled those reported for *Meis2* or *Pax6* gain-of-function models (4, 16, 19, 30), which include aberrant lens differentiation and microphthalmia. Conversely, miR-204 over-expression led to a significant down-regulation of Meis2 activity, with phenotypic consequences similar to those observed after *Meis2* loss-of-function, in which a reduction of *Pax6* gene dose was also observed (16, 19, 30). Finally, concomitant knock-down of *olMeis2* and miR-204 and protection of the *olMeis2* target site in miR-204–overexpressing embryos, significantly rescued expression of *olPax6*, *olSox2*, *olProx1*, and *olα-ACrystallin* in the lens, which is consistent with a pathway in which miR-204 controls lens differentiation through regulation of *olMeis2* levels (Fig. 4).

During lens development, the progeny of epithelial cells migrate into the transitional zone and elongate and differentiate into lens fiber cells (18, 31). Timely differentiation and correct migration of lens fibers are crucial for continuous addition of fiber mass and formation of a correctly organized lens. The miR-204–mediated control of *olMeis2* appears to modulate gene expression programs that control these events because its over-expression or inactivation produces significant changes in the expression of lens differentiation markers. miR-204 also appears to control lens morphogenesis, because lens epithelial cells were abnormally positioned in Mo-204 morphants. However, this miR-204 activity is very likely to be *Meis2*-independent, because protection of *Meis2* mRNA did not alter epithelial and lens fiber cell organi-

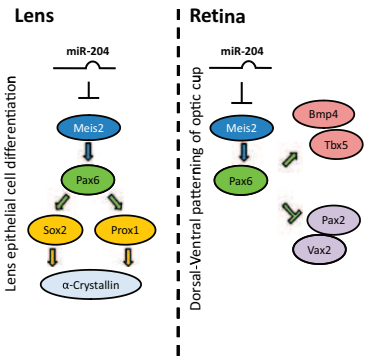

Fig. 4. Model for function of miR-204 in lens and retina development. miR-204 controls expression of the *Meis2* gene, contributing to regulation of the Meis2/Pax6 pathway in both lens and retina development.

zation. Thus, miR-204 might ensure correct control of lens morphogenesis by targeting other genes involved (e.g., in the control of cell polarity, cell-cell signaling, tissue polarity, or cell migration). This last possibility is particularly attractive, because cells with elevated miR-204 levels are highly mobile and have invasive properties (32, 33).

The miR-204 contributed to other aspects of eye morphogenesis, as expected by its specific distribution in ocular tissues other than the lens. The requirement for miR-204 in establishment of D-V polarity in the optic cup and in optic fissure closure can also be explained by its control of *Meis2* expression. Indeed, the defects in D-V polarity and optic fissure closure in the miR-204 and Meis2-TPmiR-204 morphants were rescued by coinjection with Mo-Meis2 or miR-204, respectively. This is an as yet unreported aspect of Meis2 function that is probably mediated by the observed ectopic ventral expression of *Pax6*, the overexpression of which correlates with significant down-regulation of ventral determinant genes, which leads to the formation of optic fissure coloboma (22, 23). However, the relatively low frequency of optic fissure defects in miR-204 morphants suggests that miR-204 might not serve as an "on-off" switch for the genetic program required for correct optic fissure closure.

In miR-204 morphants, eye formation was initiated and progressed normally up to the optic cup stage; thereafter, it did not advance correctly, leading to microphthalmia. This phenotype might be a consequence of alterations in apoptosis and/or cell proliferation, because previous studies have shown that members of the *Meis* gene family can directly regulate these events. However, we found that the concomitant knock-down of *Meis2* and miR-204 was insufficient to restore normal eye size (Fig. S2), possibly because Mo-Meis2 reduces the levels of *Meis2* expression well below normal levels. Indeed, a microphthalmic phenotype has been reported for loss-of-function *Meis* mutants in the chick and zebrafish (19, 29). Alternatively, the miR-204–mediated regulation of eye size involves other, as yet unidentified, transcriptional pathways.

Although miRNAs have the potential to regulate the expression of hundreds of genes, we have shown that the specific miR-204-*Meis2* interaction has multiple consequences in eye development. Of note, this action is mediated by a single miR-204 target site within the 3′-UTR of the *Meis2* gene, as demonstrated by the specific target protector assay. Previous reports have proposed that the presence of multiple target sites for the same miRNA within the 3′-UTR of a given mRNA is a strong indication of the "strength" and biological relevance of these interactions (34). However, in agreement with our data, it has also been reported that point mutations in a single miRNA recognition site have a pathogenetic role in human genetic diseases (35). Thus, the mode of action of miRNAs and their relevance in the control of basic biological processes may be more complex than initially envisaged.

In conclusion, we have begun to unravel the function of miR-204 during eye development, and we have demonstrated that this is largely mediated by *Meis2* targeting. As shown by our data, miR-204 may have additional target genes in the eye. It will be of the utmost importance to identify these and to determine whether alterations in miR-204 expression contribute to the pathogenesis of eye malformations in humans.

Materials and Methods

Medaka Stocks. Samples of the Cab strain of WT medaka fish were kept and staged as described (36).

Computational Analysis. Prediction of miRNA targets was performed using the Host gene Opposite Correlated TARgets (HOCTAR) tool (http://hoctar.tigem.it) (15).

Mo and miR-204 Duplex Injections. Mos (Gene Tools, LLC) were designed and injected into fertilized one-cell embryos, as detailed in Table S1. The specificity and inhibitory efficiency of each Mo were determined as described (14). Optimal Mo concentrations (Tables S1 and S2) were determined on the basis of morphological criteria. miRIDIAN (Dharmacon) miRNA Mimics for miR-204 were injected at a final concentration of 4 μM. Embryos injected with mm-Mo-miR-204 were used as controls.

Whole-Mount ISH. Whole-mount RNA ISH was performed, photographed, and sectioned as described (37). Digoxigenin-labeled antisense and sense riboprobes for *olMeis2*, *olPax6*, *olα-ACrystallin*, *olSox2*, *olProx1*, *olBmp4*, *olTbx5.2*, *olVax2*, and *olPax2* were used. The miRCURY detection miR-204 probe (Exiqon) was used according to Karali et al. (11).

Western Blotting. Immunoblotting was performed as described (38), with a rabbit polyclonal antibody against Meis2 (1:1,000) or an anti-β-tubulin monoclonal antibody (1:1,000; Sigma).

Immunolabeling. Medaka embryos were cryostat-sectioned, and immunochemistry was performed as described (39) using an anti-phospho-histone H3 monoclonal antibody (1:100; Cell Signaling Technology) and an anti-Meis2 rabbit polyclonal antiserum. Alexa-488–conjugated goat anti-rabbit or anti-mouse (1:1,000; Invitrogen) IgGs were used as secondary antibodies. Alternatively, a peroxidase-conjugated anti-rabbit antibody (1:200; Vector Laboratories) was used, followed by diaminobenzidine staining, as described previously (40).

Cell Transfection, qRT-PCR, and Luc Assays. The H36CE human lens epithelial cell line was grown as described (41). Cell transfections and qRT-PCR experiments were performed as described (15). Cells were transfected with either 50 nM miRIDIAN miRNA Mimics or 80 nM miRIDIAN miRNA Inhibitor (Dharmacon). Plasmids containing the 3′-UTR of the human *MEIS2* gene and psiUx plasmid constructs containing the hsa-premiR-204 sequence were used in Luc assays, as described previously (15). Each assay was performed in duplicate, and all the results are shown as means ± SD of at least three independent assays. The primer sequences used to amplify each transcript are shown in Table S1.

ACKNOWLEDGMENTS. We are grateful to M. Torres (Centro Nacional de investigaciones Cardiovasculares, Madrid) for providing the Meis2 antibody. We thank M. Studer and G. Diez-Roux (Telethon Institute of Genetics and Medicine, Naples) for critical reading of the manuscript. We thank F. Salierno, M. Pirozzi (Telethon Institute of Genetics and Medicine), and the Institute of Genetics and Biophysics Open Laboratory for technical support. This study was supported by the Italian Telethon Foundation, European Union Grants LSHG-CT-2005-512036 and PERG03-GA-2008-231068 (to S.B.) and Spanish Ministerio de Ciencia e Innovación Grant BFU2007-61774 (to P.B.). R.M.F holds an I3P-Consejo Superior de Investigaciones Cientificas Postdoctoral Fellowship.

1. Chow RL, Lang RA (2001) Early eye development in vertebrates. *Annu Rev Cell Dev Biol* 17:255–296.
2. Livesey FJ, Cepko CL (2001) Vertebrate neural cell-fate determination: Lessons from the retina. *Nat Rev Neurosci* 2:109–118.
3. Dyer MA, Cepko CL (2001) Regulating proliferation during retinal development. *Nat Rev Neurosci* 2:333–342.
4. Schedl A, et al. (1996) Influence of PAX6 gene dosage on development: Overexpression causes severe eye abnormalities. *Cell* 86:71–82.
5. Taranova OV, et al. (2006) SOX2 is a dose-dependent regulator of retinal neural progenitor competence. *Genes Dev* 20:1187–1202.
6. Fiore R, Siegel G, Schratt G (2008) MicroRNA function in neuronal development, plasticity and disease. *Biochim Biophys Acta* 1779:471–478.
7. He L, Hannon GJ (2004) MicroRNAs: Small RNAs with a big role in gene regulation. *Nat Rev Genet* 5:522–531.
8. Harfe BD (2005) MicroRNAs in vertebrate development. *Curr Opin Genet Dev* 15: 410–415.
9. Huang KM, Dentchev T, Stambolian D (2008) MiRNA expression in the eye. *Mamm Genome* 19:510–516.
10. Xu S (2009) microRNA expression in the eyes and their significance in relation to functions. *Prog Retin Eye Res* 28:87–116.
11. Karali M, Peluso I, Marigo V, Banfi S (2007) Identification and characterization of microRNAs expressed in the mouse eye. *Invest Ophthalmol Vis Sci* 48:509–515.
12. Xu S, Witmer PD, Lumayag S, Kovacs B, Valle D (2007) MicroRNA (miRNA) transcriptome of mouse retina and identification of a sensory organ-specific miRNA cluster. *J Biol Chem* 282:25053–25066.
13. Kloosterman WP, Lagendijk AK, Ketting RF, Moulton JD, Plasterk RH (2007) Targeted inhibition of miRNA maturation with morpholinos reveals a role for miR-375 in pancreatic islet development. *PLoS Biol* 5:e203.

14. Eisen JS, Smith JC (2008) Controlling morpholino experiments: Don't stop making antisense. *Development* 135:1735–1743.
15. Gennarino VA, et al. (2009) MicroRNA target prediction by expression analysis of host genes. *Genome Res* 19:481–490.
16. Zhang X, Friedman A, Heaney S, Purcell P, Maas RL (2002) Meis homeoproteins directly regulate Pax6 during vertebrate lens morphogenesis. *Genes Dev* 16:2097–2107.
17. Yang Y, et al. (2006) Regulation of alphaA-crystallin via Pax6, c-Maf, CREB and a broad domain of lens-specific chromatin. *EMBO J* 25:2107–2118.
18. Lang RA (2004) Pathways regulating lens induction in the mouse. *Int J Dev Biol* 48:783–791.
19. Bessa J, et al. (2008) meis1 regulates cyclin D1 and c-myc expression, and controls the proliferation of the multipotent cells in the early developing zebrafish eye. *Development* 135:799–803.
20. Choi WY, Giraldez AJ, Schier AF (2007) Target protectors reveal dampening and balancing of Nodal agonist and antagonist by miR-430. *Science* 318:271–274.
21. Adler R, Canto-Soler MV (2007) Molecular mechanisms of optic vesicle development: Complexities, ambiguities and controversies. *Dev Biol* 305:1–13.
22. Schwarz M, et al. (2000) Spatial specification of mammalian eye territories by reciprocal transcriptional repression of Pax2 and Pax6. *Development* 127:4325–4334.
23. Leconte L, Lecoin L, Martin P, Saule S (2004) Pax6 interacts with cVax and Tbx5 to establish the dorsoventral boundary of the developing eye. *J Biol Chem* 279: 47272–47277.
24. Koster R, Stick R, Loosli F, Wittbrodt J (1997) Medaka spalt acts as a target gene of hedgehog signaling. *Development* 124:3147–3156.
25. Zhao Y, Srivastava D (2007) A developmental view of microRNA function. *Trends Biochem Sci* 32:189–197.
26. Damiani D, et al. (2008) Dicer inactivation leads to progressive functional and structural degeneration of the mouse retina. *J Neurosci* 28:4878–4887.
27. Shi L, Ko ML, Ko GY (2009) Rhythmic expression of microRNA-26a regulates the L-type voltage-gated calcium channel alpha1C subunit in chicken cone photoreceptors. *J Biol Chem* 284:25791–25803.
28. Walker JC, Harland RM (2009) microRNA-24a is required to repress apoptosis in the developing neural retina. *Genes Dev* 23:1046–1051.
29. Qiu R, et al. (2009) The role of miR-124a in early development of the Xenopus eye. *Mech Dev* 126:804–816.
30. Heine P, Dohle E, Bumsted-O'Brien K, Engelkamp D, Schulte D (2008) Evidence for an evolutionary conserved role of homothorax/Meis1/2 during vertebrate retina development. *Development* 135:805–811.
31. Tholozan FM, Quinlan RA (2007) Lens cells: More than meets the eye. *Int J Biochem Cell Biol* 39:1754–1759.
32. Findlay VJ, Turner DP, Moussa O, Watson DK (2008) MicroRNA-mediated inhibition of prostate-derived Ets factor messenger RNA translation affects prostate-derived Ets factor regulatory networks in human breast cancer. *Cancer Res* 68:8499–8506.
33. Lee Y, et al. (2010) Network modeling identifies molecular functions targeted by miR-204 to suppress head and neck tumor metastasis. *PLOS Comput Biol* 6:e1000730.
34. Brodersen P, Voinnet O (2009) Revisiting the principles of microRNA target recognition and mode of action. *Nat Rev Mol Cell Biol* 10:141–148.
35. Meola N, Gennarino VA, Banfi S (2009) microRNAs and genetic diseases. *Pathogenetics*, 10.1186/1755-8417-2-7.
36. Iwamatsu T (2004) Stages of normal development in the medaka Oryzias latipes. *Mech Dev* 121:605–618.
37. Conte I, Bovolenta P (2007) Comprehensive characterization of the cis-regulatory code responsible for the spatio-temporal expression of olSix3.2 in the developing medaka forebrain. *Genome Biol* 8:R137.1–R137.17.
38. Mercader N, Tanaka EM, Torres M (2005) Proximodistal identity during vertebrate limb regeneration is regulated by Meis homeodomain proteins. *Development* 132: 4131–4142.
39. Flynt AS, Li N, Thatcher EJ, Solnica-Krezel L, Patton JG (2007) Zebrafish miR-214 modulates Hedgehog signaling to specify muscle cell fate. *Nat Genet* 39:259–263.
40. Del Bene F, Tessmar-Raible K, Wittbrodt J (2004) Direct interaction of geminin and Six3 in eye development. *Nature* 427:745–749.
41. Porter RM, Hutcheson AM, Rugg EL, Quinlan RA, Lane EB (1998) cDNA cloning, expression, and assembly characteristics of mouse keratin 16. *J Biol Chem* 273: 32265–32272.